Regulation of multiple developmental processes by *AtFH1* and *AtARP3* mediated actin cytoskeleton in *Arabidopsis thaliana*

A Thesis Submitted to the College of

Graduate and Postdoctoral Studies

In Partial Fulfillment of the Requirements

For the Degree of Master of Science

In the Department of Biology

University of Saskatchewan

Saskatoon

By

Abdul Halim

PERMISSION TO USE

This thesis is presenting to fulfill the partial requirements for a Master degree from the University of Saskatchewan. So, I therefore state that the Library of the University of Saskatchewan can make it freely available for inspection in any circumstance. I agree that the permission to reproduce this thesis in a part or full copy for scholarly purposes may be granted by the professor who supervised my program and thesis work. In absence of my supervisor, this permission may be granted by the Head of the Department of Biology or by the Dean of the College where my thesis work was done. It is also disclosed that use of this thesis or any information/material from this thesis for publication or copying the whole or part of this thesis for any financial gain will not be allowed without my written permission. It is further understood that any scholarly use of this thesis or any information/material from this thesis will render due recognition to me and to the University of Saskatchewan.

To copy this thesis or use of any materials in whole or part from this thesis, request should be addressed to:

Head of the Department of Biology
University of Saskatchewan
112 Science Place, Saskatoon, SK S7N 5E2

OR

Dean
College of Graduate and Postdoctoral Studies
University of Saskatchewan
116 Thorvaldson Building, 110 Science Place
Saskatoon, Saskatchewan S7N 5C9
Canada

ABSTRACT

The actin cytoskeleton plays a multifaceted role in plant biology. It is involved in several developmental processes and is needed to cope with both biotic and abiotic stresses. Actin is a highly conserved, the most abundant and multifunctional globular protein that can exist either as a globular sub-unit (G-actin) or filamentous (F-actin) form. F-actin is the microfilament part of the cytoskeleton polymerized from G-actin. Actin cytoskeleton polymerization is facilitated by several proteins like formins (polymerizing linear actin cytoskeletons) and the ARP2/3 complex (polymerizing branched actin cytoskeletons). *AtFH1* and *AtARP3* are important regulators of actin cytoskeleton in *Arabidopsis thaliana* and belong to the formins and ARP2/3 complex, respectively. The effect of *AtFH1* and *AtARP3* on actin cytoskeleton reorganization and its subsequent regulation on multiple developmental processes in *Arabidopsis thaliana* were studied using both single and double mutants of these genes. Simultaneous mutation of *AtFH1* and *AtARP3* appears to have a lethal effect. Although *fh1-1* was not a true knockout mutant, the double mutant *fh1-1/arp3-1* further recovered some expression of the *AtFH1* gene compared to *fh1-1* single mutant but a homozygous double mutant was not obtained. This double mutant showed several unique characteristics compared to the wild type and each single mutant, such as small plants with short, narrow and pale green leaves; short root, slow root growth rate; greater gravitropic response; altered lateral root locations etc. At the cellular level, the double mutant exhibited deformities in epidermal cell circularity; short root hairs; distinct trichome phenotype; small mesophyll cells with lower chloroplasts content; small pollen size, a number of which were structurally distorted. The double mutant produced tiny flowers with distinct floral organ structures that vastly affected the fertility resulted a short silique and a smaller number of seeds due to aborted ovule or embryo. Most of these characteristics were absent in the single mutants, *fh1-1* and *arp3-1*, and/or were not as severe as in the double mutant. The aberrant actin cytoskeleton organizations that were distinctive in each mutant were observed in epidermal pavement cells, trichome cells and mesophyll cells. So, *AtFH1* and *AtARP3* appears to regulate several biological processes in *Arabidopsis thaliana* by maintaining the proper organization of actin cytoskeleton.

ACKNOWLEDGEMENTS

It is a proud privilege to express my profound gratitude, sincere appreciation and heartfelt indebtedness to my supervisor Professor Dr. Yangdou Wei, Department of Biology, University of Saskatchewan, Saskatoon, SK for his constant and intellectual guidance, affectionate feelings, meaningful suggestions, constant encouragement, constructive criticisms from the beginning to the end of the research work and preparation of this thesis.

I also expresses my immense gratitude to the members of the advisory committee, Dr. Karen K. Tanino, Dr. Chris Ambrose and Dr. Ken Wilson for their kind advice, sympathetic encouragement, meaningful suggestions, constructive criticisms, scholastic guidance and all round help and cooperation for successful completion of this thesis.

I also convey my heartfelt gratitude to Dr. Hong Wang for being my external examiner.

The Department of Biology is sincerely acknowledged for providing the scholarship to complete my program. I also extends my warmest thanks to all the administrative and technical personnel of the Department for their sincere cooperation and help through the way of my success in this program.

I convey my special appreciations and thanks to the past and present members of my lab, post doc and graduate students from other lab for their friendly discussions, cooperation and sharing the feelings during the period of my program.

TABLE OF CONTENTS

PERMISSION TO USE i
ABSTRACT ii
ACKNOWLEDGEMENTS iii
TABLE OF CONTENTS iv
LIST OF FIGURES vi
CHAPTER 1: INTRODUCTION 1
1.1 Actin 1
1.2 Actin cytoskeleton 2
1.3 Formin protein family and AtFH1 4
1.4 ARP2/3 complex and AtARP3 5
1.4.1 Formin-mediated nucleation and elongation of actin filaments 5
1.4.2 Nucleation and branch assembly of actin filaments by ARP2/3 complex 6
1.5 The actin cytoskeleton in plants 7
1.5.1 Plant organogenesis and the actin cytoskeleton 8
1.5.2 Plant cell morphogenesis and the actin cytoskeleton 12
1.6 Root gravitropism and the actin cytoskeleton 15
1.7 Relation of actin cytoskeleton to the content of chlorophyll 16
1.8 Actin cytoskeleton and plant fertility 17
1.9 Rationale of the thesis 19
1.10 Objectives 20
CHAPTER 2: MATERIALS AND METHODS 21
2.1 Plant material and growth conditions 21
2.2 RNA-Extraction and cDNA Synthesis 22
2.3 Quantitative real-time PCR (qPCR) 22
2.4 Morphometric analysis 23
2.5 Estimation of chlorophyll and preparation of mesophyll cells for chloroplast counting 24
2.6 *In vitro* Pollen Germination 25
2.7 Aniline blue staining of pollen tube in pistil 25
2.8 Development of GFP-ABD2-GFP expressing lines under genetic background of all mutants 26
2.9 Confocal laser scanning microscopy 26
2.10 Scanning electron microscopy 27

2.11 Image analysis and measurement 28
2.12 Statistical analysis 28
CHAPTER 3: RESULTS 30
3.1 Development of the *fh1-1/apr3-1* double mutant 30
3.2 The distinct phenotypes of the actin cytoskeleton disrupted mutants 32
3.3 Aberrant root growth of the actin cytoskeleton disrupted mutants 35
3.3.1 Root phenotype and root growth rate 35
3.3.2 Gravitropic response 38
3.3.3 Root hair structure and density 40
3.3.4 Lateral root development and location 43
3.4 Changes in cellular structures of the actin cytoskeleton disrupted mutants 45
3.4.1 Leaf epidermal pavement cells 45
3.4.2 Trichome cells 49
3.4.3 Mesophyll cells 54
3.5 Diminished fertility of the actin cytoskeleton disrupted mutants 59
3.5.1 Flower and floral organ structures 59
3.5.2 Pollen structure and number of pollen produced 60
3.5.3 *In vitro* pollen germination rate 62
3.5.4 Pollen tube germination on the stigma 64
3.5.5 Size of the silique 65
CHAPTER 4: DISCUSSION 70
4.1 *AtFH1* and *AtARP3* genes mutation affect normal plant morphology 70
4.2 *AtFH1* and *AtARP3* are involved in normal root development of *Arabidopsis* 71
4.3 *AtFH1* and *AtARP3* are required for normal cell morphogenesis 79
4.4 The overall fertility of *Arabidopsis* is vastly affected by combined mutation of both *AtFH1* and *AtARP3* genes 85
CHAPTER 5: SUMMARY AND CONCLUSIONS 89
REFERENCES 93
APPENDICES 123

LIST OF FIGURES

Figure 3.1: Gene structure of *AtFH1* and *AtARP3* 31
Figure 3.2: The relative expressions of *AtFH1* gene 32
Figure 3.3: Morphology of the plants at 3 weeks of plant age (rosette leaf stage). 33
Figure 3.4: Stem Morphology of mature wild-type and mutant plants at the age of 8 weeks. 34
Figure 3.5: The histogram shows the average area of the whole plant 34
Figure 3.6: The histogram shows the average rosette leaf size 35
Figure 3.7: Root growth phenotypes 36
Figure 3.8: The histogram shows the average root growth rate 37
Figure 3.9: The histogram shows the average thickness of the roots 38
Figure 3.10: The root tip curvature at 12.5 hrs post gravistimulation 39
Figure 3.11: The histogram shows the average root tip angles 40
Figure 3.12: The root hairs length and density in primary roots 41
Figure 3.13: The histogram shows the average root hair length 42
Figure 3.14: The histogram shows the average root hair density 43
Figure 3.15: The images show the lateral roots number and location 44
Figure 3.16: The histogram shows the average lateral root density 45
Figure 3.17: The confocal images of the leaf pavement cells 47
Figure 3.18: The histogram shows the average circularity of leaf pavement cells 48
Figure 3.19: Actin cytoskeleton organization in leaf pavement cells. 49
Figure 3.20: SEM images of mature leaf trichomes 51
Figure 3.21: The images show the difference in trichome size and morphology 52
Figure 3.22: Actin cytoskeleton organizations in mature trichome 53
Figure 3.23: The histogram shows the total chlorophyll content of leaf 55
Figure 3.24: Chloroplast content of mesophyll cells 56
Figure 3.25: The histogram shows the average number of chloroplasts 57
Figure 3.26: The actin cytoskeleton organizations in leaf mesophyll cells 58
Figure 3.27: Different stages of flower development 60
Figure 3.28: Scanning electron microscopy (SEM) images of mature pollens 61
Figure 3.29: The SEM images show the normal and distorted pollens of the double mutant 62
Figure 3.30: Light microscopic images show *in vitro* pollen germination 63
Figure 3.31: The histogram shows *in vitro* pollen germination rate 64
Figure 3.32: Growth of pollen tube along the transmitting tissues of pistils 65
Figure 3.33: Sizes of the siliques in different stages of their development 66
Figure 3.34: The histogram shows the average length of siliques 67
Figure 3.35: The seed content of the siliques 68
Figure 3.36: The histogram represents the average seed content of siliques 69

CHAPTER 1: INTRODUCTION

1.1 Actin

Actin is highly conserved and one of the most abundant proteins, found in almost all eukaryotic cells (Pollard and Cooper, 1986). Actin is a member of a structural superfamily that also contains ARP proteins (Robinson et al., 2001), sugar kinases, hexokinases and Hsp70 proteins (Bork et al., 1992) and prokaryotic actin such as MreB (van den Ent et al., 2001) and ParM (van den Ent et al., 2002). Actin exists either as globular (G actin) actin monomer, or filamentous (F actin) polymer (Dominguez and Holmes, 2011).

The actin monomer is a rectangular prism like structure of 375 amino acid long polypeptides consisting of 5.5 nm x 5.5 nm x 3.5 nm dimension with a molecular mass of approximately 42 kDa (Dominguez and Holmes, 2011). Actin folds into two major domains α and β that are also known as the outer and inner domains based on their localization within the actin filament. These domains are different in size as revealed by electron microscopy images, and hence they are also called small and large domains, respectively (Dominguez and Holmes, 2011). These two major domains were further divided into four subdomains of which 1 and 2 subdomains belong to the small major domain and subdomains 3 and 4 represent the large major domain (Kabsch et al., 1990). Filamentous actin will be reviewed in 1.2 under the heading Actin cytoskeleton.

The transition between G and F actin is regulated mainly by nucleotide hydrolysis of F actin (Dominguez and Holmes, 2011). There are two active states of actin, the ATP and ADP states, of which ATP-actin (G) is more stable. When the G actin is in its ATP state, the activated actin monomer is attached to the fast-growing barbed (+) end of the actin filament. During the hydrolysis of actin filaments, the ADP-actin (G) monomers are released separating from the filamentous actin. This polymerization and de-polymerization of actin is called actin filament treadmilling (Wegner and Isenberg, 1983).

There are three main actin isoforms, α, β- and γ that are expressed in vertebrates. Among them α-actin isoforms are in skeletal, cardiac and smooth muscles, whereas non-muscles and muscles cells

express the β- and γ-isoforms (Dominguez and Holmes, 2011). There are a few variations of the amino acid sequence, mainly towards the N-terminus which are observed among the actin isoforms (Hanson and Lowy, 1963). Different actin genes are expressed in different organs of *Arabidopsis* based on steady state RNA level and GUS reporter gene expressions (An et al., 1996; Huang et al., 1997; McDowell et al., 1996). The mRNA level studies revealed that *ACT7* is a vegetative actin highly expressed in roots, stems, leaves, floral organs and siliques, but it is not detected in pollen. In contrast, *ACT1* is expressed in all the organs at a very weak level, but it is strongly expressed in pollen and hence it is called reproductive actin (Meagher et al., 2000; McDowell et al., 1996). Among the ten *Arabidopsis* actin genes, *ACT5* and *ACT9* are pseudogenes which are not expressed at a detectable level (Meagher et al., 2000). Studies using GUS reporter gene constructs showed that *ACT1* and *ACT3* are strongly expressed in pollen, pollen tube, and other organ primordia such as root, shoot and inflorescences. *ACT7* is highly expressed in the expanding hypocotyl and seed coat and interestingly *ACT7* complements the lack of the *ACT2* gene within these organs (An et al., 1996; Meagher et al., 2000). In addition *ACT1* also responds to the majority of the phytohormones including auxins, cytokinins and abscisic acid and *ACT7* contains a large number of phytohormone responsive elements in its promoter region (Meagher et al., 2000; McDowell et al., 1996). *ACT4* and *ACT12* expression is also observed in the late stage of pollen, but *ACT1* exhibited the strongest expression (Meagher et al., 2000).

1.2 Actin cytoskeleton

Actin is a multifunctional globular protein that can exist either as G-actin or F-actin form. F-actin is the microfilament part of the cytoskeleton polymerized from G-actin sub unit and is found in muscle and non-muscle cells as contractile apparatus. The actin filaments are assembled typically at the cell periphery from the site of membrane extension. Following nucleation, the actin filament starts to grow by addition of actin monomer at both the ends of the filament. The rate of monomeric actin addition is five to ten times higher at the barbed (+) end comparing to that of the pointed (-) end. The actin binding proteins influence the specific structure of actin filaments to form. These actin filaments can exist in two dimensional networks or three dimensional gels and can create linear bundles (Cooper, 2000). Negatively stained electron microscopy of actin fibers showed that two chains of filamentous actin gradually around each other forming a right-handed twisted long

helix of two chains (Graceffa and Dominguez, 2003; Dominguez and Holmes, 2011). As a general concept of an actin filament, it has a total rise of 27.3 Å between two sub units of nearer strands and a rotation of 166.15° around the axis (Egelman et al., 1982). The flexible F-actin has a helical repeat every 37 nm and the diameter ranges from 5-9 nm. The actin filament also has 13 actin subunits between each cross-over point (Egelman, 1985; Egelman, 2003). As an exception in the sperm, the actin filament exists in an inactive coil state being controlled by a cross linker protein and it can be extended upon activation (Schmid et al., 2004).

Actin filaments provide mechanical support, determine cell shape, and allow cell surface movement such as production and extension of cytoplasmic protrusions (lamellipodia, filopodia) formed by pushing plasma membrane outward during actin polymerization and adhesion of these protrusions to some elements of the anchoring point by being accumulated beneath the plasma membrane. The ionic strength of the actin solution regulates the polymerization and de-polymerization of the actin filaments. Addition of Mg^{+}, K^{+}, or Na^{+} increases the ionic strength of the actin solution that allows spontaneous polymerization of actin filaments, whereas de-polymerization occurs in a weak ionic solution (Lodish et al., 2000). ATP also influences the polymerization of actin filaments as actin monomers can exist in two different states: ATP-bound and ADP-bound. When the G actin is in its ATP state, the activated actin monomer is attached to the fast-growing barbed (+) end, enabling five to ten times more polymerization of the actin filament comparing to ADP state at the pointed end. Upon hydrolysis of ATP, the unstable ADP-actin leads to de-polymerization of the filament (Dominguez and Holmes, 2011; Pollard, 2007). So, actin polymerization is a reversible process in which actin monomers can be aggregated to form the actin filaments, and the actin filaments can be de-polymerized contributing monomeric actin. This process has an apparent equilibrium that is dependent on the concentration of free actin monomers. This concentration is proportional to the rate of polymerization or de-polymerization. There is a specific concentration when the polymerization is equal to de-polymerization that is called the critical concentration of actin monomers (Pollard, 2007; Wegner, 1976). There are two different structures: actin bundles and fine actin networks that play different roles in the cell. In a bundle, actin filaments are compactly cross-linked into parallel array, whereas they are loosely cross-linked into an orthogonal array in a network (Cooper, 2000).

1.3 Formin protein family and AtFH1

The Formin protein family stands as the third major protein family for nucleation of actin filaments utilizing G- actin and profilin-actin (Kovar et al., 2006; Faix and Grosse, 2006; Goode and Eck, 2007). The first Formin family member, formin1 was reported as being responsible for a limb deformity defect when mutated in mice in the early 1990s (Mass et al., 1990; Woychik et al., 1990). Formins contain multiple functional domains and are large proteins that have from 1000 to 2000 amino acid residues. They control the regulation as well as assembly of actin filaments. The formin proteins are divided into two distinct clades based on their phylogenies as type-I and type-II formins. *Arabidopsis thaliana* contains 21 members (AtFHs) of which AtFH1 to AtFH11 have been included in the type-I formins and the rest (AtFH12 to AtFH21) belong to the type-II formins (Cvrcková et al., 2004). There are two functional domains of formins involved in actin filament nucleation: FH1 (Formin Homology domain1) and FH2 (Formin Homology domain2). Type1 formins have also an extracellular signal peptide, a proline/serine rich region, and a transmembrane domain which has been shown for *AtFH1* (Banno and Chua, 2000) and *AtFH2* to *AtFH8* (Cvrcková, 2000). On the other hand, class II formins contain phosphatase tensin (PTEN) domains in their N-termini along with conserved FH1 and FH2 domains (Cvrcková et al., 2004).

As a class I formin, AtFH1 consists of a 21 amino acid (aa) signal peptide, an extracellular serine/proline rich domain of 64 aa, a transmembrane domain of 23 aa, and conserved FH1 (46 aa), and FH2 (412 aa) domain. It has been shown that the intra-space proline rich region between the membrane anchor and the transmembrane domain has a similarity to the extensin proteins which are associated with the cell wall (Liu et al., 2015; Blanchoin and Staiger, 2010). The trans-membrane domain also indicates the localization of type-I formins along the plasma membrane. The membrane location of *AtFH1* has been suggested based on the findings of a cell-fractionation experiment where this protein was associated with the microsomal fraction (Banno and Chua, 2000). Finally, the study using FH1-GFP fusion confirmed its membrane localization in *Arabidopsis thaliana* (Martinière et al., 2011). Some type-I formins which are highly associated with the actin, are localized to the endoplasmic reticulum (ER) (Cvrčková et al., 2014; Boevink et al., 1998).

1.4 ARP2/3 complex and AtARP3

ARP2/3 complex is a seven protein complex which includes two actin related proteins, ARP2 and ARP3 and five unique polypeptides, ARPC1, ARPC2, ARPC3, ARPC4 and ARPC5 (Zigmond, 2004; Beltzner and Pollard, 2004; Millard et al., 2004) and is responsible for nucleation and assembly of branched actin filaments (Mullins et al., 1998). The ARP2/3 complex itself cannot perform the polymerization of actin filaments without being activated with its associated regulatory proteins called nucleation promoting factors (NPFs), such as Wiskott-Aldrich syndrome family proteins (WASP, N-WASP, WASH etc.) and SCAR/WAVE (Rohatgi et al., 1999; Machesky et al., 1999). The activation of the ARP2/3 complex is tightly regulated by WASP and/ or SCAR/WAVE allowing the formation of sufficient branched filaments (Blanchoin et al., 2000; Pantaloni et al., 2000) as the ARP2/3 complex is responsible for .

As an actin-related protein that mimics the actin monomer, *AtARP3* contains only a single 420 aa domain of actin in *Arabidopsis thaliana*. *ARP3* is localized to the actin nucleation site (in the apex of the polarized, terminal cells of a file) in tobacco (Maisch et al., 2009), and preferentially to the plasma membrane in *Arabidopsis*, as the ARP2/3 complex is strongly associated to the plasma membrane in *Arabidopsis* (Zhang et al., 2013a). In *Arabidopsis,* both *AtARP2* and *AtARP3* start to nucleate branches of actin filaments upon activation by SCAR/WAVE (Szymanski, 2005).

1.4.1 Formin-mediated nucleation and elongation of actin filaments

The formins are integral membrane proteins that are common in the plant kingdom and responsible for the formation, or nucleation, of linear actin filament. The formin proteins modulate the affinity between G-actin monomers to initiate and facilitate the nucleation of new, unbranched actin filaments (Dominguez, 2010). Sometimes the formin proteins establish a structural interaction between the two ends of the protein and are auto-inhibited continuously (Li and Higgs, 2003). But their activation can be induced by GTP-bound Rho GTPases (Watanabe et al., 1997).

Recently it has been shown that the binding of adenomatous polyposis coli (APC), a tumor suppressor gene, to the mammalian Formin mDia1 inhibits the capping protein and profilin mediated suppression allowing the initiation and elongation of actin filaments (Breitsprecher et

al., 2012). In this model, the APC-mDia1 complex separates during polymerization, where mDia1 remains associated with growing barbed end, and APC remains attached to the nucleation site of the filaments (Breitsprecher et al., 2012).

Formin proteins act as a dimer upon activation and forms a donut-shaped structure around the actin subunit, recruiting the subunits to the filament's barbed end where the formin proteins remain bound, to initiate the formin-mediated nucleation and elongation of the actin filament (Romero et al., 2004). The bindings between the actin monomers is facilitated by the FH2 domain. These formin dimers then capture the G-actin bound profilin units. This capture process is mediated by poly proline residues within the formin homology domain1 or FH1 of formin proteins (Paul et al., 2008a; Higgs, 2005). Profilin induces the exchange of ADP to ATP nucleotides on G-actin and maintains a continuous supply of actin monomers to accelerate nucleation by adding the ATP-G-actin to the growing end of the actin filament (Romero et al., 2004). The binding of formin at the growing, barbed end of the actin filament maintains a continuous growth of the filament by preventing capping to the elongation site of the filamentous actin (Pring et al., 2003).

1.4.2 Nucleation and branch assembly of actin filaments by ARP2/3 complex

The ARP2/3 complex was first identified as a profilin-binding protein (Machesky et al., 1994). It consists of seven subunits, two of which are Actin-Related Proteins *ARP3* and *ARP2* (Suetsugu and Takenawa, 2003; Pollard, 2007). The ARP2/3 complex controls the de novo assembly of branched actin filaments by acting as a nucleation core (Suetsugu and Takenawa, 2003; Machesky et al., 1999; Mullins et al., 1998). Upon addition of G-actin, the ARP2/3 complex can mimic actin trimer formation (Robinson et al., 2001) and hence continue rapid actin polymerization without delay of actin trimer formation (Suetsugu and Takenawa, 2003). *ARP2* and *ARP3* are structurally closely related to monomeric actin and both serve as the actin filament nucleation site. Being attached to the nucleation site of the existing actin filament the ARP2/3 complex initiates the new daughter branch filament on this site of the mother actin filament. The ARP2/3 complex attaches the pointed end of the new branched filament at a distinctive angle of 70^0 (Svitkina, 2012) to the mother filament and elongates the branched filament by adding G-actin to the filament's barbed end (Pollard, 2007; Suetsugu and Takenawa, 2003).

The ARP2/3 complex itself cannot perform the polymerization of actin filament without being activated with its associated regulatory proteins called nucleation promoting factors (NPFs), such as Wiskott-Aldrich syndrome family protein (WASP, N-WASP, WASH etc.) and SCAR/WAVE (Rohatgi et al., 1999; Machesky et al., 1999). Structural analysis revealed that changes in structure of ARP2/3 complex is essential for actin filament polymerization. Three dimensional image analysis showed that the orientations of *ARP2* and *ARP3* subunits in the complex would block the trimer core activity for actin filament polymerization (Robinson et al., 2001). Cryo-electron microscopy also revealed that the dynamic conformational changes in *ARP2* and *ARP3* that are needed for addition of G-actin to the ARP2/3 complex are achieved by association of WASP (Volkmann et al., 2001). Therefore, activation of the ARP2/3 complex is tightly regulated by the Wiskott-Aldrich syndrome family protein that allows the formation of sufficient branched filaments (Blanchoin et al., 2000; Pantaloni et al., 2000). The number of barbed ends increases with the elongation of each branch which is proportional to the speed of polymerization (Suetsugu and Takenawa, 2003).

Based on the branching points on the mother filament, two different models have been proposed. One is a side-branching model and another is a barbed-end branching model. In the side branching model, the *ARPP2/3* complex attaches to the mother filament at a different point, other than nucleation site from where it initiates the branching at the nucleation site (Dayel and Mullins, 2004). By contrast, in the barbed-end branching model, the ARP2/3 complex is only associated with the barbed end to allow both the elongation of the original filament and the formation of a branched-actin filament (Pantaloni et al., 2000). However, later the research results increasingly favor the side-branching model instead of the barbed-end model of ARP2/3-mediated branch actin polymerization (Suetsugu and Takenawa, 2003).

1.5 The actin cytoskeleton in plants

Actin cytoskeletons play a multifaceted role in plant biology. It provides the major tracks that facilitate the intracellular transport of different cell organelles such as the Golgi apparati (Boevink et al., 1998), peroxisomes (Mathur et al., 2002) and mitochondria (Van Gestel et al., 2002). These organelles follow the actin filaments to move inside the cell as a part of the mass intracellular or

cytoplasmic movement that mediates the cytoplasmic streaming. The driving force for the movement of these organelles is provided by a molecular motor protein 'myosin' (Holweg and Nick, 2004). Actin filaments and myosin motor proteins are also thought to mediate the intracellular transport of vesicles within the endomembrane system of plants as it is established in the case of yeast and mammals (DePina and Langford, 1999).

The actin cytoskeleton also plays a part in cell division that is crucial besides its basic function in the cell. The actin filaments mostly facilitate the early stage of mitosis, but are also needed for the formation of the cell plate during cytokinesis to separate the newly formed daughter cells (Valster et al., 1997). The stomatal opening is modulated by actin filaments that stimulate the guard cells at the non cuticular part of the leaves (Hwang et al., 1997). It also maintains cell-to-cell communication through plasmodesmata (Aaziz et al., 2001). The gravitropic signal transduction into the root cells (Braun et al., 2004) and the outcome of plant-microbe interactions (Takemoto and Hardham, 2004) are also mediated by the dynamic reorganization of actin filaments.

The actin filament is responsible for the focal assembly of exocytic vesicles at the site of growing tips in plant root hairs and pollen tubes but this process is dispensed by microtubules (Vidali et al., 2001; Baluska et al., 2000). The complex morphogenesis of leaf trichomes in *Arabidopsis thaliana* depend on the organization of actin filaments (Szymanski et al., 1999), but the branching of the trichome is dependent on stabilized microtubules (Mathur and Chua, 2000). A variety of research findings established that actin is very much needed for the establishment and maintenance of cellular polarity in plants.

1.5.1 Plant organogenesis and the actin cytoskeleton

The development of several plant organs relies on the proper organization and distribution of the actin cytoskeleton within the cells of respective organs, such as the primary root, lateral root, flower and silique. Root growth is the result of cell divisions in the meristematic zone, anisotropic cell expansion in the elongation zone and cell differentiation in the differentiation zone (Rosero et al., 2013). The fate of root cells is determined during germination when the longest primary root apical meristem (RAM) is built up by divisions and reactivation of cell growth. Subsequently, the meristem tends to shorten resulting in slower root growth rate and reduced cell files (Shishkova et

al., 2007; Barlow and Baluska, 2000; Rost and Baum, 1988; Baum et al., 2002). When the elongation rate of the primary root is at its peak, the size of the RAM is greatest. It gradually decreases until elongation stops (Shishkova et al., 2007; Rost and Baum, 1988). This happens when the dynamic organization of the RAM changes with the aging of the roots from 1 to 4 weeks post-germination (Baum et al., 2002). The rate of root growth is boosted with the enlargement of RAM due to the increased number of divided cells from the root apical meristem (Verbelen et al., 2006; Beemster and Baskin, 1998; Beemster and Baskin, 2000). The actin cytoskeleton is needed for increasing the number of dividing cells, because disruption of the actin cytoskeleton reduces the cell division rate of the root apical meristem (Kushwah et al., 2011). In short, root growth is the combined result of controlled cell division and anisotropic cell expansion in the apical meristem and elongation zones, respectively (Vaughn et al., 2011). Most of the cytoskeletal disrupted mutations affect root growth, as well as root hair development (Thitamadee et al., 2002; Gilliland et al., 2003; Abe and Hashimoto, 2005). Among the cytoskeleton, actin filaments and microtubules play dominant roles in cell division, cell shape determination, cell expansion and organelle movement (Blancaflor et al., 2006). It is now established that microtubules determine the polar axis and actin cytoskeletons regulate the delivery of components required for growth of all growing cells, including root cells. Thus, disruption of actin cytoskeleton by mutation or drug treatments, misdirects or depletes vesicles delivery to the cell cortex, resulting in cellular distortion or growth reduction (Mathur and Hülskamp, 2002). Plant hormones have a marked effect on root growth where auxin acts antagonistically and cytokinin acts synergistically to root growth (Beemster and Baskin, 2000). Actin cytoskeletons are redistributed to establish the proper auxin gradient throughout the whole plant (Lanza et al., 2012). Disruption of the actin cytoskeleton causes differential cell elongation across the root through differential auxin transport. Thus, auxin reduces root growth by arresting cell elongation without decreasing the cell number, and by contrast, de-polymerization of the actin cytoskeleton reduces root growth by decreasing the number of dividing cells (Kushwah et al., 2011).

The lateral roots are initiated from the pericycle cell layer that lies between the vascular bundle and the endodermis of the primary root. The lateral root founder cells of the pericycle cell layer possess a deep outgrowth of overlying endodermal, cortical and epidermal cell layers to produce the lateral roots at the surface of the primary root (Lavenus et al., 2013; Péret et al., 2009; Vilches-

Barro and Maizel, 2015). In *Arabidopsis thaliana*, the developmental process of lateral root formation is dependent on accommodating space and the intrinsic pressure imposed by overlying epidermal, endodermal and cortical cell layers (Lucas et al., 2013; Vermeer et al., 2014). In angiosperms the initiation of lateral root primordia occurs in advance of visible growth of the lateral root (Hinchee and Rost, 1992). The lateral roots which are formed in response to several environmental cues, such as drought, are used by the plant to foster water and nutrient absorption as well as anchoring (Malamy and Ryan, 2001). The hormonal regulation of lateral root formation, its growth and development, are well reported, such as (i) auxin triggers lateral root formation and specifies the lateral root founder cells (Vermeer and Geldner, 2015), (ii) cytokinin antagonizes the auxin effect on lateral root formation, but its effect on auxin transport is essential for mitotic division of lateral root founder cells (Bielach et al., 2012; Marhavý et al., 2014), (iii) auxin plays the central role in initiation and growth of lateral roots in *Arabidopsis* (Chang et al., 2013). The oscillation of auxin concentration determines the acquisition of the fate of lateral root founder cell. When the auxin concentration reaches a maximum to a subset of undifferentiated pericycle cells, they become primed to form lateral root founder cells that produce lateral roots following subsequent developmental stages (De Smet et al., 2007; De Smet, 2012). Actin cytoskeletons are redistributed to establish the proper auxin gradient through the whole plant (Lanza et al., 2012).

The development of the entire flower including floral organs is the primary determinant for the reproductive success of the flowering plants, as the plants can produce unisexual or sterile flowers by degeneration or abortion of reproductive floral organs like developing stamens and/or pistils (Smith and Zhao, 2016). Flowers which are the reproductive organs of plants, are developed through a long, complex process of four sequential stages including flowering transition, floral meristem identity, floral organ identity, and floral organ morphogenesis. In *Arabidopsis*, flowers are indefinitely generated on raceme-type indeterminate inflorescence (Smith and Zhao, 2016). The transition from the vegetative to reproductive phase of plant development is tightly regulated by a highly complex gene regulatory network (GRN). There are several environmental cues including temperature, photoperiod, nutrient availability and endogenous signals (Paul et al., 2008b; Wahl et al., 2013) play a pivotal role for timing in floral transition (Srikanth and Schmid, 2011; Andrés and Coupland, 2012) that directs the conversion of shoot apical meristem (SAM) to inflorescence meristem (IM) in order to form a complete flower (Ó'Maoiléidigh et al., 2014). The

floral organs in a typical *Arabidopsis* flower are arranged within four different whorls. There are four sepals in first whorls, four petals in second whorls, six stamens or male reproductive organs in third whorls and two fused carpels or female reproductive organs that form gynoecium in the fourth whorl (Robles and Pelaz, 2005; Yang et al., 2003; Smith and Zhao, 2016). Numerous genes required for flower development have been identified through molecular genetic studies. Among these genes which regulate the floral organs identities in all four whorls are classified into four major classes, i.e., class A genes [APETALA1 (*AP1*) and APETALA2 (*AP2*)], class B genes [APETALA3 (*AP3*) and PISTILLATA (*PI*)], class C gene [AGAMOUS (*AG*)], and the semi-redundant class E genes [SEPALATTA1-4 (*SEP1-4*) in *Arabidopsis thaliana*. To show the functional interactions among these classes of genes a simple ABC [now ABCE (Smith and Zhao, 2016; Myakushina et al., 2009)] model was proposed and this model is now established. According to this model, class A and E genes are needed to specify four sepals in first whorl. To regulate petal identity in the second whorl, a combination of class A, B and E genes are required. The stamen identity is regulated by class B, C, and E genes in the third whorl, and in the fourth whorl class C and E genes are required for specifying the carpels (Smith and Zhao, 2016; Ditta et al., 2004). Other than mutation of genes involved in floral organs identity several *Arabidopsis* genes mutants including *clavata1*, *clavata2*, *clavata3*, *fasciata1*, *fasciata2*, *tousled*, and *revoluta* that are defective in floral organ development have been characterized (Running and Meyerowitz, 1996). In addition, auxin is also responsible for mediating the linkage between outgrowths of floral primordia from inflorescence meristem (IM) and specification of floral meristem (FM) (Ó'Maoiléidigh et al., 2014; Li et al., 2013). Furthermore, actin related proteins (*ARP*s) like *ARP4*, *ARP6* and *ARP7* deficiency resulted defect in floral organ morphology, male and female fertility and exhibited embryo lethality (Meagher et al., 2005; Meagher et al., 2007; Deal et al., 2005; Kandasamy et al., 2004; Kandasamy et al., 2005).

Furthermore, the fertilization following the successful pollination leads to the formation of embryo and endosperm (Goldberg et al., 1994; Horner and Palmer, 1995; Lord and Russell, 2002) which determine the length of the siliques (Wang, 2015; Meinke and Sussex, 1979). In *Arabidopsis*, seed sets also determine the length of the silique, as fewer seed containing siliques are shorter (Wang, 2015; Meinke and Sussex, 1979). At the time of pollination, the total number of ovules determines the number of seeds in a silique. Normally unfertilized ovules containing siliques cannot be

elongated resulting in a short size of silique (Meinke and Sussex, 1979). Auxin can induce plant to produce fruits which are seedless without fertilization (Gustafson, 1936). There were several gene mutations like a short glycine-rich domain containing gene (*AtGRDP1*) (Rodríguez-Hernández et al., 2017), SWITCH1 gene (*SWI1*) (Mercier, 2001; Motamayor et al., 2000), a putative heterotrimeric G-protein β subunit (*AGB1*) (Lease et al., 2001), SHAGGY-LIKE PROTEIN KINASES 32 *(ASK32*) (Dong et al., 2015) resulted in non-elongated short siliques, mostly with a reduced seed phenotype.

1.5.2 Plant cell morphogenesis and the actin cytoskeleton

The actin cytoskeleton regulates several cellular processes that control the growth and morphology of eukaryotic cells (Hussey et al., 2006). The filamentous actin (F-actin) mediates the cytoplasmic streaming and guides the transportation of materials necessary for plant cell growth to the exocytosis zones (Valster et al., 1997). The growth, expansion and development of several cell types, like root hair, epidermal pavement cell, trichome, pollen tube depends on the accumulation of dynamic F-actin configurations to the cell surface area (Hussey et al., 2006; Mathur and Hülskamp, 2002; Mathur, 2004; Miller et al., 1999; Fu et al., 2002).

The single cellular root hairs are long tubular extensions of root epidermal cells or trichoblasts (Grierson et al., 2014). The trichoblasts are the specialized root epidermal cells that produce the root hairs in majority of the plants. Trichoblasts are arisen from the cleft between two underlying cortical cell files in *Arabidopsis thaliana* (Dolan et al., 1993; Galway et al., 1994; Balkunde et al., 2010; Grebe, 2012). There are three basic steps including specification of the root hair cell fate, initiation of a root hair outgrowth, and elongation of the hair via tip growth are involved in root hair development process (Huang et al., 2017). The formation and elongation of root hairs in a plant are strictly controlled genetically, but the external environmental stimuli like hormone, nutrient, physical and chemical stresses are also aided in this process (Cho and Cosgrove, 2002; Pitts et al., 1998; Müller and Schmidt, 2004). The application of auxin or ethylene synthesis inhibitors enhanced root hair development (Cho and Cosgrove, 2002). But internally this auxin production and distribution in the root cells are controlled by several genes like PINs. The mutation effect of these controlling genes may be minimized externally, such as root hairless mutant *rhl* and

root hair defective mutant *rhd6* of *Arabidopsis* produce normal root hair when the root grows in contact with air (Cho and Cosgrove, 2002; Müller and Schmidt, 2004). The cytoskeleton organization is highly dynamic in root hair cell. Actin cytoskeleton disrupted trichome and pavement cell phenotype is well reported, but the root hair growth and development also depend on actin cytoskeleton polymerization (Hepler et al., 2001). Actin cytoskeleton visualization studies revealed that a dense actin cytoskeleton meshwork decorated the root hair tips, but low density actin filaments were seen at the base of root hair (Baluska et al., 2000; Tominaga-Wada et al., 2011).

The development of jigsaw puzzle shaped interdigitating pavement cell layers in the epidermis of cotyledons and leaves are associated with the coordinated cell wall expansions among the neighboring cells (Ivakov and Persson, 2013; Jacques et al., 2014). The assembly of protruding microtubule bundles (Panteris and Galatis, 2005), ARP2/3 complex mediated nucleation and assembly of actin cytoskeleton (Mathur, 2005), myosins (Ojangu et al., 2012), some microtubule-binding proteins, microtubule cytoskeleton (Wang et al.; 2007; Ambrose et al., 2007), and the active function of membrane trafficking apparatus (Falbel et al., 2003; Zhang et al., 2011a) at the indentation or the neck region are involved for the formation of harmonized lobes in the pavement cells. The cortical microtubule band that is located in the cell neck region, controls the interdigitating growth of neighboring cells and prevents the expansion of the neck areas, but the patches of microfilaments supports the anticlinal cell wall expansion at lobe tip resulting the lobe formation in pavement cell (Fu et al., 2005**;** Fu et al., 2009**;** Xu et al., 2010). Microtubules also play a central role in lobe out growth and it initiate the lobbing with periclinal cell wall expansion. After initiation of the lobe the actin filament is being enriched at the lob tip (Armour et al., 2015). RIC1/ROP6 pathway inhibits RIC4/ROP2 pathway and induces microtubule bands in neck regions that promote the assembly of microfilaments in the lobes. So, to study the cytoskeleton coordination and membrane dynamics epidermal pavement cell can provide an important model (Jacques et al., 2014).

The dynamics and organization of actin cytoskeleton are specially regulated by several actin binding proteins whose mutations showed a wide range of plant phenotypes. Irregular expansion and shape of the trichome is a common characteristics of these mutants (Mathur, 2005; Mathur,

2006). Trichomes that are specialized epidermal cells of the plants originate from the specific mother cells of epidermal layer and are distributed uniformly on leaves and stems (David Marks, 1994; Hülskamp et al., 1994). These trichome fate cells then undergo at least four rounds of endoreduplication and form mature trichomes following a series of morphological changes (Folkers et al., 1997). In general, a mature leaf trichome has two branch points and a large single nucleus containing an average ploidy of 32C located at the lower branch point (Li et al., 2012; Hülskamp et al., 1994). There are several groups of mutants that are initially screened based on distorted trichome cell shape and size. These mutants were studied based on genetic and cytological analysis to uncover the sequence of developmental steps including specification of the trichome cell, regulation of cell size, local outgrowth, expansion growth and branching in trichome morphogenesis (Hülskamp et al., 1994). Actin cytoskeleton polymerizing protein mutations, like components of ARP2/3 (Mathur, 2003; Li, 2003) and SCAR/ WAVE complexes (Basu, 2004; Basu, 2005) mutations are well reported for distinct trichome cell shape and size. The trichomes of these mutants are small, irregular in size, expanded and elongated stalk and short branched (Zhang, 2005; Szymanski et al., 1999). Some other phenotypically similar mutant like myosin mutant *xi-k*, the WD40/BEACH domain protein mutant- *spirrig* showed reduced distortion in size and shape of trichome cells and considered as weak distorted mutants (Ojangu et al., 2012).

The pollen tube is generated from the vegetative cell of the pollen in all flowering plants (Tanaka, 1997). This pollen tube provides route to deliver the non-motile sperm cells into the embryo sac to fuse the female gametes (Gao et al., 2016). The pollen tube growth is started with the landing of pollen onto the stigma and germination of the pollen grain after pollination. This compatible pollen germination onto the stigma is determined by the successful pollen-stigma interaction (Edlund et al., 2004; Hiscock and Allen, 2008). A series of events including pollen adhesion onto the stigma, pollen hydration and germination, polarized growth of pollen tube across the transmitting tissue of pistil occur during pollen-stigma interactions (Gao et al., 2016). Several studies revealed the crucial role of actin cytoskeleton for pollen tube growth (Taylor and Hepler, 1997; Gibbon et al., 1999; Hepler et al., 2001; Vidali et al., 2001; Smith and Oppenheimer, 2005; Hussey et al., 2006; Chen et al., 2009; Fu, 2010; Staiger et al., 2010). The long distance migration of the pollen tube cell is facilitated by actin cytoskeleton which aids the pollen tube to deliver the sperm cells to the embryo sac for fertilization. This migration of the pollen tube is mediated by an

actin cytoskeleton-based polar growth process in which the growth is restricted to the tube apex (Derksen et al., 1995; Hepler et al., 2001). In order to describe the function of actin cytoskeleton during pollen tube growth, several models have been proposed. All of these models propagate a common idea that actin cytoskeleton provides the track for intracellular movement of Golgi-derived vesicles containing cell wall synthesis and membrane fusion materials to the tip of the pollen tube (Pierson and Cresti, 1992; Hepler et al., 2001; Vidali and Hepler, 2001). As a structural component, actin cytoskeleton also provide the turgor pressure as a driving force to maintain rapid pollen tube growth (Picton and Steer, 1982; Steer and Steer, 1989; Derksen et al., 1995). In addition, polymerization of actin cytoskeleton is also important in pollen tube growth (Gibbon et al., 1999; Vidali et al., 2001).

1.6 Root gravitropism and the actin cytoskeleton

Gravitropism is the directional growth or changes in growth direction of a plant in response to gravity (Blancaflor et al., 2006). There are three major phases of gravitropism in higher plants including gravity sensing, gravity signal transduction and gravitropic responses (Blancaflor and Masson, 2003) which mediate the directional growth of plant organs. Gravity sensing occurred in different cells in different organs i.e., root cap columella cells of root and endodermal cells of shoot (Morita, 2010). It was proposed that gravitropism is vastly regulated by actin cytoskeleton (Blancaflor, 2013). Several actin cytoskeleton inhibitor studies showed that disruption of actin cytoskeleton enhanced the gravitropism in higher plant (Yamamoto and Kiss, 2002; Hou et al., 2003; Palmieri and Kiss, 2005; Mancuso et al., 2006). The cytoskeleton and endomembrane derived non-homogeneous structures of statocytes significantly affected the complex movements of amyloplasts and disruption of actin cytoskeleton reduced the statolith movement, increased the statolith sedimentation resulting increased gravitropic response (Saito et al., 2005; Nakamura et al., 2011). The changes in tension of actin cytoskeletons which act as a sensor of amyloplast displacement initiate a signaling cascade by activating ion channels in the plasma membrane to mediate curvature (Blancaflor, 2002). The novel signaling roles for the actin cytoskeleton in root gravitropism was found at the root cap. Because actin disruption extended the duration of gravity-induced pH changes in the root cap, which are linked to the initial events of signaling and gravity perceptions (Hou et al., 2004).

Asymmetric auxin distribution is needed for influencing gravitropism (Hou et al., 2004). The actin cytoskeletons that regulate gravitropism in higher plants by modulating auxin transport are responsible for the polar auxin transport in shoots, indicating actin dynamics facilitate the auxin transporting machinery within the plants (Muday and Murphy, 2002). The localization of PIN proteins within the transporting cells determines the auxin transport through the cell file. As reported, the PIN1, PIN3, PIN4 and PIN7 facilitate the auxin transport acropetally/root-ward through pro-vascular cell files whereas PIN2 protein turns root-ward auxin stream back to the elongation zone (Su et al., 2017; Adamowski and Friml, 2015). Thus PIN proteins increase auxin concentration to the root tip by mediating the downward efflux of auxin resulting its redistribution in response to gravitropism (Müller et al., 1998; Friml et al., 2002a; Friml et al., 2002b). Between the plasma membrane and endosomes, PIN proteins go under constitutive recycling process that involves a complex interplay within molecules and proteins (Dhonukshe et al., 2005). This recycling process is depended on the actin cytoskeleton which is responsible for proper PIN protein compartmentalization (Geldner et al., 2001).

1.7 Relation of actin cytoskeleton to the content of chlorophyll

Chlorophyll content of the chloroplast can significantly change the color of plant leaves (Guan et al., 2016). Mutations of the genes involved in chlorophyll biosynthesis, its degradation and chloroplast development produced varying leaf colors in the plant (Terao et al., 1985; Zhang et al., 2006; Yoo et al., 2009; Yu et al., 2009). These type of chlorophyll deficient leaf color mutations have been reported in different higher plant including *Arabidopsis* (Carol et al., 1999). There are several genes in different plants like *elm1*, *elm2*, *vyl-Chr.1* and *vyl-Chr.9* in maize (Sawers et al., 2004; Shi et al., 2013; Xing et al., 2014); *ygl1*, *ygl2*, *ygl3*, *ygl7*, *ygl98* and *YGL138*(*t*) in rice (Wu et al., 2007; Chen et al., 2013; Deng et al., 2014; Zhang et al., 2013b); and *chaos*, *egy1*, *apg1*, and *var3* in *Arabidopsis* (Chen et al., 2005; Motohashi et al., 2003; Naested et al., 2004) that are responsible for the leaf color have been characterized. These have built up the advanced understanding on leaf color mutations in plant.

To decrease the CO2 diffusion resistance, chloroplasts are usually located between the plasma membrane and tonoplast, adjacent to the intercellular space (Terashima et al., 2011; Kubínová et al., 2014). The number of chloroplasts per cell is a quantitative anatomical parameter depending on various internal and external conditions (Kubínová et al., 2014), such as ploidy and CO2 concentration (Wang et al., 2004; Teng et al., 2006; Kubínová et al., 2014). The number and size of the chloroplasts are involved in photosynthesis rate and chlorophyll content of the plants (Kariya and Tsunoda, 1972; Gabrielsen, 1948).

In the mesophyll cells, actin cytoskeleton mainly controls the chloroplasts positioning and movements by forming a longitudinal array of thick and randomly oriented thin actin filaments network. This thin actin network normally extends from the thick array and binds to the outer envelope of the chloroplasts (Luesse et al., 2006; Kandasamy and Meagher, 1999), thus controls the positioning of the chloroplasts. Chloroplast positioning influences the light-use efficiency of leaves (Xiao et al., 2016) and in the mesophyll cell light induced chloroplast positioning for photosynthetic optimization is mediated by actin cytoskeleton (Kimura and Kodama, 2016). The chloroplast in the cells may be aligned along the thick bundles or closely associated with thin actin filaments network. By contrast, microtubules have no effect on chloroplast positioning and movements (Kandasamy and Meagher, 1999; Tlałka and Gabryś, 1993).

1.8 Actin cytoskeleton and plant fertility

The evolutionary success and the reproductive fitness in the flowering plants are determined by the functional specialization of male gametophyte (Honys and Twell, 2004). As the important fundamental studies in plant reproduction, physiological, biochemical and molecular analyses of male gametophyte development including pollen grain rehydration, pollen germination and pollen tube growth (Boavida and McCormick, 2007) are crucial to determine the potentiality of male reproduction. Pollen development is an important process in plant reproduction, but it can also be considered as an ideal system to study several plant biological aspects including cell fate determination, cellular differentiation, intracellular and intercellular signaling and polar growth (Procissi et al., 2001). Male sporogenesis is the process for producing pollen grains containing one vegetative and two sperm cells. Through this process, diploid sporophytic cells undergo mitotic division to produce a sporogenous cell which subsequently produces pollen mother cells following

several mitotic divisions. This pollen mother cell then undergoes two rounds of mitosis. The pollen mitosis I produces a large vegetative cell and a smaller generative cell and then pollen mitosis II divides the generative cell into two sperm cells. The produced vegetative cell then takes control for developing the pollen grain as well as the pollen tube and continue its control to deliver the sperm cells into the embryo sac (Suzuki et al., 2008; McCormick, 1993; Bedinger et al., 1994; Preuss, 1995; Franklin-Tong, 1999). Pollen grains that contain a haploid vegetative cell enclosed two haploid sperm cells in *Arabidopsis* are important part of male reproductive organ (Loraine et al., 2013). Pollen provides the powerful model to study the formation and deposition of a complex extracellular structure. This structure is assembled in a complicated 3D pattern to form the pollen wall called exine which exhibits a wide range of morphological diversity across the higher plant species (Reeder et al., 2016; Suzuki et al., 2008). In *Arabidopsis,* the surface structure of the pollen grain consists of two layers, intine and exine, that form a reticulate sculpture with uniform mesh size. The main components of intine are cellulose and pectin. The exine is composed of sporopollenin which is a polymer of fatty acid derivatives and phenylpropanoids (Suzuki et al., 2008; McCormick, 1993; Scott, 1994; Owen and Makaroff, 1995; Paxson-Sowders et al., 1997; Scott et al., 2004; Morant et al., 2007).

Pollen viability that can generally be determined by *in vitro* pollen germination rate (Shivanna et al., 1991), is the ability of the pollen grain to deliver its sperm cells into the embryo sac following a compatible pollination (Boavida and McCormick, 2007). The alterations in germination or tube growth preference can be detect through *in vitro* pollen germination test (Cole et al., 2005; Hashida et al., 2007; Procissi et al., 2003; Steinebrunner et al., 2003). Because unsuccessful *in vitro* assays is normally difficult to perform *in vivo* (Boavida and McCormick, 2007). Although numerous protocols have been discussed (Johnson-Brousseau and McCormick, 2004; Azarov et al., 1990; Fan et al., 2001; Li et al., 1999; Mouline et al., 2002; Thorsness et al., 1993), but in general the *in vitro* pollen germination in a tri-nucleate pollen like *Arabidopsis* pollen is extremely challenging in terms of reproducibility of its results (Boavida and McCormick, 2007; Johnson-Brousseau and McCormick, 2004; Preuss et al., 1993; Taylor and Hepler, 1997; Scholz-Starke et al., 2003). Even though reproducibility of these protocols is difficult, the pollen tube growth following *in vitro* pollen germination is invaluable for investigating several processes underlying tip growth (Johnson and Kost, 2010). Without any other cell contaminations, growing a large number of

pollen tube is possible *in vitro* for RNA isolation and biochemical analysis (Klahre et al., 2006). *In vitro* grown pollen tubes are transparent and free from auto-fluorescence which provides excellent material for live-cell imaging (Johnson and Kost, 2010). This imaging technology revealed that network like structure containing filamentous actin (F-actin) plays crucial roles in both pollen germination and pollen tube growth (Cao et al., 2013).

1.9 Rationale of the thesis

Actin cytoskeleton reorganization is essential for many cellular functions in eukaryotic organisms. In animal cells actin cytoskeleton polymerization is changed by extracellular signals and alters cell morphology, movement, membrane dynamics, and other processes. In plant, actin cytoskeleton plays important roles in many cellular and developmental processes, such as cell morphogenesis, intracellular organelle movement, organogenesis, stomatal movement, gravitropism, cell polarity and polarized cell growth, and cell division. Actin cytoskeleton is reorganized differently to control different processes in plants. The reorganization of actin cytoskeleton is regulated by several actin-binding proteins. Among the actin-binding proteins, actin cytoskeleton polymerizing proteins play the pivotal roles in this reorganization processes, as these proteins control the distribution of actin cytoskeleton in plant cells. The *AtARP3* and *AtFH1* are the important members of the major actin cytoskeleton polymerizing proteins ARP2/3 complex and Formins in *Arabidopsis thaliana*. The mutation studies of *AtARP3* and *AtFH1* reported few cellular and developmental processes, such as epidermal pavement cell, hypocotyl epidermis and trichome cell shape, and root and pollen tube growth which are regulated by these proteins. But, as the important actin polymerizing proteins, they may control most of the actin cytoskeleton mediated processes in *Arabidopsis thaliana*. During the development of a double mutant of *AtARP3* and *AtFH1* genes, homozygous double mutant was not obtained in the present study. The preliminary observations on the heterozygous double mutant plants revealed several developmental defects. So, it is hypothesized that simultaneous mutation of *AtFH1* and *AtARP3* has lethal effect on plant life cycle and *AtARP3* and *AtFH1* genes controls actin cytoskeleton reorganization during several developmental processes in *Arabidopsis thaliana*. To prove this hypothesis the experiments (to perform on the actin cytoskeleton disrupted double and single mutants) were designed to achieve the following objectives.

1.10 Objectives

i. To elucidate *AtFH1* and *AtARP3* mediated cell morphogenesis and organ development in *Arabidopsis thaliana*

ii. To study *AtFH1* and *AtARP3* mediated actin cytoskeleton reorganization during cell morphogenesis in *Arabidopsis thaliana*

iii. To investigate the effect of *AtFH1* and *AtARP3* on the fertility of *Arabidopsis thaliana*

CHAPTER 2: MATERIALS AND METHODS

2.1 Plant material and growth conditions

The SALK mutants, *fh1-1* (SALK_071705), the insertion mutant of *AtFH1* (AT3G25500), and *arp3-1* (SALK 010045), the insertion mutant of *AtARP3* (AT1G13180) seeds were collected from TAIR. The wild type (Col-0) and both the mutants were grown in the soil in a controlled growth chamber under 22/18 ^{0}C day/night temperature, 16 hrs photoperiod with a light intensity of 130 $\mu molm^{-2}s^{-1}$ with a relative humidity 60% to 70%. One week after germination, the genomic DNA of the wild type and both the mutants were extracted from first emerged true leaves according to the method described in (Dinh et al., 2014). The mutant plants were screened using both genomic and insertion specific T-DNA left border primer and genomic reverse primer pair.

AtFH1 genomic primer pairs:
Forward primer – 5' TAATGTTTGTTGCCCCAAAAC 3'
Reverse primer – 5' TTGGGTCTGATGAAGATGGAG 3'

AtARP3 genomic primer pairs:
Forward primer – 5' AATTGCTGGCAAAGATGTCAC 3'
Reverse primer – 5' AGCTCTTCGTGTGTCAATTGG 3'

T-DNA left border primer – 5' ATTTTGCCGATTTCGGAAC 3'

Using the above primers, T-DNA insertions were confirmed in both the mutants. Wild type DNA served as a control using the same primers for each PCR reaction. *AtARP3* knockout mutation was confirmed by screening distorted trichome phenotype of the mutant. For the confirmation of *AtFH1* knockout mutation RT and qRT-PCR was performed. The *fh1-1/arp3-1* double mutant was developed by performing reciprocal crossing artificially between *fh1-1* and *arp3-1* single mutants. Following crossing, F2 generation plants were screened by PCR using above mentioned primers for the confirmation of insertions. The knockout mutation of *AtARP3* in the double mutant were

confirmed by screening distorted trichome phenotype. For the determination of *AtFH1* knockout mutation in the double mutant RT and qRT-PCR were performed.

2.2 RNA-Extraction and cDNA Synthesis

The total RNA from the leaves of three week old plants of the wild type, the *fh1-1/arp3-1* double mutant and the *fh1-1* single mutant were extracted using the RNeasy Plant Mini Kit (www.quiagen.com) according to the manufacturer's protocol. Total RNA was quantify using Thermo Scientific™ *NanoDrop*™ spectrophotometer. The cDNA was synthesized by reverse transcription using SuperScript™ First-Strand Synthesis System for RT-PCR (www.thermofisher.com) following manufacturer's recommendations. All cDNA samples were diluted to a same concentration quantifying by Thermo Scientific™ *NanoDrop*™ spectrophotometer. The cDNA primers were designed from the cDNA sequence of *AtFH1* using Primer3 (version 0.4.0) software. The purity of the cDNA was confirmed by RT PCR using primer pairs designed from two different exons.

2.3 Quantitative real-time PCR (qPCR)

Quantitative real-time PCR analysis was performed on an *iQ5* Multicolor *Real Time PCR* Detection *System* (Bio-Rad, USA) using PowerUp™ SYBR™ Green Master Mix (www.thermofisher.com). The primer pair for the qPCR was 5' TACACCGCCTTCACATCCTT 3' (forward), 5' TCACGATCCGAACTTGCTCT (reverse) with an amplicon length of 168 base pairs and glyceraldehyde 3 phosphate dehydrogenase (GAPDH) gene was used as reference which produced amplicon of 62 base pairs with the primer pairs 5' TTGGTGACAACAGGTCAAGCA 3' (forward) and 5' AAACTTGTCGCTCAATGCAATC 3' (reverse). The reaction volume was 20 µl each and each reaction mix contained 200 ng of each primer and 10:1 diluted cDNA 1 µl. The qPCR conditions were 95^0C five minutes initial denaturation, then 35 cycles of 95°C at 15 s and 62°C at 60 s. A no template control (NTC) was run to check the contaminations. The mean Ct values of triplicate designed sampling was calculated for each sample. The $2^{-\Delta\Delta Ct}$ method (Livak and Schmittgen, 2001) was performed to find out the mRNA fold change of *AtFH1* gene in *fh1-1/arp3-1* and *fh1-1* cDNA mRNA samples compared to the wild type control.

2.4 Morphometric analysis

The wild type, the *fh1-1/arp3-1* double mutant and both the *fh1-1* and *arp3-1* single mutants were grown in a growth chamber under 22/18 ^{0}C day/night temperature, 16 hrs photoperiod with a light intensity of 130 μmolm^{-2}s^{-1} with a relative humidity 60% to 70%. At the rosette stage (3 week old plant), whole plant images were taken for each genotype using Nikon digital camera (Nikon D70s, Nikon Inc. Japan). At least ten different plants for each genotype were measured. At the same stage, the average size of the leaf of each genotype were calculated. At least 70 rosette leaves from 10 different plants for each genotype were imaged.

The flowers of all stages were collected from a single florescence of each genotype and imaged using Zeiss dissection microscope (Zeiss Stemi 2000-C, West Germany). For the determination of silique size of the wild type and all the mutants, all the siliques of a branch were considered for measuring their lengths. Accordingly, the siliques were collected from each genotype and imaged with Zeiss dissection microscope (Zeiss Stemi 2000-C, West Germany). The number of seeds per silique were counted fixing the siliques in carnoy's solutions (ethanol: chloroform: glacial acetic acid = 6:3:1) (Chen et al., 2002) that allowed seed counting in the siliques making those transparent. The images of transparent siliques were captured using Zeiss dissection microscope (Zeiss Stemi 2000-C, West Germany).

The seedlings of all the phenotypes were grown in half strength MS media in petri dishes within the incubator under 22/18 ^{0}C day/night temperature, 11 hrs photoperiod with a light intensity of 130 μmolm^{-2}s^{-1} with a relative humidity 50% to 60%. At 3 DAG the seedlings were transferred to new petri dishes and at 4 DAG the petri dishes were turned at a 90^0 angle (Zou et al., 2016) to impose gravistimulation. At 4 DAG just before turning the petri dishes and every 2.5 hrs interval post gravistimulation, the images were taken using a Nikon digital camera. After 12.5 hrs post gravistimulation the absolute root growth and the curvature made by the elongated root with the primary root axis were documented in the images. For root hair and lateral root studies the seedlings were grown in the same conditions in same incubator. At 4 DAG the seedlings were transfer in new petri dishes and at 6 DAG the root hairs images were taken using Zeiss dissection

microscope (Zeiss Stemi 2000-C, West Germany). At 8 DAG the same seedlings were imaged with Nikon digital camera (Nikon D70s, Nikon Inc. Japan) for the lateral root study.

2.5 Estimation of chlorophyll and preparation of mesophyll cells for chloroplast counting

Chlorophylls a, b and total chlorophyll content of the leaves of all plants genotypes were determined spectrophotometrically by acetone extraction method (Wellburn, 1994) using a SmartSpec Plus spectrophotometer (Bio-Rad-Laboratories, Hercules, CA, USA). 4 days old leaves of each genotype were collected and chlorophyll contents were determined based on fresh weight of the leaves. The leaf samples were ground with a pre-chilled mortar and pestle using 80% (v/v) pre-chilled acetone (HPLC Grade; EMD Millipore, Darmstadt, Germany) and sand (EM Science, Merck KGaA, Darmstadt, Germany) until homogenized. The slurry was transferred to 50 ml falcon tube (VWR International; Radnor, PA, USA) and centrifuged at 4500 rpm for 10 minutes at 4^0C. The supernatant were transfer to the new tubes and based on spectrometer reading the chlorophyll was calculated using the equation of (Lichtenthaler and Wellburn, 1983).

The total number of chloroplast of the mesophyll cells in the leaf of each genotype were counted separating the individual mesophyll cell following the protocol described in (Possingham and Smith, 1972; Boffey et al., 1979). According to this protocol 4 day old leaves from 21 days old plants were fixed in Eppendorf tube containing 3.5% glutaraldehyde for one hr in the dark. After fixation, the glutaraldehyde was removed carefully using micro-pipette and added 0.1M Na_2EDTA (pH 9) to the tube up to covering the leaves. The tubes were heated at 60^0C temperature in a shaking water bath with 100 shakes/minute for 2 hrs. The prepared metal green samples were cooled in room temperature and stored them at 4^0C in the refrigerator. The next day a piece of each prepared leaf sample were taken on the slide containing a drop of Na_2EDTA and covered with coverslip. The sample under the coverslip was pressed gently but firmly with the blunt end of a scalpel. Then the slides were examined under confocal laser scanning microscope (ZEISS LSM 510 Confor2, Carl Zeiss, West Germany).

2.6 *In vitro* Pollen Germination

In vitro pollen germination was performed following the procedure described (Lee et al., 2008) with some modifications. The flowers were collected from each plant at 1-2 weeks after bolting for *in vitro* pollen germination. The pollens were germinated in liquid media containing 1 mM $CaCl_2$, 1 mM $Ca(NO_3)_2$, 1 mM $MgSO_4$ and 0.01% H_3BO_3 (pH 7). About 20 opened flowers per sample were taken in Eppendorf tube containing 500 µl pollen germination media, vortexed 30 seconds and centrifuged them for 4 minutes at 5000 rpm. The supernatant with all floral parts except pollens pellet were removed and the pollens were re-suspended in 100 µl of pollen germination media. The pollen suspensions were then spread to cell culture dishes (35mm x 12mm) containing pollen germination media. The dishes were placed in the dark and after 6 hrs post spreading the pollen, the pollen germinations were observed with Epifluorescence microscope (Zeiss Axioplan, Carl Zeiss, Germany). The pollen germination rate were calculated from direct observation of pollen germination through microscope.

2.7 Aniline blue staining of pollen tube in pistil

The visualization of pollen tubes in pistils were achieved by aniline blue staining following the protocol described (Wu et al., 2010) with some modifications. The self-pollinated flowers from the wild type, the double mutant and both the single mutants were collected and pistils were removed from the flowers emasculating by dissecting forceps. The pistils were then taken in the Eppendorf tubes containing the fixative (ethanol:acetic acid = 3:1) and fixed for 3 hours at room temperature. The fixed pistils were softened in 8 M NaOH overnight after three consecutive wash of 10 minutes each with distilled water. After softening, the pistils were washed three times for 1 hrs each wash with distilled water. After washing, the pistils were stained with aniline blue solution containing 0.1% aniline blue in 0.1 M K_2HPO_4-KOH buffer (pH 11) for 3 hrs. The pistils were then taken on the slides containing a drop of 0.1 M K_2HPO_4-KOH buffer (pH 11) and covered with coverslip carefully to avoid damage of super soft pistils. The slides contained pistils were then studied with Epifluorescence microscope (Zeiss Axioplan, Carl Zeiss, Germany) and images were taken under UV light.

2.8 Development of GFP-ABD2-GFP expressing lines under genetic background of all mutants

With a view to visualize the actin cytoskeleton organizations inside the cells GFP tagged actin binding domain2 of fimbrin protein (GFP-ABD2-GFP) expressing lines under genetic background of all the mutants were developed. The reciprocal crossings were performed artificially between GFP-ABD2-GFP expressing Col-0 (Col-0/ GFP-ABD2-GFP) and each mutant. In case of *fh1-1* mutant following crossing, F2 generation plants were screened first for GFP expression with confocal microscope (Zeiss LSM510 META). From the GFP-ABD2-GFP expressing plants, *AtFH1* insertion mutation was confirmed using gene specific and insertion specific T-DNA border primers pairs. In case of *fh1-1/arp3-1* double mutant and *arp3-1* single mutant, *AtARP3* mutation was confirmed first by screening distorted trichome phenotype. Then screened with confocal microscope for GFP-ABD2-GFP expressions. At last distorted trichomes containing GFP-ABD2-GFP plants of the double mutant were screened for *AtFH1* mutation using gene specific and insertion specific T-DNA border primers pairs. The GFP expressing line Col-0/GFP-ABD2-GFP under genetic background of the wild type, *fh1-1/arp3-1*/ GFP-ABD2-GFP under genetic background of the double mutant (*fh1-1/arp3-1*), *fh1-1*/ GFP-ABD2-GFP under genetic background of *fh1-1* single mutant and *arp3-1*/ GFP-ABD2-GFP under genetic background of *arp3-1* single mutant were grown in the growth chamber under 22/18 ^{0}C day/night temperature, 16 hrs photoperiod with a light intensity of 130 μmolm^{-2}s^{-1} within a relative humidity 60% to 70% for subsequent analysis.

2.9 Confocal laser scanning microscopy

The leaves were collected from 18 days old plants of the wild type, the double mutant and both the single mutant and were incubated 10 to 15 minutes in 0.1mg/ml propidium iodide (PI) in water at room temperature (Falbel et al., 2003). After incubation the leaves were taken in slides containing a drop of water and studied under confocal laser scanning microscope (ZEISS LSM 510 Confor2, Carl Zeiss, West Germany) with HeNe1 laser using PI fluorochrome spectra (excitation/emission = 535nm/617nm). The images of epidermal pavement cells were taken from the abaxial side of the leaves.

All the actin cytoskeleton images were taken with the confocal laser scanning microscope using argon laser with GFP fluorochrome spectra (excitation/emission = 488nm/510nm). The leaves from the GFP expressing lines of the wild type, the double mutant and both the single mutants were collected from 18 days old plants and actin cytoskeleton organizations within the epidermal pavement cells were studied under confocal laser scanning microscope (ZEISS LSM 510 Confor2, Carl Zeiss, West Germany). The Z-stack images of almost all the clear optical sections within the pavement cells were taken. The actin cytoskeleton organizations in mature leaf trichome cells were studied by confocal laser scanning microscope. The leaves from three week old plants were collected and Z-stack images of all clearly visible optical sections within the trichome cells were captured.

The Z-stack images of fixed and separated leaf mesophyll cells of the wild type, the double mutant and both the single mutants were taken with confocal laser scanning microscope using argon laser and chloroplast auto-fluorescent. 4 days old leaves from three week old plants of all GFP expressing lines were collected to study the actin cytoskeleton organizations within the leaf mesophyll cells. Z-stack images of clearly visible optical sections within the mesophyll cells were taken with confocal microscope (ZEISS LSM 510 Confor2, Carl Zeiss, West Germany).

2.10 Scanning electron microscopy

Leaves with mature trichomes of the wild type, the double mutant and both the single mutants were prepared following the protocol (Talbot and White, 2013). According to this protocol the leaves were fixed in the 6 well culture plates containing 100% methanol for 10 minutes plus about 2 minutes taken to sink the leaves in methanol. Then the methanol was removed with a micro-pipette and 100% ethanol were added to the culture plates for 2 hrs followed by 2 changes of 100% ethanol for 30 minutes each. After that critical point drying (CPD) was performed following the manufacturer protocol. Following CPD the leaf samples were carefully but quickly placed (facing the adaxial part of the leaves up) over the double sided tape on the sample stubs and gold/palladium coating were done immediately to avoid absorbing the moisture by the samples. The trichomes of the coated samples were imaged by Phenom G2 desktop scanning electron microscope. For pollen

images, anther from the wild type, the double mutant and both the single mutants were collected from the open flower using dissecting forceps. The pollens were released by gently tapping the anther onto the double sided taps stuck on the sample stubs. The samples were dehydrated for one hours and the images were taken using scanning electron microscope (Phenom G2 desktop, Phenom-world, Eindhoven, Netherlands).

2.11 Image analysis and measurement

All the images were analyzed with Fiji ImageJ software (https://imagej.net/ImageJ). Whole plant images were analyzed for plant sizes or total green areas of the plants, the leaves images were analyzed for leaf size, root images of the seedlings were analyzed for root growth rate, root thickness, root curvature, root hair length and density, the mature siliques images were analyzed for silique sizes, the pavement cells images were analyzed for pavement cell sizes, Individual mesophyll cells were analyzed for counting the chloroplast in each mesophyll cells. Every maximum projection image was produced from each Z-stack series of images like Z-stack series of pavement cells, trichome cells, mesophyll cells and individual separated mesophyll cells and guard cells.

2.12 Statistical analysis

All the statistical analyses were performed using One Way ANOVA for Means, Standard deviations of the means and Standard errors of the means. The multiple comparison tests were performed by Holm-Sidak multiple comparison test. All the replicable experiment were done with triplicate and each replication was analyzed statistically. For plant size and leaf size measurement, at least ten different plants for each genotype were measured. At the same stage, the average size of the leaf of each genotype were calculated. At least 70 rosette leaves from 10 different plants for each genotype were measured. The analysis of silique size was performed considering 300 siliques per genotype. To determine the seed content per silique, 300 siliques were taken for each genotype to count their average seed content of the siliques. About 50 seedlings were considered to measure and analyze the root growth rate, root thickness, root curvature upon gravistimulation and lateral root density. The length and density of root hair considering at least 300 root hairs per genotype. For determination of pavement cell circularity at least 50 leaf epidermal pavement cells were

measured and analyzed. For chloroplast estimation and analyzed at least 30 separated individual mesophyll cells were considered. For *in vitro* pollen germination rate about 1000 pollens per genotype were counted for analysis.

CHAPTER 3: RESULTS

3.1 Development of the *fh1-1/apr3-1* double mutant

The double mutant [*fh1-1*/*apr3-1*] under the present study is a heterozygous double mutant that possessed heterozygous mutant for *AtFH1* (AT3G25500) gene and homozygous mutant for *AtARP3* (AT1G13180) gene. The SALK mutant lines of *AtFH1, fh1-1* (SALK_071705) and *AtRP3, apr3-1* (SALK 010045) were collected from TAIR and their homozygosities were confirmed by double PCR using gene specific primers and mutant specific insertion primers. The insertion point in the *fh1-1* mutant is in the promoter region within 300 bp upstream of *AtFH1* gene, whereas the *apr3-1* mutant contains the insertion within the 5th intron from the 5' end of *AtARP3* coding sequence (Figure 3.1). The RT-PCR result showed some expressions of *AtFH1* gene in *fh1-1* single mutant (Figure 3.2) indicating that the *fh1-1* mutant is not fully knocked out. The qRT-PCR results revealed that *AtFH1* expression was 2.73 fold down regulated in *fh1-1* single mutant and 1.66 fold down regulated in *fh1-1*/*apr3-1* double mutant compared to the wild type expression of *AtFH1*. The distorted trichome phenotype further confirmed that both *apr3-1* single and *fh1-1*/*apr3-1* double mutant were truly knocked out for *AtARP3* gene.

These two mutant lines were crossed and screened for the homozygous double mutant in F3 generation. After a long series of screening through hundreds of PCRs, homozygous double mutant was not found. Following F3 generation, several generations were screened, but the results were same. Double heterozygotes were obtained and those plants were phenotypically in the middle of *fh1-1/apr3-1* and wild type with normal trichomes. After all screenings, a double mutant harboring homozygous mutation for *AtFH1* and heterozygous for *AtARP3* genes was also not found. That suggests that in absence of *AtARP3* gene, homozygous mutation of *AtFH1* has lethal effect on the plant life cycle. So, we selected *AtFH1* partial knockout and *AtARP3* complete knockout double mutant (hereafter referred to as *fh1-1/apr3-1*) and both the single mutants for this study. Wild type Col-0 ecotype was used as the control under this study.

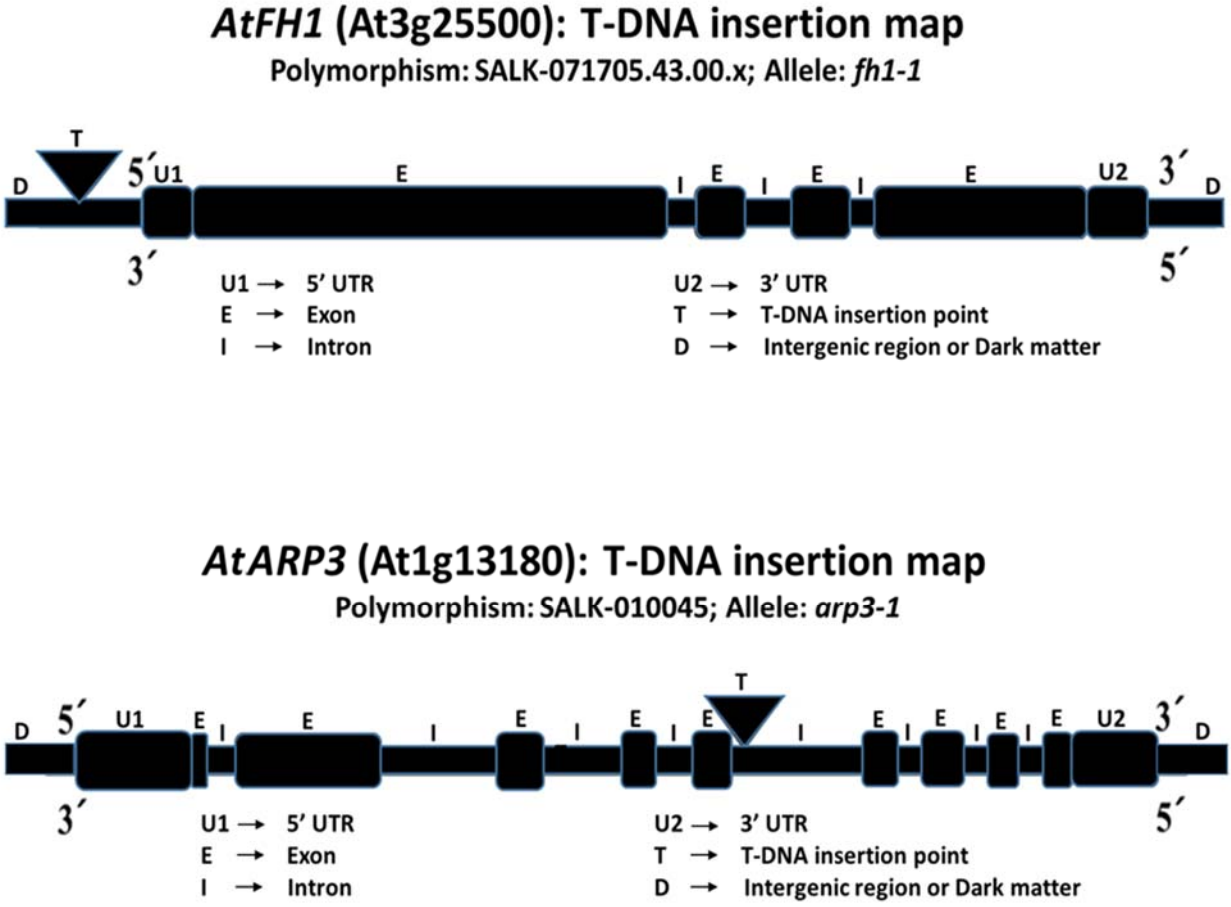

Figure 3.1: Gene structure of *AtFH1* and *AtARP3* showing the T-DNA insertion points.

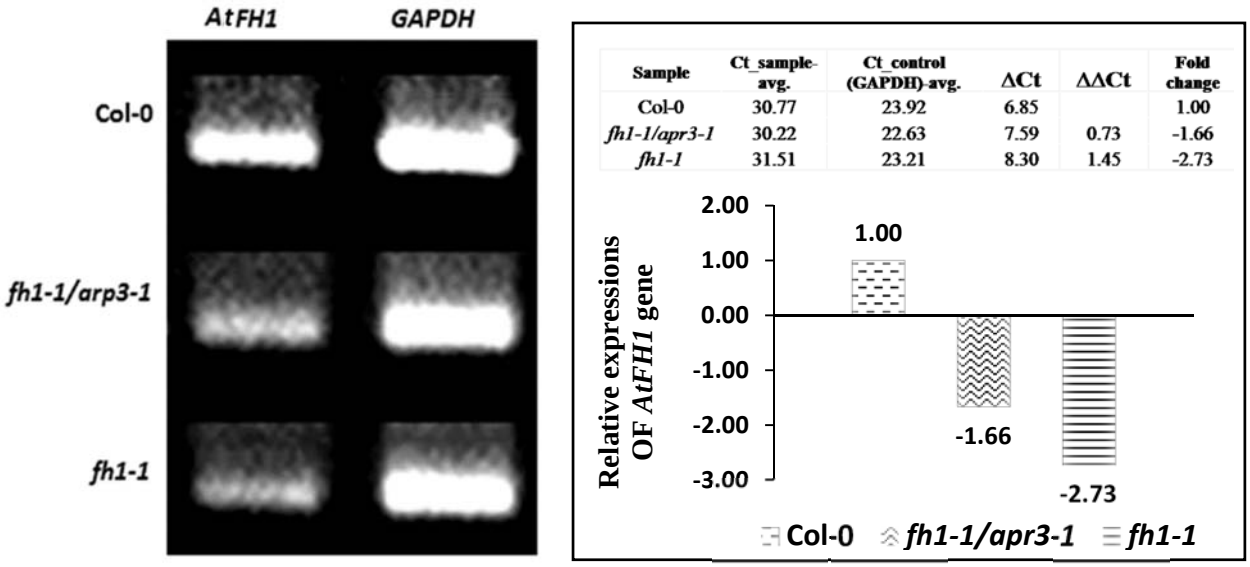

Figure 3.2: The relative expressions of *AtFH1* gene detected through RT-PCR (A) and qRT-PCR (B) in the wild type (Col-0), the double mutant (*fh1-1*/*apr3-1*) and the formin1 single mutant (*fh1-1*). GAPDH was used as reference gene for normalization of the expressions.

3.2 The distinct phenotypes of the actin cytoskeleton disrupted mutants

On phenotypic observations, *fh1-1/arp3-1* mutant produced small plants (less than half of the wild type at the rosette leaf stage) with short, narrow and pale green leaves compared to wild type and both the single mutants (Figure 3.3). The number of rosette leaves of *fh1-1/arp3-1* plants was similar to the wild type but the length of the petioles was shorter and the shape of the leaves was mostly oval with sharp serrations at the edge of the leaf blades (Figure 3.3). The mature plants of the double mutant were less branched with short siliques, some of which lacked seeds whereas the wild type and both the single mutants produced similar highly branched plants with plenty of normal siliques containing enough seeds (Figure 3.4). At the rosette leaf stage the average size of the whole plants of *fh1-1/arp3-1* mutant was 9.41±0.33 mm^2 which was less than half of wild type and *fh1-1* mutant and two third of *arp3-1* mutant plants (Figure 3.5). The average rosette leaf size of the double mutant was 1.45±0.03 mm^2 that was significantly smaller than wild type (3.67±0.06 mm^2), and single mutants *fh1-1* (3.39±0.06 mm^2) and *arp3-1* (2.71±0.06 mm^2) (Figure 3.6). There was no significant difference in whole plant sizes between *fh1-1* single mutant and the wild type, but the *arp3-1* mutant produced significantly smaller plants compared to the wild type and *fh1-1*

single mutant at the rosette leaf stage (Figure 3.5). All the mutants and the wild type plants produced significantly different sizes of the rosette leaves under the present study.

Figure 3.3: Morphology of the plants at 3 weeks of plant age (rosette leaf stage). All plants were grown in the same growth chamber in 16/8 hours day/night condition with a relative humidity 60% to 70%.

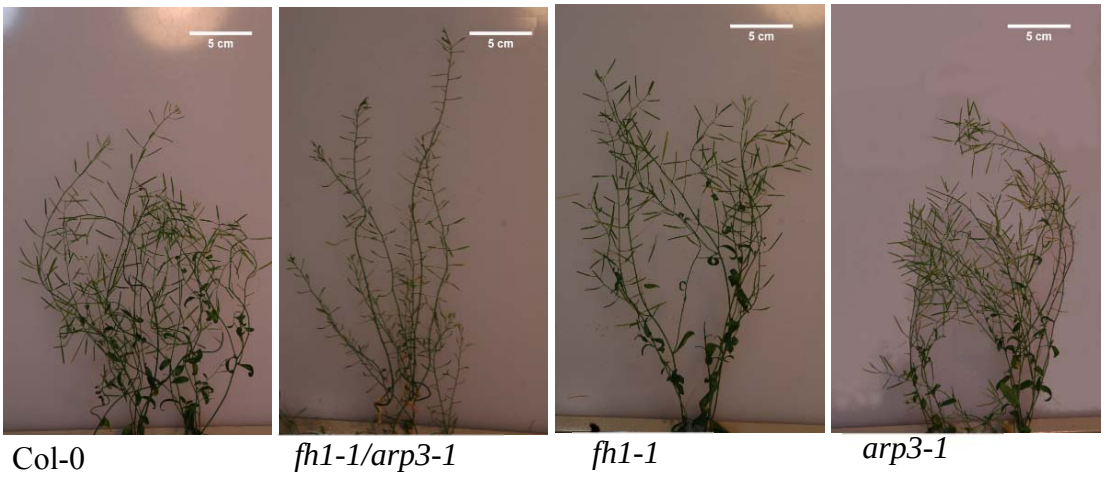

Figure 3.4: Stem Morphology of mature wild-type and mutant plants at the age of 8 weeks.

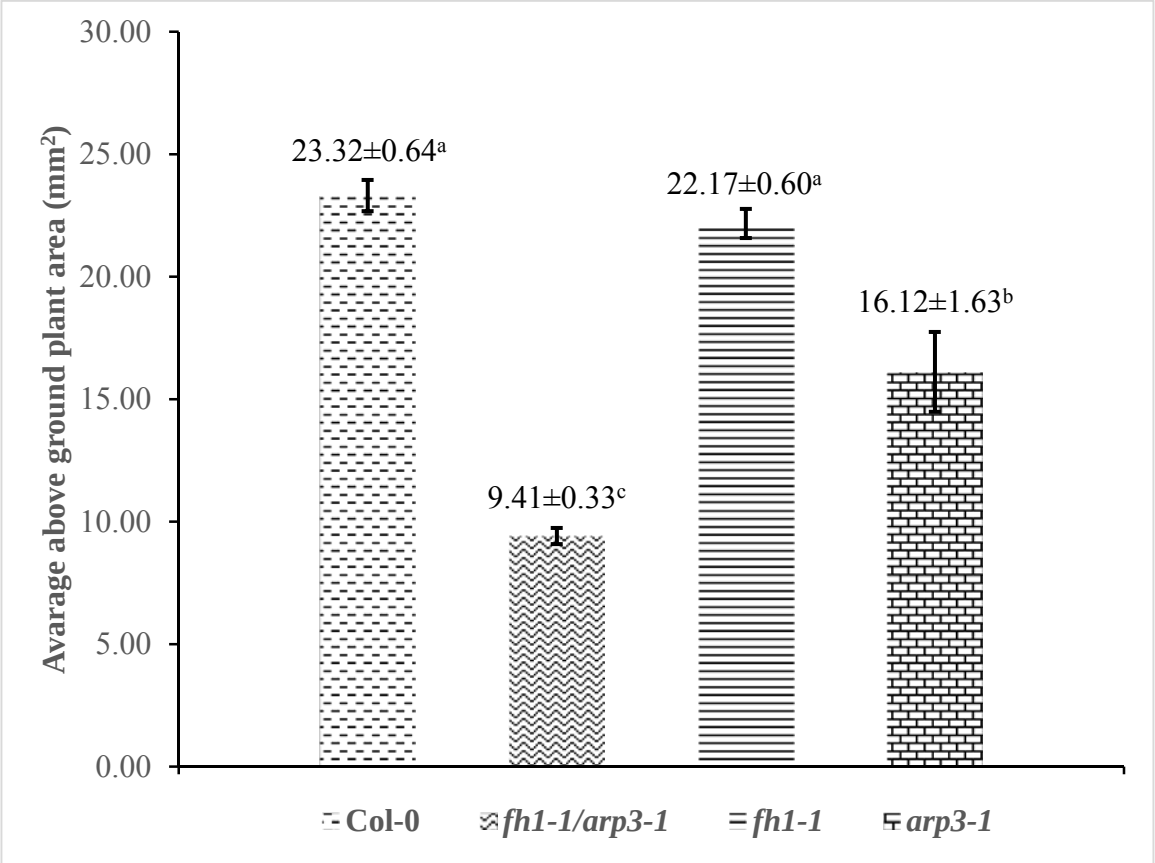

Figure 3.5: The histogram shows the average area of the whole plant (total green area) at rosette leaf stage. Total green area was measured from the image using ImageJ software. At least 32 plants for each line were measured. For statistical analysis, One way ANOVA with Holm-Sidak multiple comparison method was used. The error bars represent the standard error of the means.

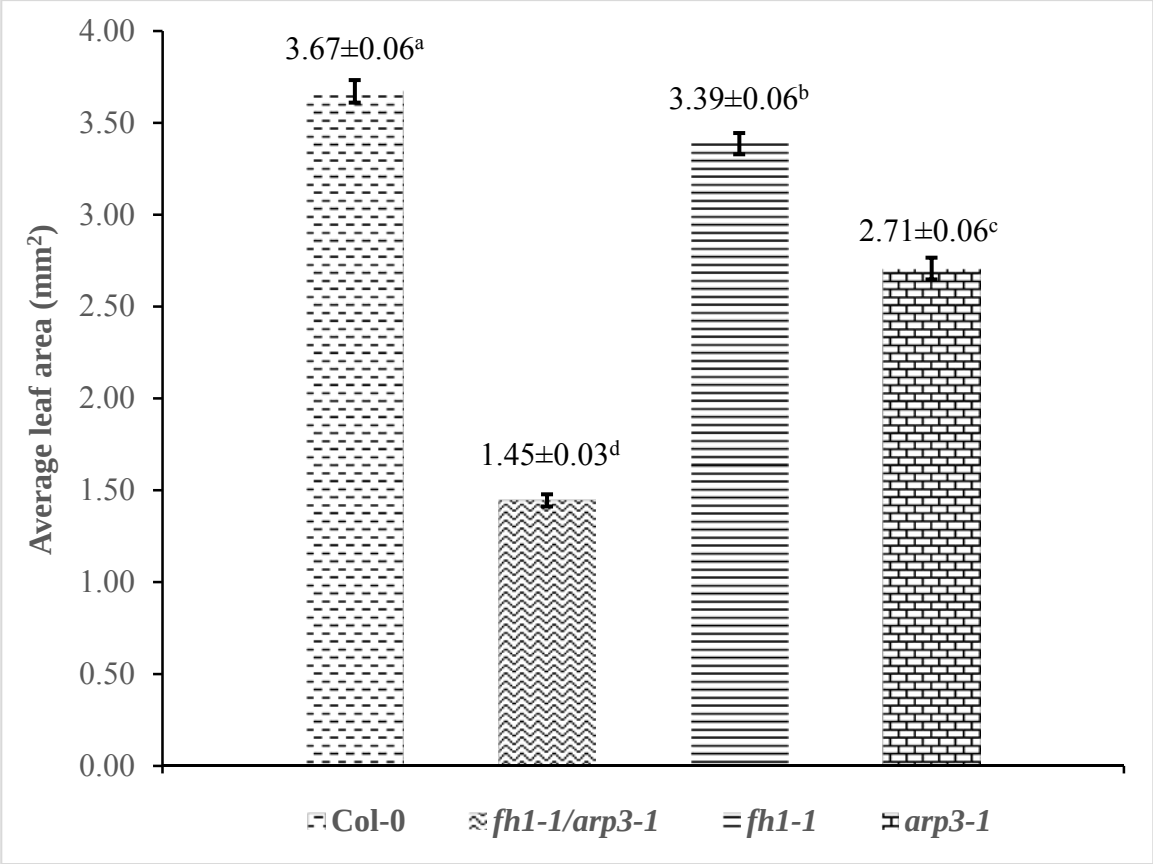

Figure 3.6: The histogram shows the average rosette leaf size of the wild type, the double mutant and both the single mutants. ImageJ softwar was used to measure the leaf size from the leaf images. At least 72 leaves from each line were used for calculation. One way ANOVA with Holm-Sidak multiple comparison method was used for statistical analysis. The error bars exhibit the standard error of the means.

3.3 Aberrant root growth of the actin cytoskeleton disrupted mutants

3.3.1 Root phenotype and root growth rate

Seedlings of the *fh1-1/arp3-1* mutant line exhibited a short root phenotype compared to the Col-0 wild type controls, as well as the other single mutants (*fh1-1* and *arp3-1*) (Figure 3.7). At 4 DAG (days after germination) the primary root growth rate of *fh1-1/arp3-1* was an average of 0.20 mm/hr less than Col-0 wild type and *fh1-1* and *arp3-1* single mutant seedlings (Figure 3.8). In addition, primary roots of the double mutant were on average 0.1 mm thicker in diameter compared

to *fh1-1* and *arp3-1* single mutants and wild type seedlings (Figure 3.9). a*rp3-1* single mutant and the double mutant also produced 2-3 lateral roots per seedling, whereas the *fh1-1* single mutant and wild type seedlings did not produce any lateral roots (Figure 3.7). The root growth rate in the *arp3-1* mutant was 0.40 mm/hr that is significantly higher than all other plants under the present study. There were also no significant differences in root growth rate between *fh1-1* and wild type plants (Figure 3.8).

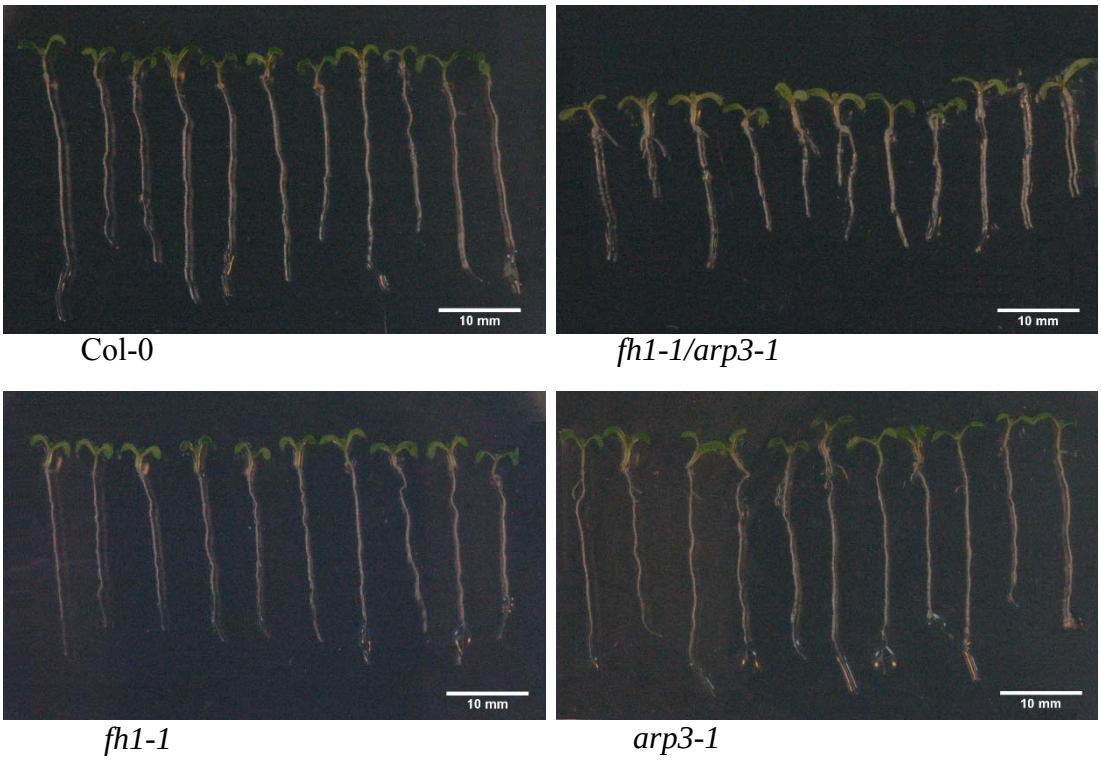

Figure 3.7: Root growth phenotypes of the wild type (Col-0), the double mutant (*fh1-1/arp3-1*) and both the single mutants (*fh1-1* and *arp3-1*) at 4 days after germination (DAG). The seedlings were grown in petridishes and at 4 DAG the images were captured with a Nikon digital camera.

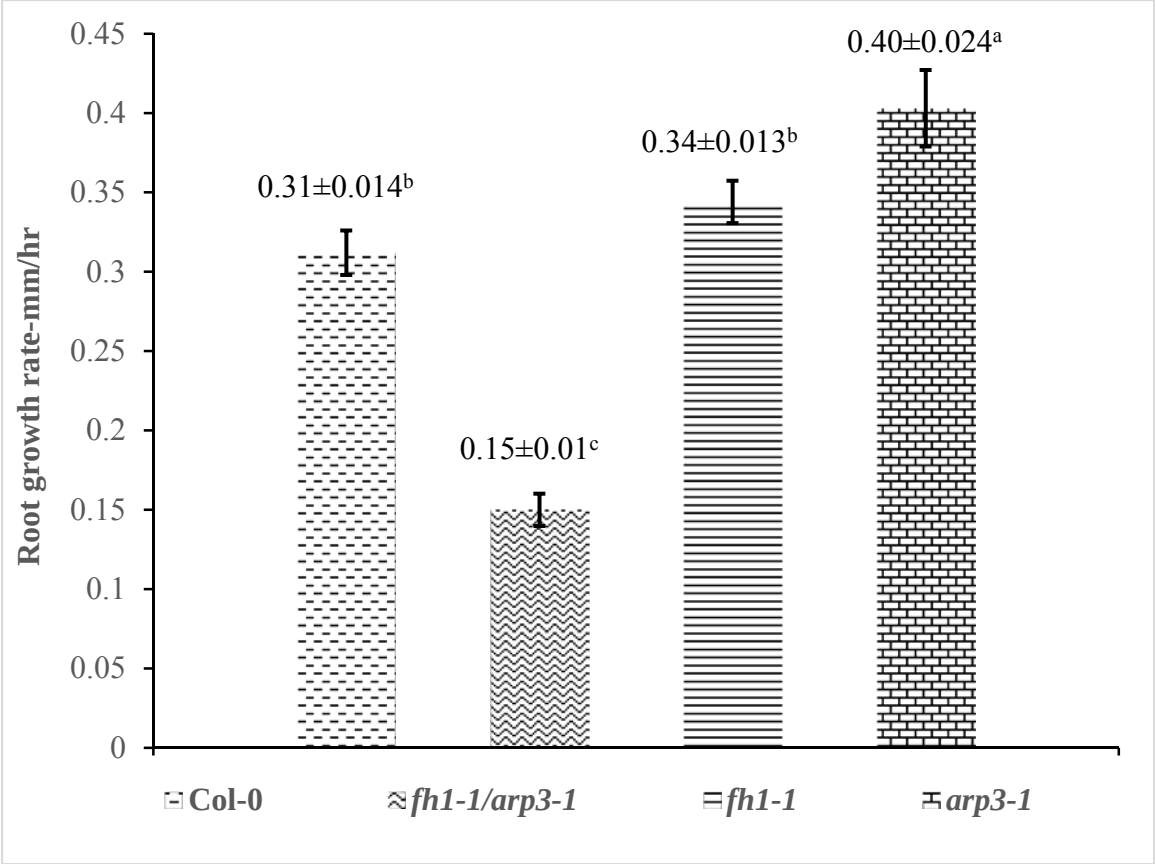

Figure 3.8: The histogram shows the average root growth rate. The absolute root length of 12.5 hours post gravistimulation was measured from the image (taken within different intervals) using ImageJ software and the average root growth rate was calculated. Around 50 seedlings per line were measured for this calculation. One way ANOVA with Holm-Sidak multiple comparison method was used for statistical analysis. The error bars represent the standard error of the means.

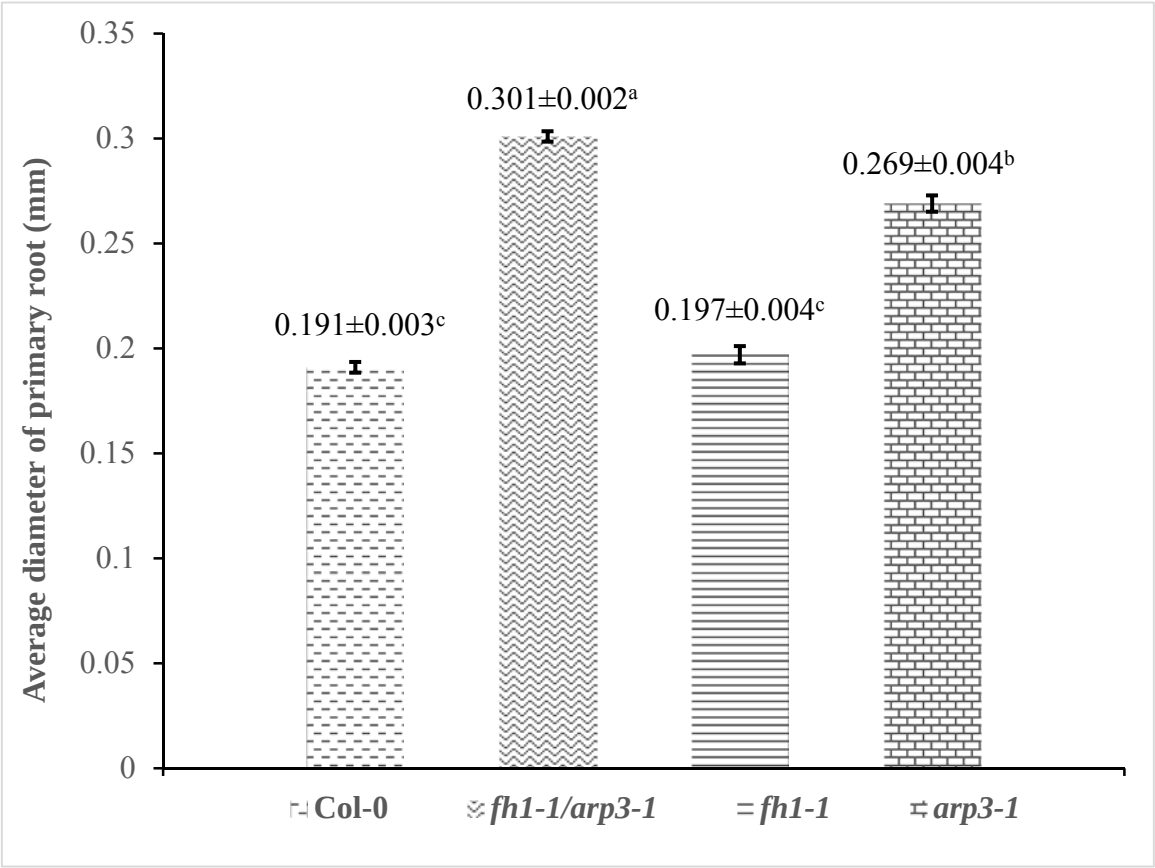

Figure 3.9: The histogram shows the average thickness of the roots of the seedlings at 4 DAG. The thickness of roots was measured from the images (taken by Zeiss dissection microscope) using ImageJ software. Around 50 seedlings per line were measured for this calculation. One way ANOVA with Holm-Sidak multiple comparison method was used for statistical analysis. The error bars show the standard error of the means.

3.3.2 Gravitropic response

The gravistimulation on the seedlings grown in half strength MS media under 22/18 ^{0}C day/night temperature, 11 hr photoperiod with a light intensity of 130 µmolm^{-2}s^{-1} was imposed by turning the petri dishes at a 90^0 angle (Figure 3.10). After gravistimulation 90^0 angle of root tip with the vertical axis of the root considered as the highest gravitropic response and the deviation of root tip angle (either positive or negative) is negatively correlated with gravitropism. At 12.5 hrs post gravistimulation *fh1-1/arp3-1* seedlings showed the highest gravitropic responses producing (90 + 18.98)^0 angle of the root tip with the vertical axis of the roots. The *fh1-1/arp3-1* seedlings showed

an average 18.98^0 deviation from 90^0 that was the lowest deviation in root tip angle compared to wild type (Col-0) and *fh1-1*, *arp3-1* single mutants that showed 28.88^0, 28.64^0 and 30.79^0 average deviation respectively (Figure 3.11). The *fh1-1* single mutant and the wild type exhibited almost similar average deviation whereas *arp3-1* showed slightly higher deviation from 90^0 in root tip angle, but statistically they had no significant difference (Figure 3.11). Only *fh1-1/arp3-1* showed the deviation in root tip angle from 90^0 that was significantly different from wild type and both single mutants.

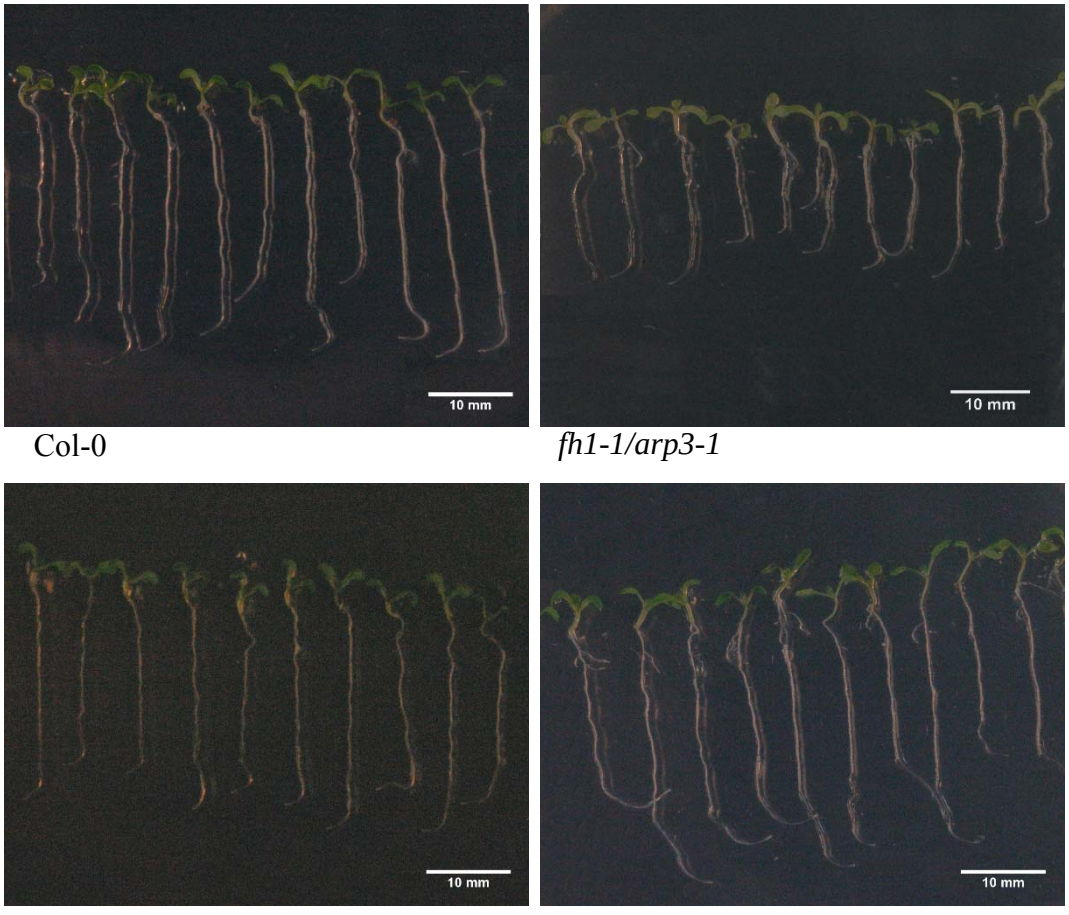

Col-0 *fh1-1/arp3-1*

fh1-1 *arp3-1*

Figure 3.10: The root tip curvature at 12.5 hrs post gravistimulation in the wild type, the double mutant and both the single mutants. The images were taken by Nikon digital camera.

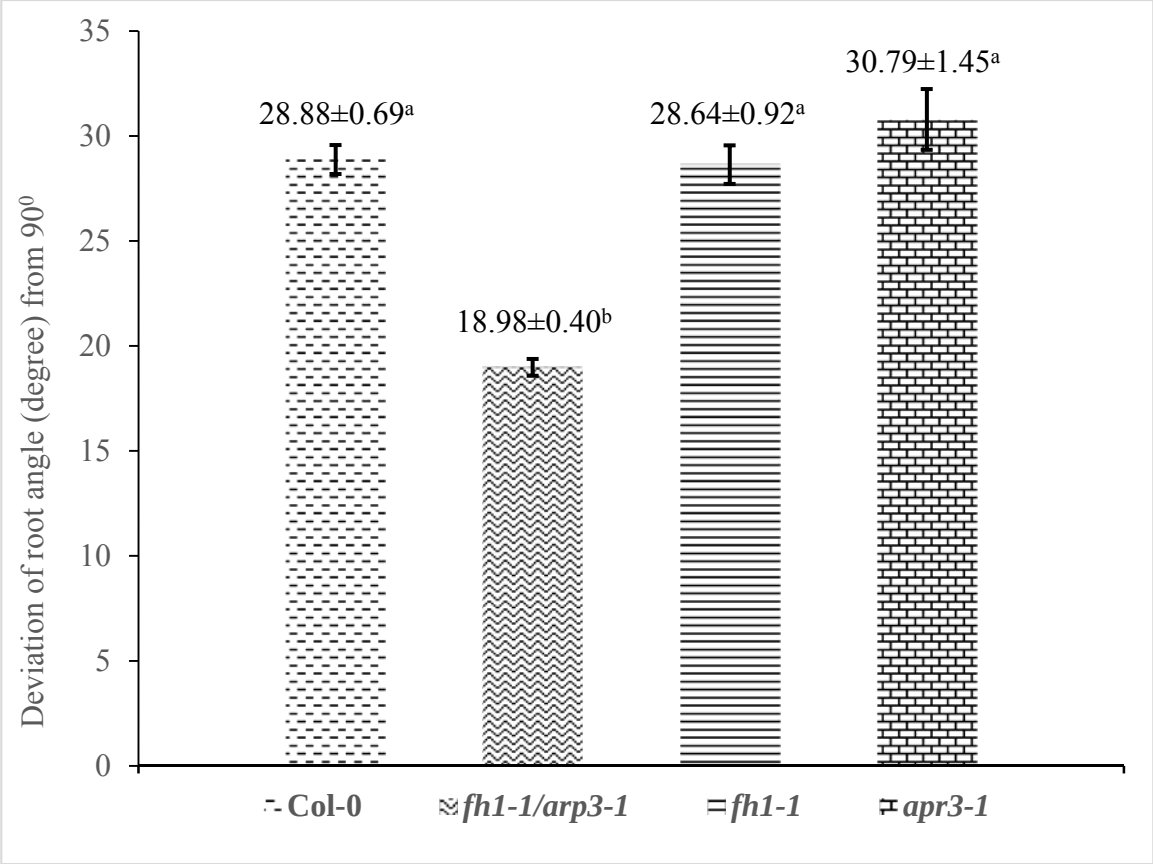

Figure 3.11: The histogram shows the average root tip angles formed with the primary root axis within 12.5 hrs post gravistimulation. The root tip angles were measured from the seedling images using ImageJ software and around 50 seedlings per line were used for the calculation. One way ANOVA with Holm-Sidak multiple comparison method was used for statistical analysis. The error bars represent the standard errors of the means.

3.3.3 Root hair structure and density

The seedlings were grown in petri dishes containing half strength MS media within controlled growth chamber under 22/18 ^{0}C day/night temperature, 11 hr photoperiod with a light intensity of 130 µmolm^{-2}s^{-1}. At 6 DAG root hair length and density of the double mutant *fh1-1/arp3-1*, wild type Col-0 and both single mutants *fh1-1*, *arp3-1* seedlings were studied by taking the images with dissection microscope (Figure 3.12). The average root hair length of *fh1-1/arp3-1* double mutant was 0.219 mm that was significantly shorter than wild type and both *fh1-1*, *apr3-1* single mutants which had average root hair length 0.31 mm, 0.369 mm and 0.26 mm respectively (Figure 3.13). The average root hair lengths of all the mutants and wild type were significantly different from

each other. Both the double mutant and *arp3-1* single mutant exhibited same root hair density of 15 root hair per mm root length that was significantly lower than wild type and *fh1-1* single mutant (Figure 3.14). The *fh1-1* single mutant produced the densest 21 root hair per mm that was also significantly higher than wild type with a root hair density of 19 root hair per mm (Figure 3.14).

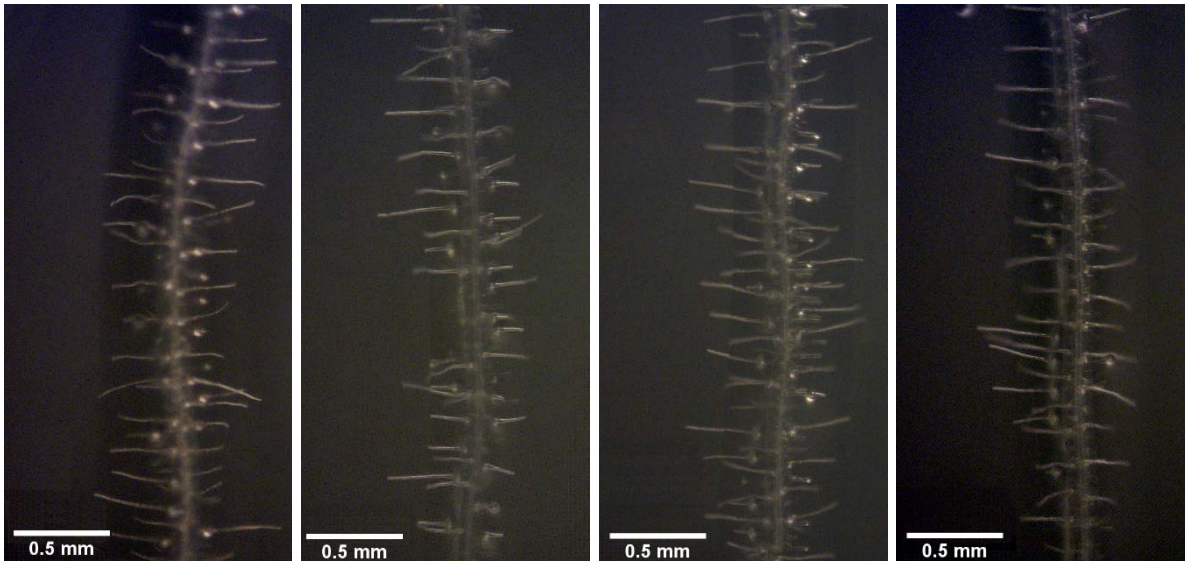

Col-0 *fh1-1/arp3-1* *fh1-1* *arp3-1*

Figure 3.12: The root hairs length and density in primary roots of the wild type, the double mutant and both the single mutants at 6 DAG. The seedlings were grown in half strength MS media in petridishes and at 6 DAG root hairs images were taken with Zeiss dissection microscope (Zeiss Stemi 2000-C, West Germany).

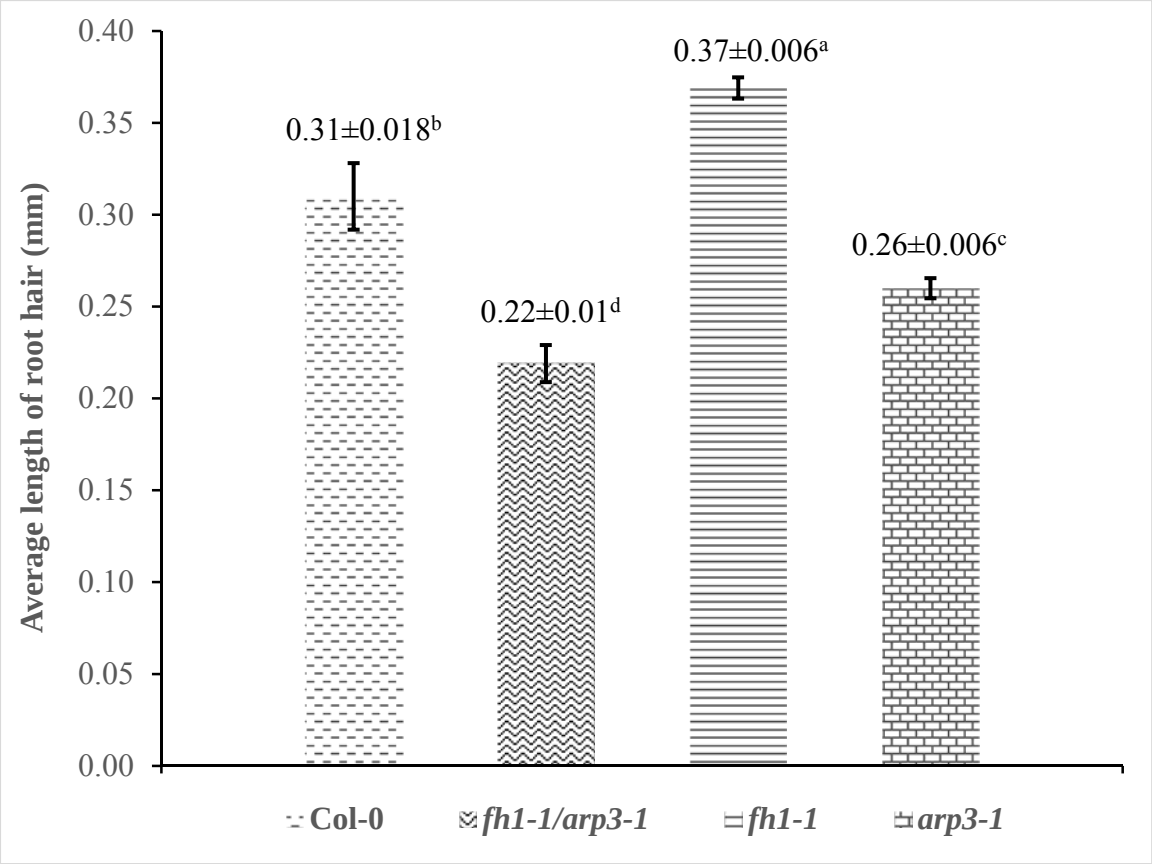

Figure 3.13: The histogram shows the average root hair length. From the root hair images which were taken at 6 DAG of the seedlings of the wild type, the mutants, the length of the root hairs were measured using imageJ software. At least 300 root hairs from images of twelve different seedlings were counted for this calculation. One way ANOVA with Holm-Sidak multiple comparison method was used for statistical analysis. The error bars stands for the standard errors of the means.

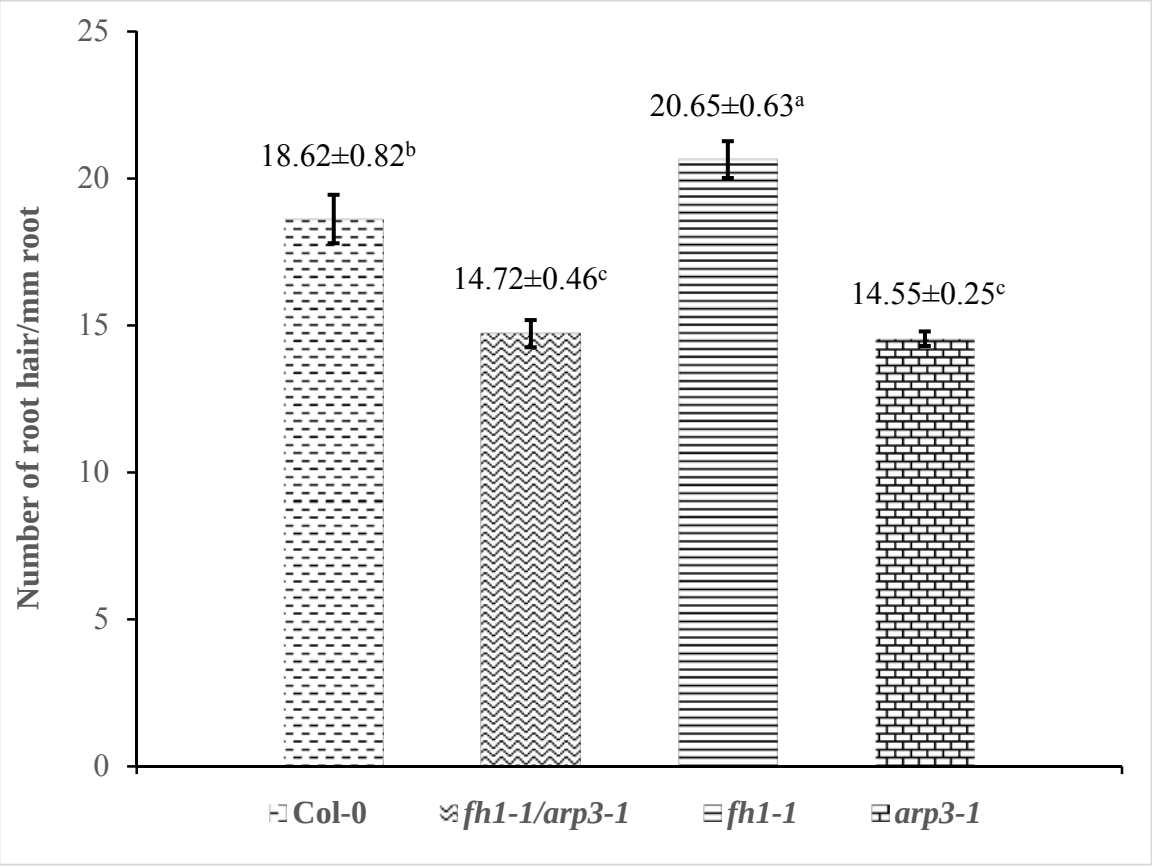

Figure 3.14: The histogram shows the average root hair density per mm length of root. From the root hair images that were taken at 6 DAG of the seedlings, the density of the root hairs was calculated using ImageJ software. About 50 mm length of primary root from 12 different seedlings of each line were considered for calculation of root hair density. One way ANOVA with Holm-Sidak multiple comparison method was used for statistical analysis.The error bars represent the standard errors of the means.

3.3.4 Lateral root development and location

All the mutants and wild type seedlings were grown in half strength MS media within the controlled environment of 22/18 ^{0}C day/night temperature, 11 hr photoperiod with a light intensity of 130 μmolm^{-2}s^{-1} in the growth chamber. At 8 DAG of the seedlings, the double mutant *fh1-1/arp3-1* produced distinguishable lateral root phenotype (Figure 3.15). In this double mutant the lateral roots were emerged in a bunch from the root shoot junction and were distributed within one-third region from the base of the primary roots. Both the single mutants and the wild type

plants produced lateral root along the whole length of primary root mostly in alternate arrangements (Figure 3.15). The average lateral root density was 5.58 in *fh1-1/arp3-1* seedlings the was lowest number compared to both *fh1-1* and *arp3-1* single mutants and the wild type bearing the lateral root densities of 8.78, 13.68 and 11.38 respectively (Figure 3.16). The lateral root densities were significantly different among all the mutants and the wild type seedlings.

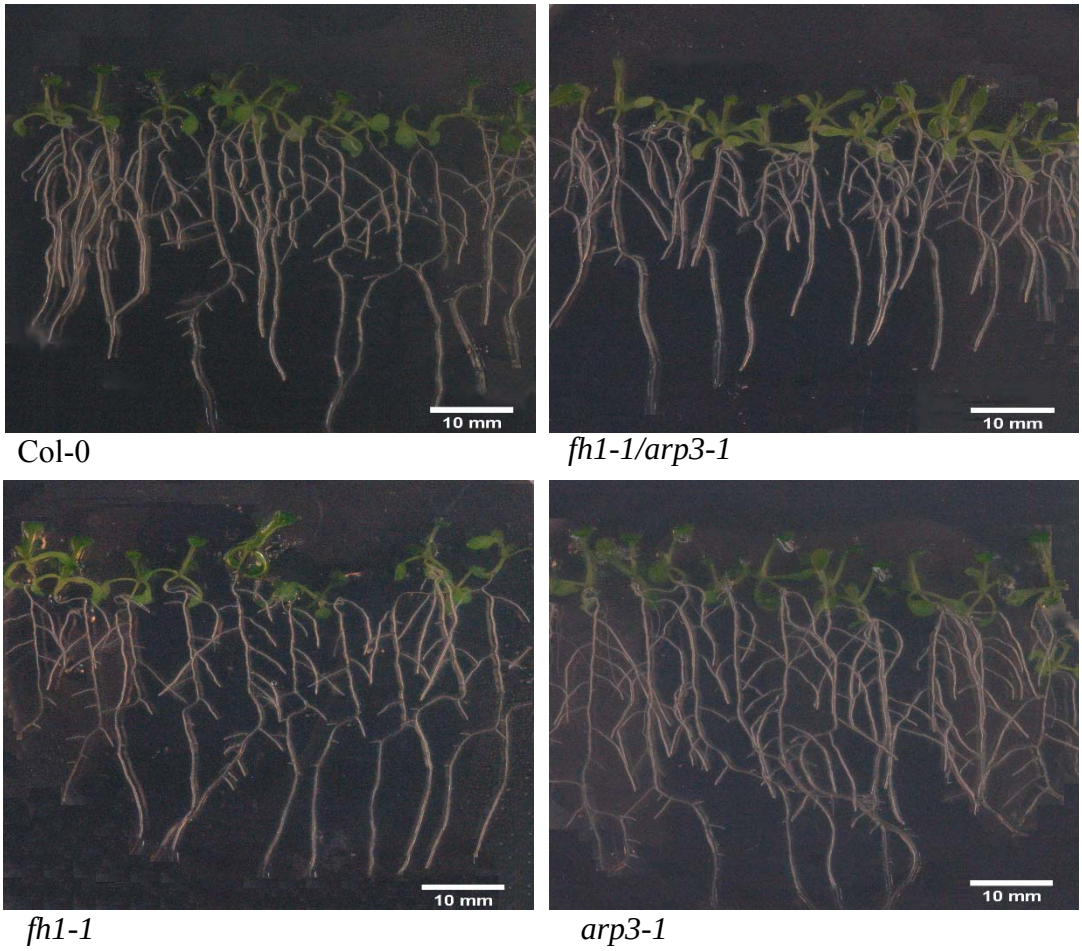

Figure 3.15: The images show the lateral roots number and location. The seedlings were grown in half strength MS media. At 8 DAG the seedlings were observed and images were taken with Nikon digital camera for secondary or lateral root growth.

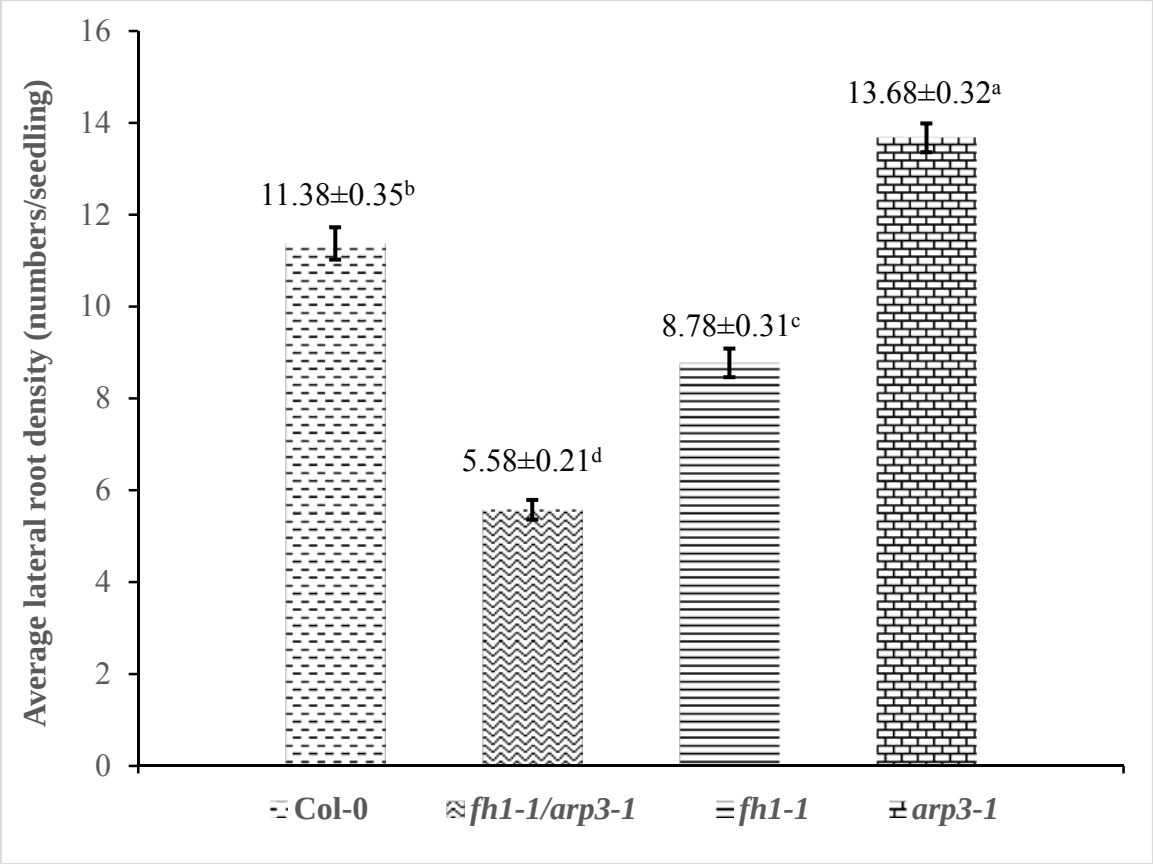

Figure 3.16: The histogram shows the average lateral root density at 8 DAG of the seedlings. The number of total lateral roots per seedling was counted from the images. At least 40 seedlings per line were used to calculate the number of lateral roots. One way ANOVA with Holm-Sidak multiple comparison method was used for statistical analysis. The error bars show the standard errors of the means.

3.4 Changes in cellular structures of the actin cytoskeleton disrupted mutants

3.4.1 Leaf epidermal pavement cells

Both the double mutant *fh1-1/arp3-1* and *fh1-1* single mutant produced elongated lobes with jigsaw puzzle shape indentations resulting in decreased circularity in the leaf epidermal pavement cells (Figure 3.17). Although the wild type plants produced some increased circularity 0.0083 in the pavement cells, but statistically there was no difference in circularity of leaf epidermal pavement cells among the double mutant *fh1-1/arp3-1*, single mutant *fh1-1*, or the wild type

Arabidopsis producing an average pavement cell circularity 0.0078 (Figure 3.18). *arp3-1* mutant produced highest circularity 0.0102 that was significantly different than both the double mutant and *fh1-1* single mutant (Figure 3.18). The average circularity of wild type cells was in between the double mutant and *arp3-1* mutant and hence also had no significant difference with the pavement cell circularity of *arp3-1* compared to the wild type (Figure 3.18). The difference in pavement cells circularity between *fh1-1/arp3-1* and Col-0 was not statistically significant, although the average pavement cell circularity of *fh1-1/arp3-1* was higher with elongated lobbing than that of wild type (Col-0).

Since both *AtARP3* and *AtFH1* are responsible for actin cytoskeleton polymerization, we investigate the actin cytoskeleton organizations and distributions using actin cytoskeleton marker lines in the wild type, the double mutant and both the single mutants. The epidermal pavement cells of wild type showed a densely compact actin filament network distributed through each individual pavement cell whereas in the *fh1-1/arp3-1* double mutant, the actin cytoskeletons were absent in most of the areas of pavement cells (Figure 3.19). In addition, in the double mutant few acting filaments crosslinked with each other and were distributed irregularly in the pavement cells. The *arp3-1* single mutant exhibited thick actin filament bundle, but no obvious actin cytoskeleton network owing few long actin filaments irregularly and un-uniformly distributed in the pavement cells. The *fh1-1* single mutant produced loose and thin actin cytoskeleton network comparing to wild type (Figure 3.19).

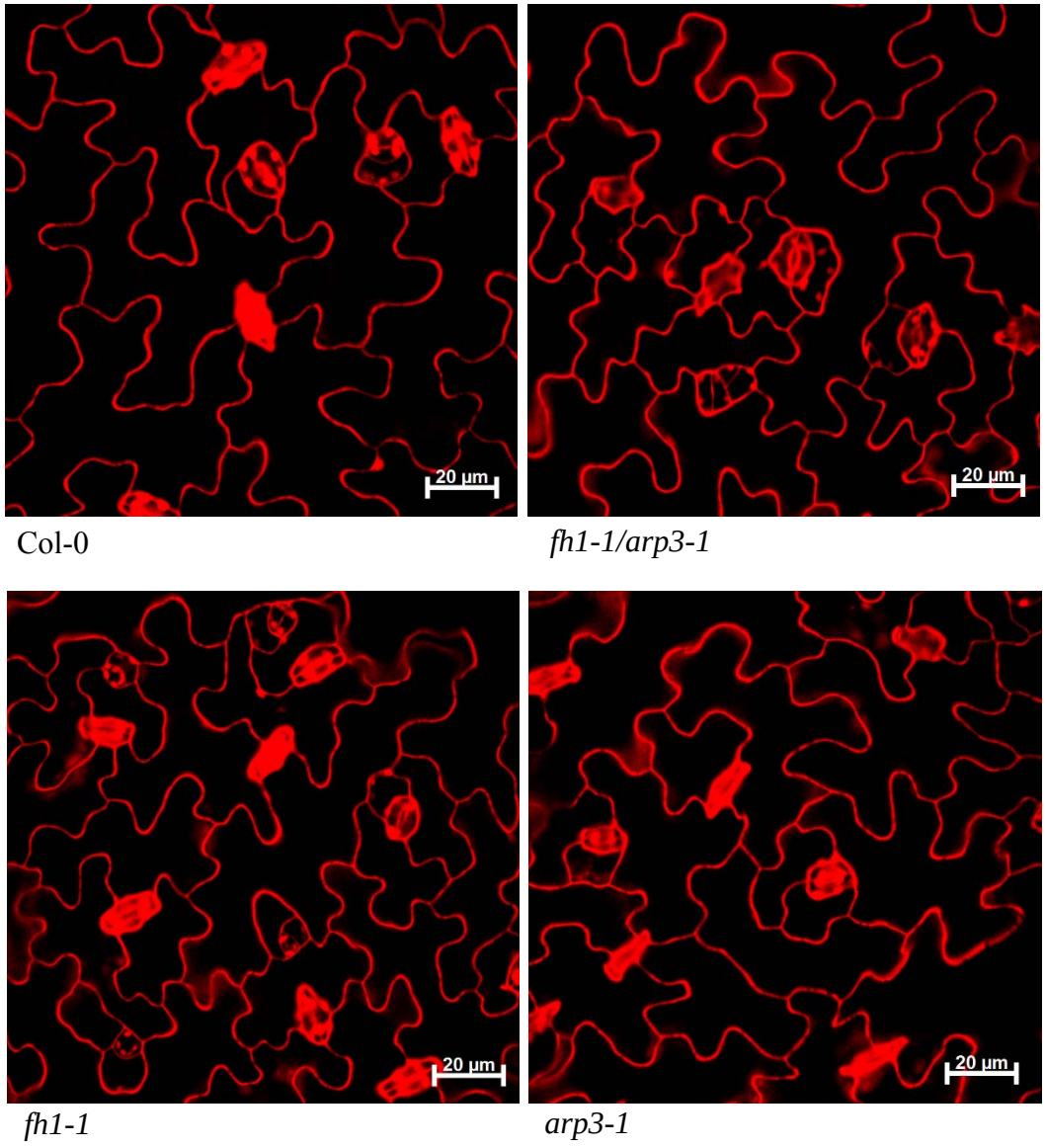

Figure 3.17: The confocal images of the leaf pavement cells. The leaves from the wild type, the double mutant and both the single mutants from 18 days old plant, stained with propidium iodide and images of the pavement cells from the abaxial side of the leaves were taken with Zeiss Confocal laser scanning microscope.

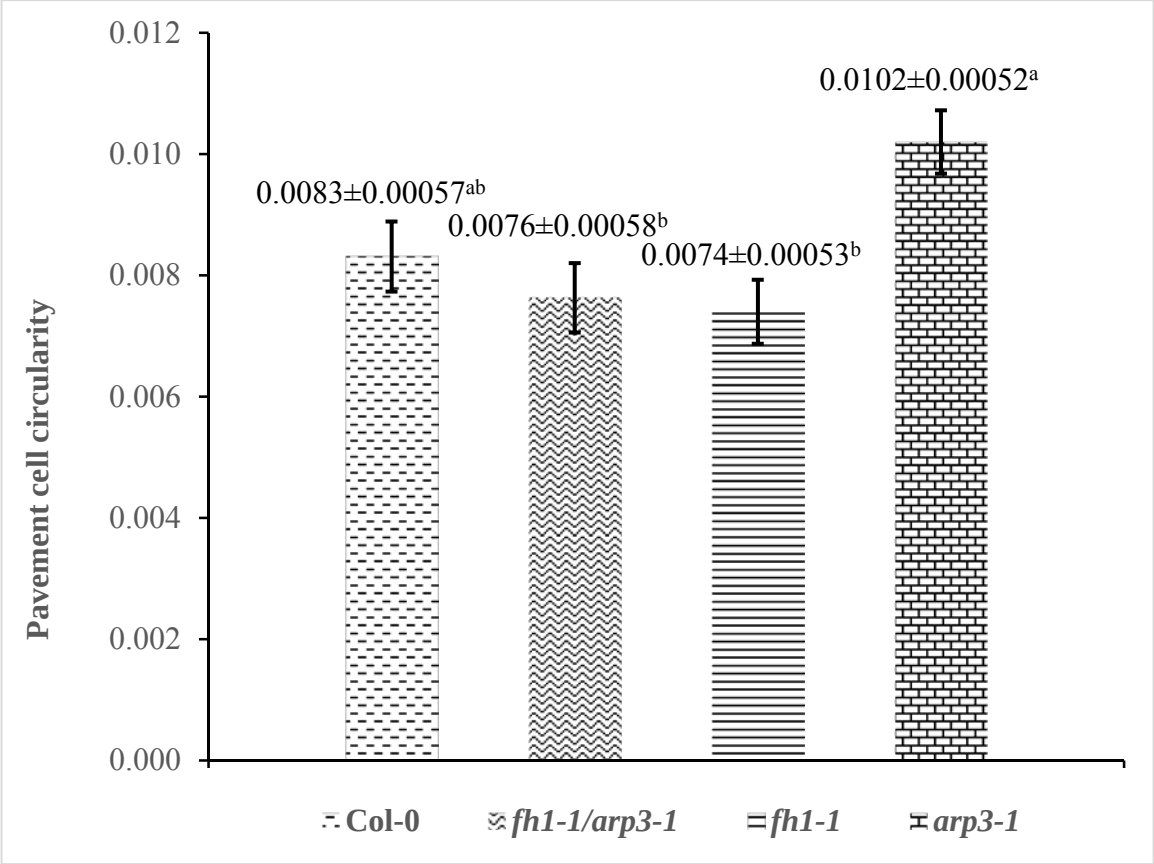

Figure 3.18: The histogram shows the average circularity of leaf pavement cells of the wild type, the double mutant and both the single mutants. The circularities were measured from the confocal images using ImageJ software. At least 30 pavement cells from each leaf sample and 3 samples per line were measured. For statistical analysis, One way ANOVA with Holm-Sidak multiple comparison method was used.The error bars represent the standard errors of the means.

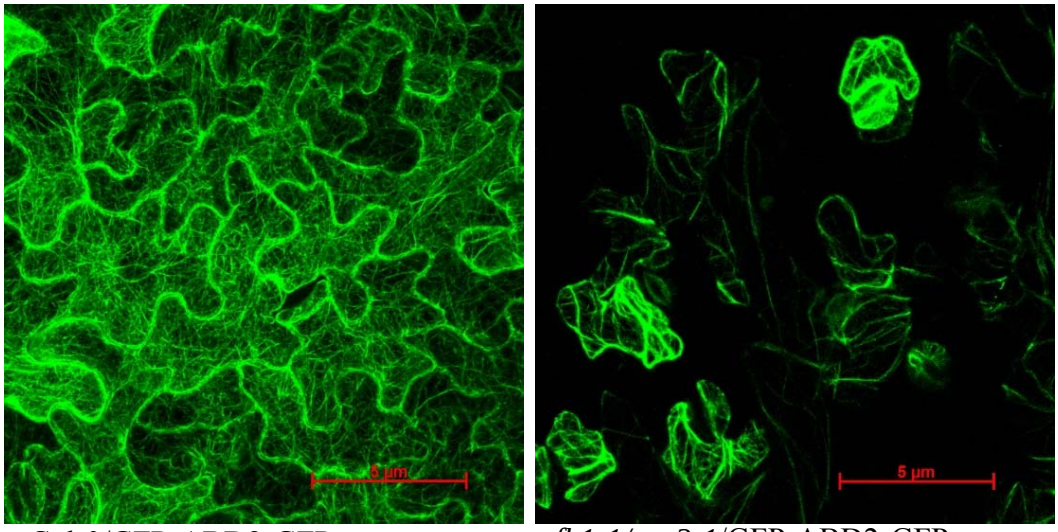

Col-0/GFP-ABD2-GFP *fh1-1/arp3-1*/GFP-ABD2-GFP

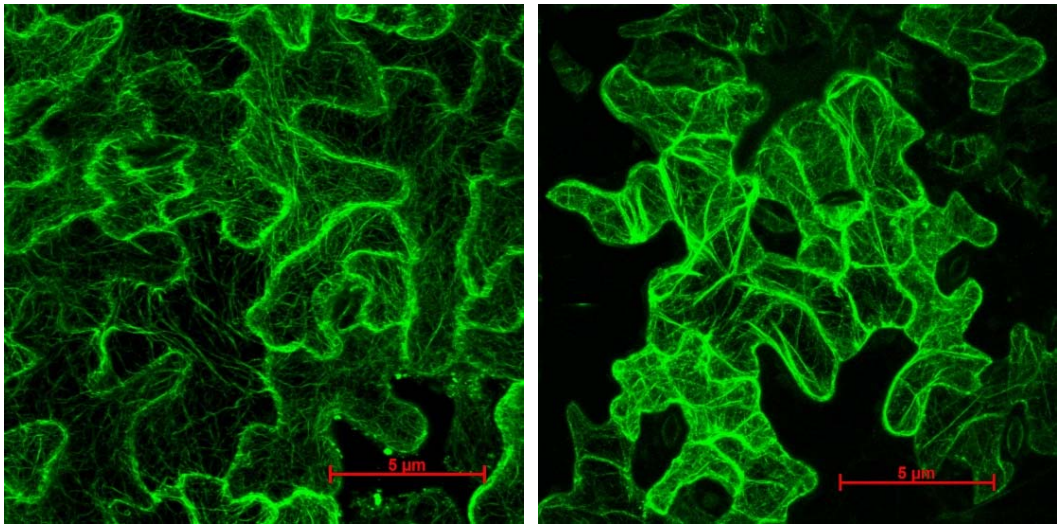

fh1-1/GFP-ABD2-GFP *arp3-1*/GFP-ABD2-GFP

Figure 3.19: Actin cytoskeleton organization in leaf pavement cells. The actin cytoskeleton organization of leaf epidermal pavement cells of the double mutant (*fh1-1/arp3-1*) and all single mutants (*fh1-1* and *arp3-1*) plants expressing GFP tagged actin binding domain2 (GFP-ABD2-GFP) were visualized under confocal microscope and Z-stack images were taken for each sample. From the Z-stack, the maximum projection images were produced using ImageJ software.

3.4.2 Trichome cells

The double mutant *fh1-1/arp3-1* and single mutant *arp3-1* produced distorted leaf trichomes compared to the wild type and *fh1-1* single mutant (Figure 3.20). The *fh1-1/arp3-1* mutant

exhibited irregular shaped long stalked and short branched trichomes comparable to the well reported trichome distorted mutant *arp3-1* (Figure 3.20). But some of the trichomes of *fh1-1/arp3-1* were very long with an expanded stalk and long branch that were not found in *arp3-1* mutant (Figure 3.21). So *fh1-1/arp3-1* double mutant may be considered as the less distorted trichome mutant. The *fh1-1* single mutant showed the normal trichome phenotype like wild type. Both *fh1-1* mutant and wild type plants produced short stalk and long branched trichomes. With a few exceptions of two or four branched types, most of the trichomes of these plants are three-branched (Figure 3.20).

The actin cytoskeleton organization in the trichome cells were studied using GFP tagged ABD2 marker under genetic background of the wild type (Col-0/ GFP-ABD2-GFP), the double mutant (*fh1-1/arp3-1*/ GFP-ABD2-GFP), *fh1-1* single mutant (*fh1-1*/ GFP-ABD2-GFP) and *arp3-1* single mutant (*arp3-1*/ GFP-ABD2-GFP). Starting from the base of the trichome, the actin filament elongated up to the branch point from where new actin filaments were distributed longitudinally to the end of the branch in wild type whereas, without stopping in the branch point the long actin filaments were eventually and longitudinally distributed from base to the end of the branch along the stalk in double mutant trichomes (Figure 3.22). In the double mutant and *arp3-1* single mutant most of the areas along the circumferences of the stalk and branch were occupied by the vacuole and a few actin filaments were distributed in the trichome cells. In the *fh1-1* mutant, the actin filaments initiated at the base of trichome, then elongated longitudinally through the stalk and stopped at the branch point where a compact actin nest that was not found in wild type or any other mutants was formed. Arising from that actin nest, new actin filaments parallel to the branch were distributed up to the end of each branch (Figure 3.22).

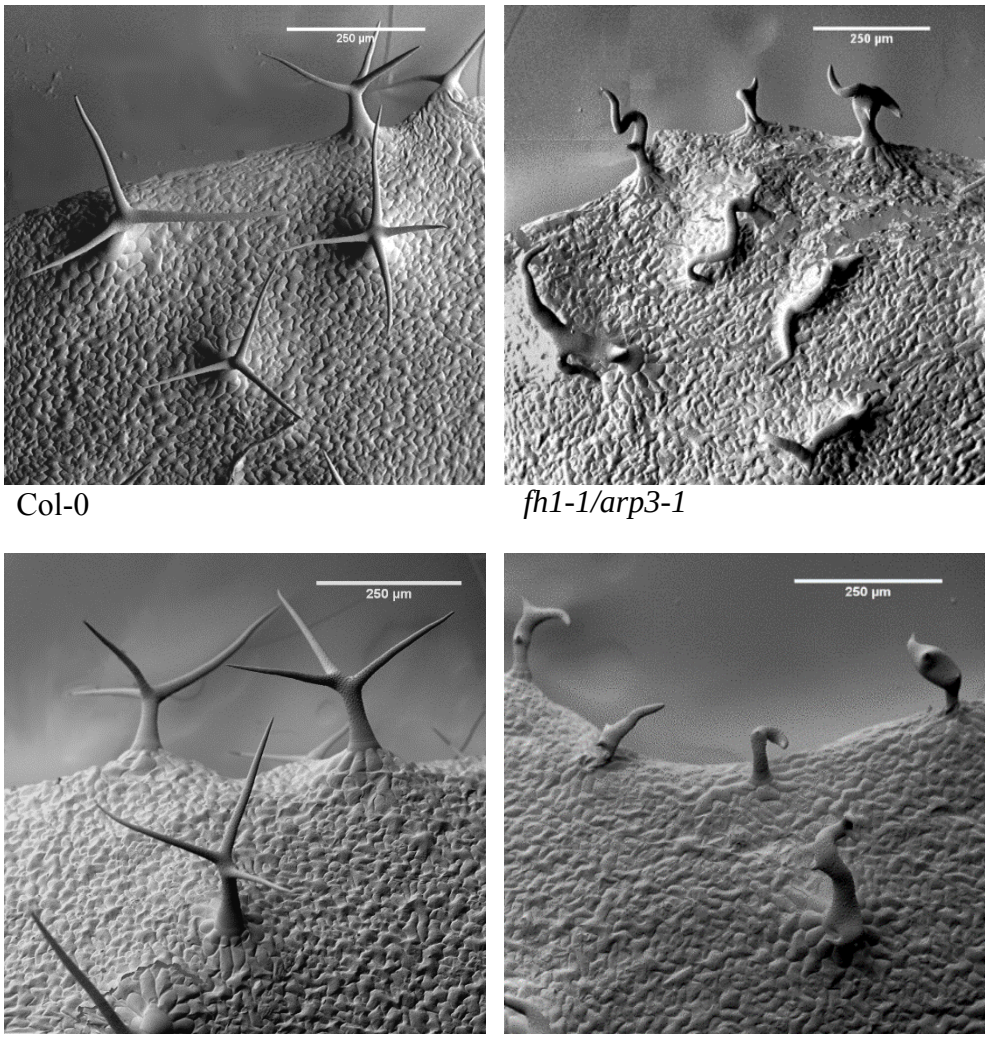

Figure 3.20: SEM images of mature leaf trichomes. The leaf samples were prepared by fixation with Methanol/ Ethanol fixative and scanning electron microscopic images were taken following CPD (critical point drying) and gold-palladium coating.

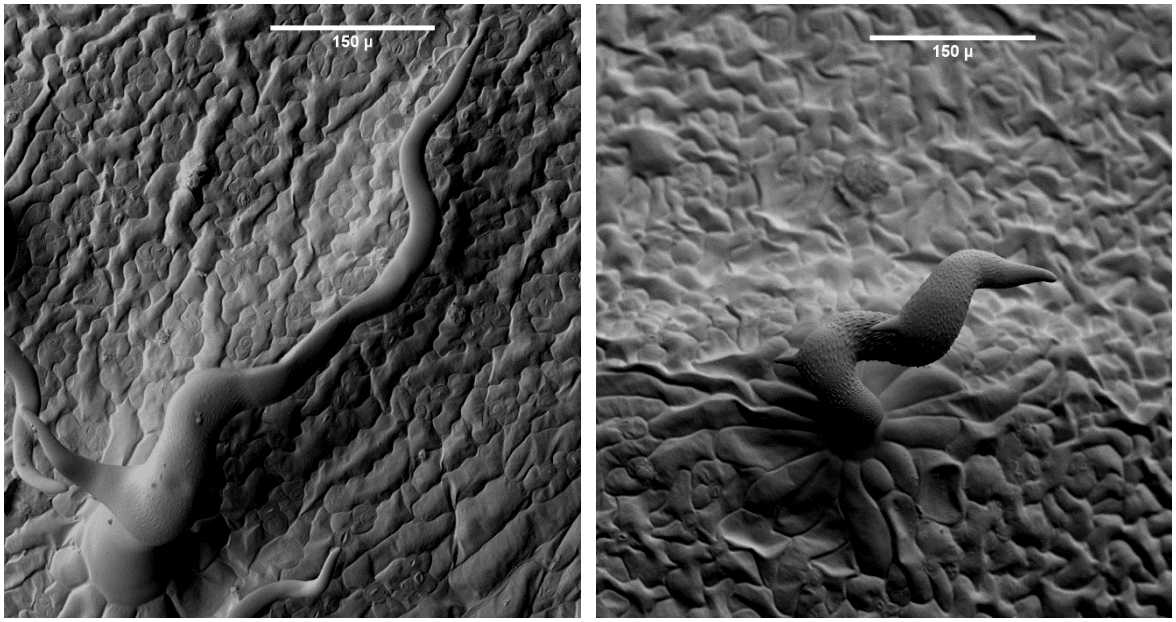

One of the largest trichome of *fh1-1/arp3-1* One of the largest trichome of *arp3-1*

Figure 3.21: The images show the difference in trichome size and morphology of two different distorted trichome in mutants *fh1-1/arp3-1* and *arp3-1*.

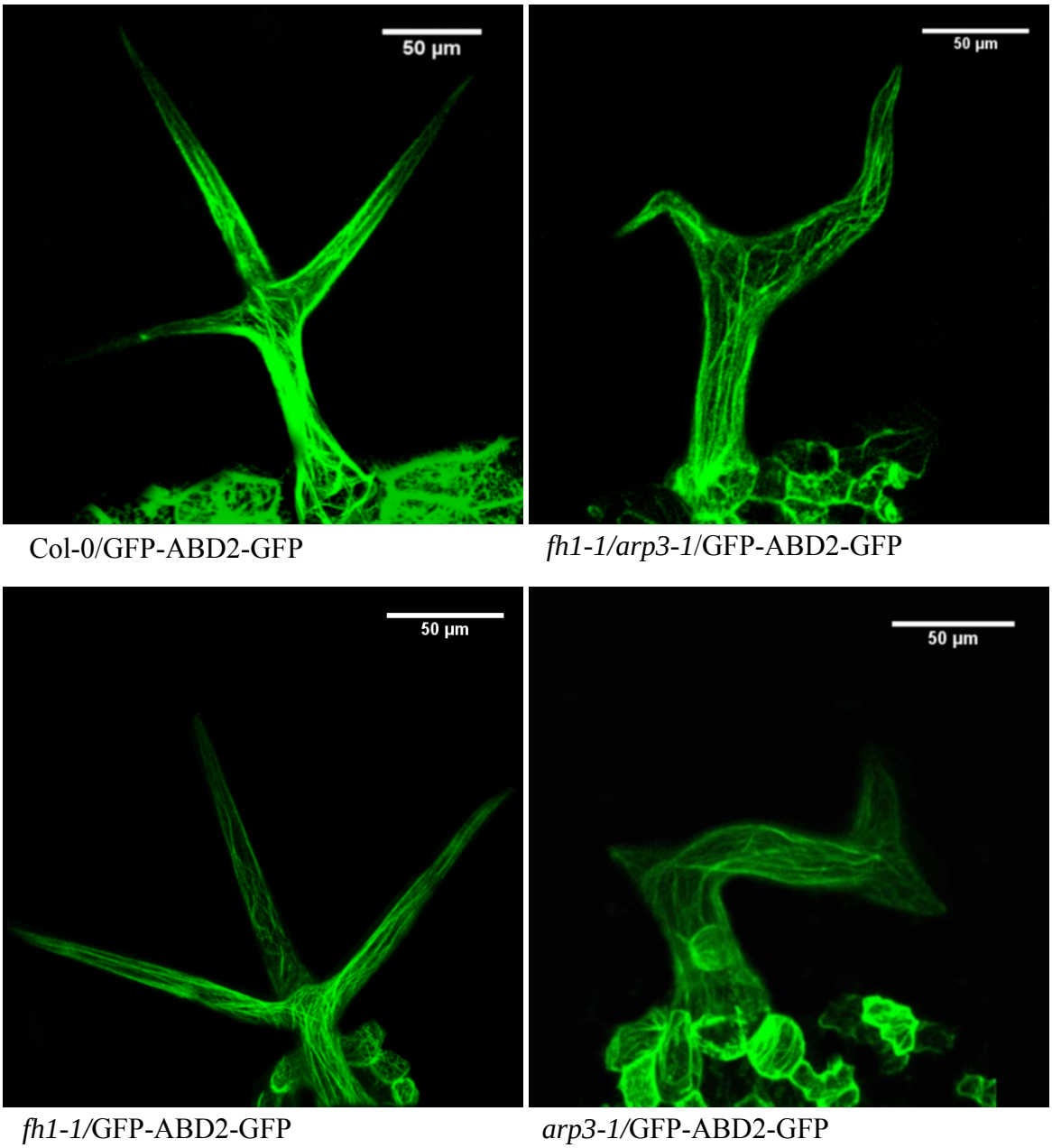

Col-0/GFP-ABD2-GFP *fh1-1/arp3-1*/GFP-ABD2-GFP

*fh1-1/*GFP-ABD2-GFP *arp3-1/*GFP-ABD2-GFP

Figure 3.22: Actin cytoskeleton organizations in mature trichome. The trichomes were collected from mature leaves of three weeks plants of the wild type and the mutants expressing GFP-ABD2 and the actin cytoskeleton organization in trichome cells was observed with Zeiss confocal laser scanning microscope. The Z- stack series images of each sample were captured from which the maximum projection image was created using ImageJ software.

3.4.3 Mesophyll cells

Chlorophyll content of the double mutant was only about 2/3 of the wild type and all other single mutants (Figure 3.23). The wild type, *fh1-1* and *arp3-1* single mutants have no significant difference in chlorophyll content of the leaves, whereas *fh1-1/arp3-1* contained significantly lower amount of chlorophyll compared to that of wild type and other single mutants (Figure 3.23). The leaf color of *arp3-1* mutant was also lighter than wild type, but was not as much as the double mutant and did not differ with wild type in chlorophyll content of leaves. The leaf color was almost same within wild type and *fh1-1* single mutant and there was no difference in chlorophyll content. The average chlorophyll content of 1.00g fresh leaves of wild type, *fh1-1/arp3-1* double mutant, *fh1-1* and *arp3-1* single mutants were 1450.38 µg, 911.92 µg, 1550.4 µg and 1543.73 µg respectively (Figure 3.23).

As an effort to identify the mechanism behind the lower chlorophyll content of the double mutant the size, shape and chloroplast content of the mesophyll cells of wild type, double mutant and both the single mutants were studied. The size and shape of the mesophyll cells in wild type and *fh1-1* mutant were the same with the same distribution pattern of chloroplasts inside these cells. The shape of the mesophyll cells and distribution pattern of chloroplasts in *fh1-1/arp3-1* double mutant were the same but the cells were smaller than that of wild type and *fh1-1* mutant (Figure 3.24). The size and shape of the mesophyll cells were irregular and the chloroplasts were compactly bound to each other inside the mesophyll cells of *arp3-1* single mutant (Figure 3.24). All the mutants and wild type plants contained significantly different numbers of chloroplasts per mesophyll cells. The average numbers of chloroplasts per mesophyll cells were 54 (wild type), 33 (double mutant), 50 (fh1-1) and 38 (arp3-1) (Figure 3.25).

In mesophyll cells of the double mutant, the longitudinal thick actin arrays were more apparent, but very few fine actin filaments thinly and un-uniformly organized actin filaments network associating the chloroplasts, whereas uniformly distributed thin actin filament network associating all the chloroplasts was seen in wild type mesophyll cells (Figure 3.26). In the *fh1-1* single mutant, compact thin actin filament network that covered the entire mesophyll cell was formed. The longitudinal thick actin filament arrays and randomly oriented thin actin filaments network both were clearly visible in the *arp3-1* single mutant, largely similar to the wild type (Figure 3.26).

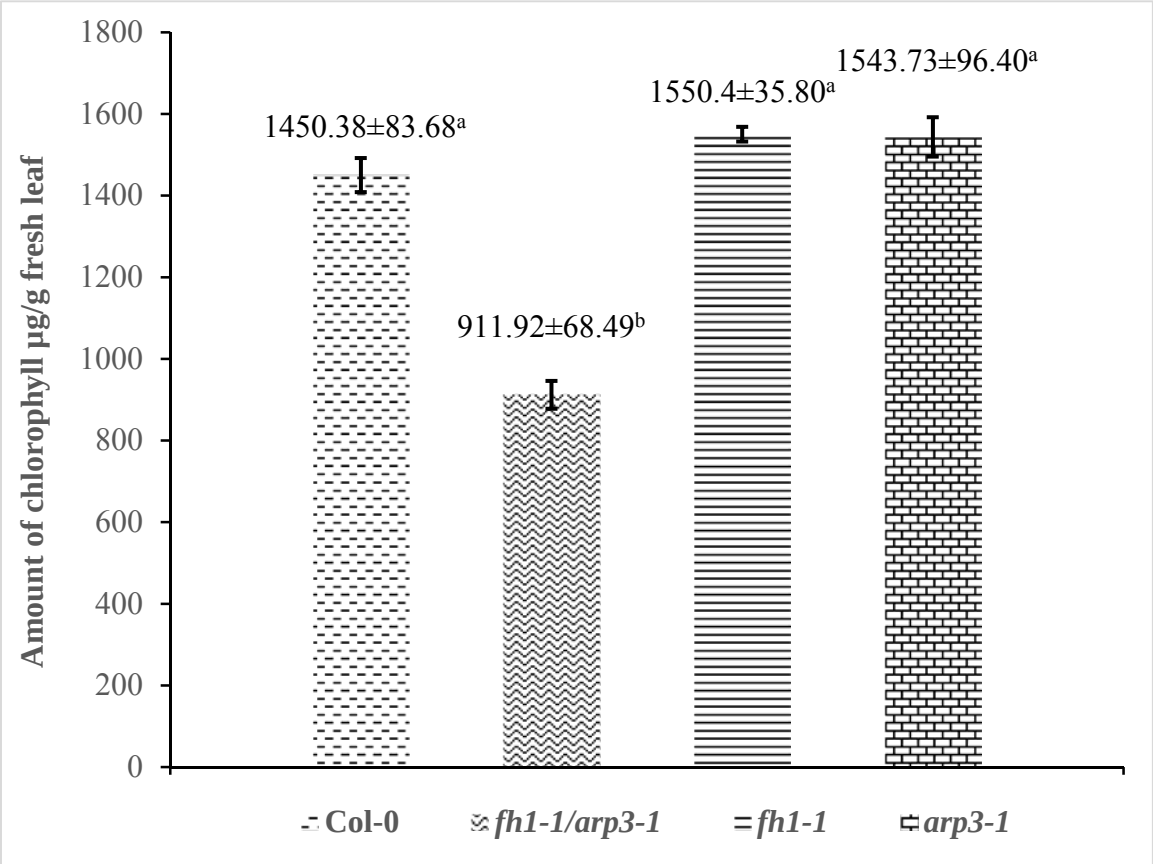

Figure 3.23: The histogram shows the total chlorophyll content of leaf in the wild type, the mutants. 4 days old leaves from 21 days old plants were collected from each sample to estimate the total chlorophyll based on fresh leaf weight. At leat 4 samples with 4 replication per line were analyzed for total chlorophyll estimation. One way ANOVA with Holm-Sidak multiple comparison method was followed for statistical analysis. The error bars represent the standard error of the means.

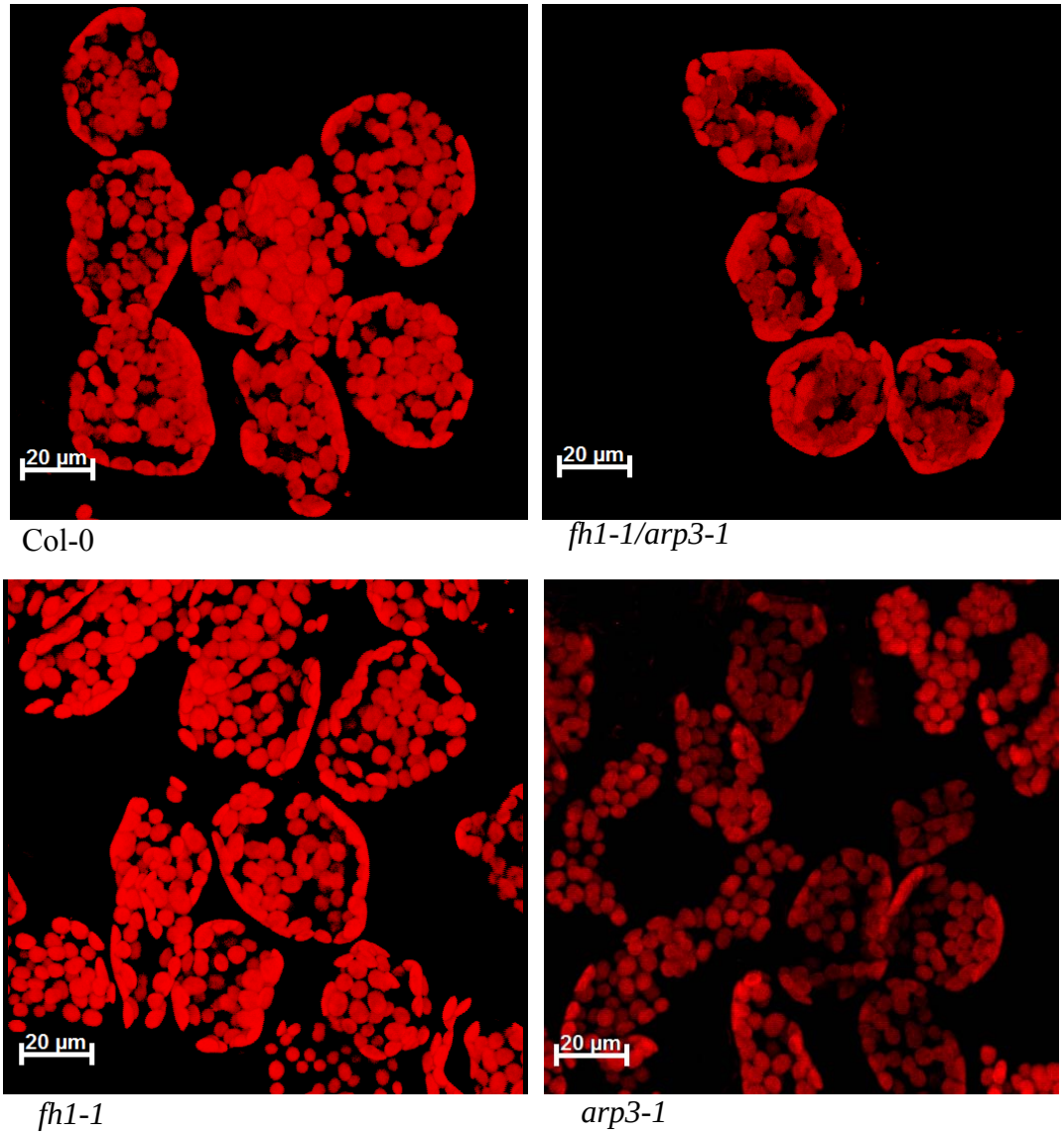

Figure 3.24: Chloroplast content of mesophyll cells. 4 days old leaves from a mature plant for all genotypes were collected and separated the intact mesophyll cells to count the chloroplast perfectly. After separating the cells Z-stack images were taken with confocal laser scanning microscope using chloroplast auto-fluorescence. The maximum projection images were created from the Z-stack images to count the chloroplasts from each mesophyll cell.

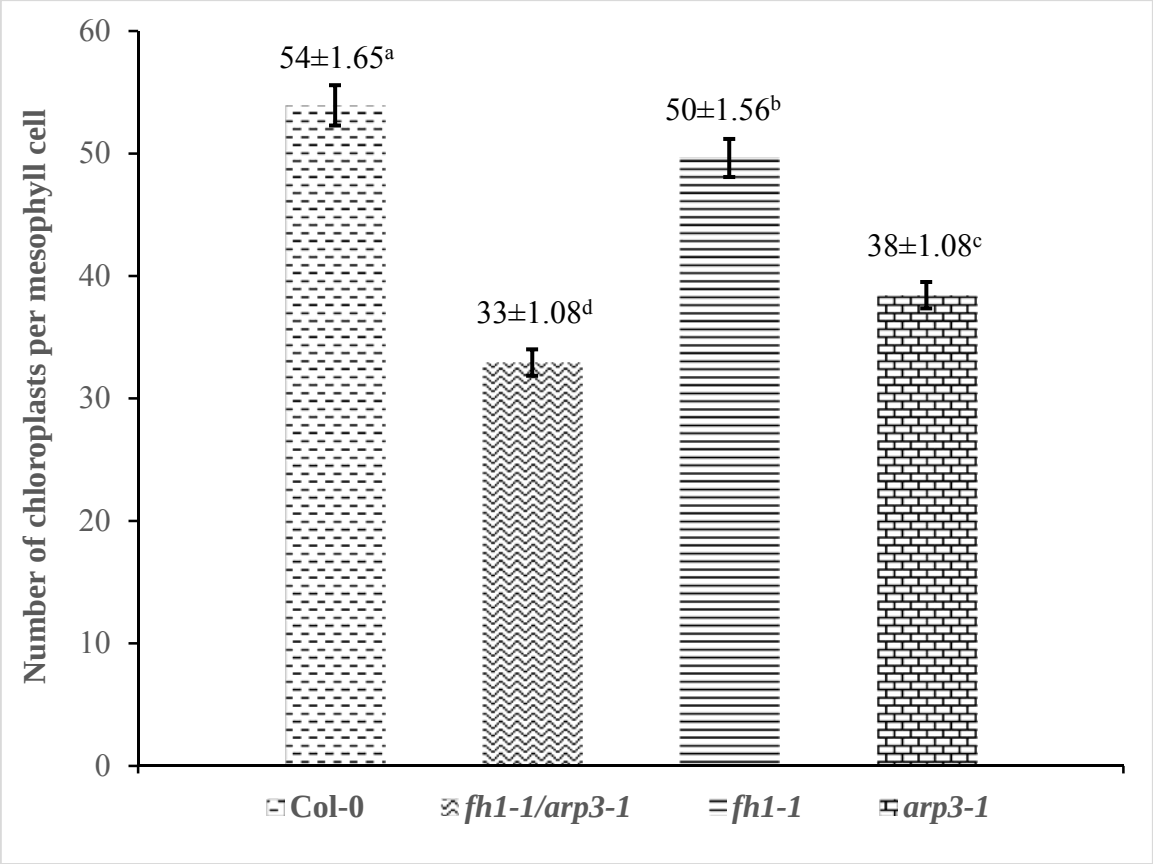

Figure 3.25: The histogram shows the average number of chloroplasts in the mesophyll cells of the wild type, the double mutant and both the single mutants. The total number of chloroplasts from 30 intact leaf epidermal cells for each line were counted from the maximum projection images. For statistical analysis, One way ANOVA with Holm-Sidak multiple comparison method was used. The error bars stands for the standard error of the means.

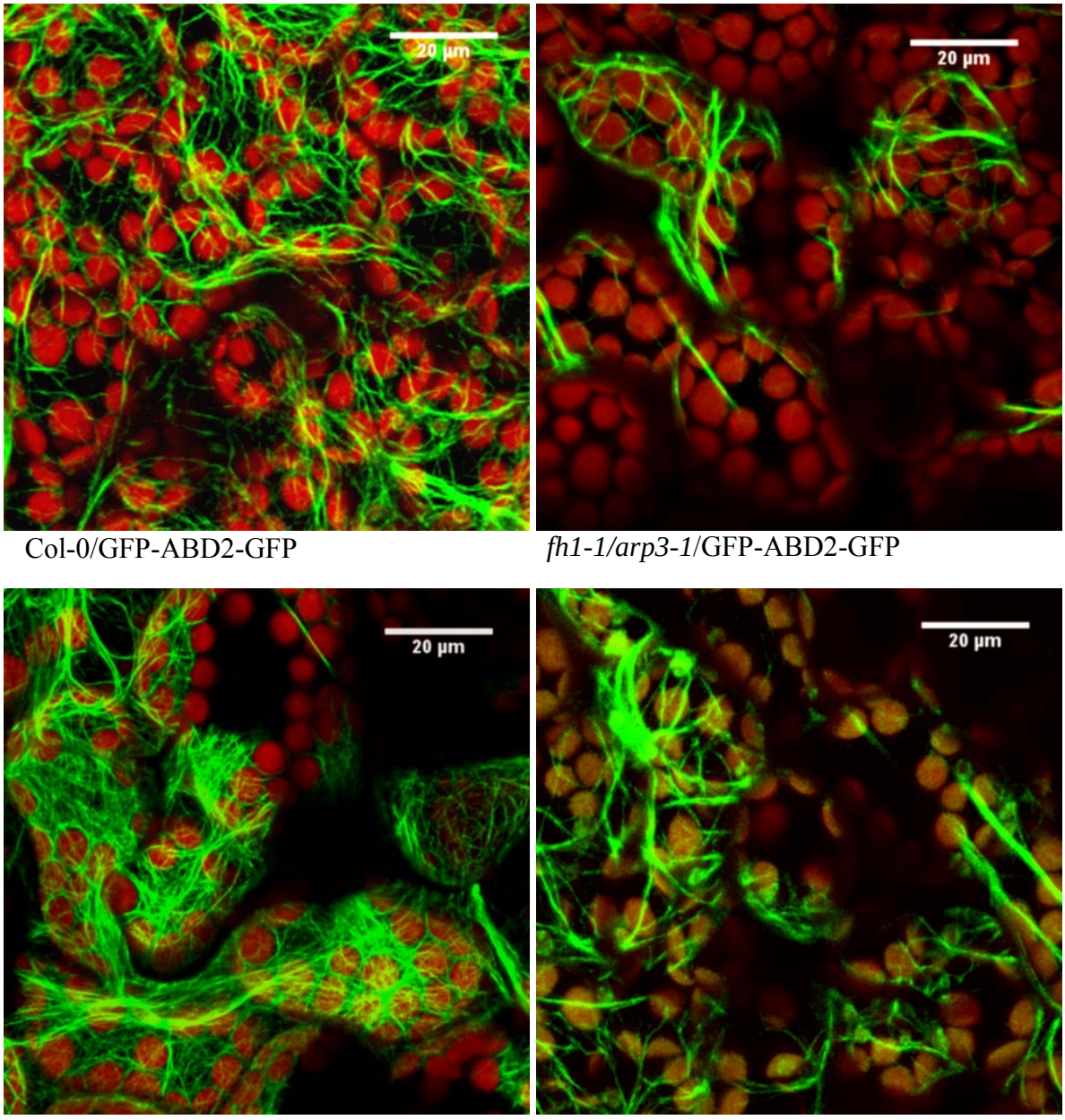

Col-0/GFP-ABD2-GFP

fh1-1/arp3-1/GFP-ABD2-GFP

*fh1-1/*GFP-ABD2-GFP

*arp3-1/*GFP-ABD2-GFP

Figure 3.26: The actin cytoskeleton organizations in leaf mesophyll cells of the wild type and mutants expressing GFP-ABD2-GFP. 4 days old leaves from three weeks plants were collected for each line. The actin cytoskeleton organizations in mesophyll cells were studied with Zeiss confocal laser scanning microscope using GFP fluorochrome spectra. The Z-stack images were captured and the maximum projection images were created using ImageJ software.

3.5 Diminished fertility of the actin cytoskeleton disrupted mutants

3.5.1 Flower and floral organ structures

The double mutant *fh1-1/arp3-1* produced tiny flowers with distinct floral organ structure compared to wild type and both the single mutants *fh1-1* and *arp3-1* (Figure 3.27). At thirteen stage of flower development, four sepals were separated from their base in the double mutant and the *fh1-1* single mutant whereas in wild type and *arp3-1* single mutant the sepals were separated almost from their mid portions. Before blooming, the stigma came out of the sepals first when the petals were covered with the sepals in the double mutant, but the petals came out first when the stigma were covered with the petals in wild type and both the single mutants. In the double mutant the sepals and petals were almost similar size in a mature flower whereas petals were much larger than sepals in wild type and both the single mutant (Figure 3.27). The stamens were of variable sizes, some were longer than the pistil and some were shorter than the pistil in the double mutant, but all the stamens were almost similar length to pistil in wild type and both the single mutants (Figure 3.27).

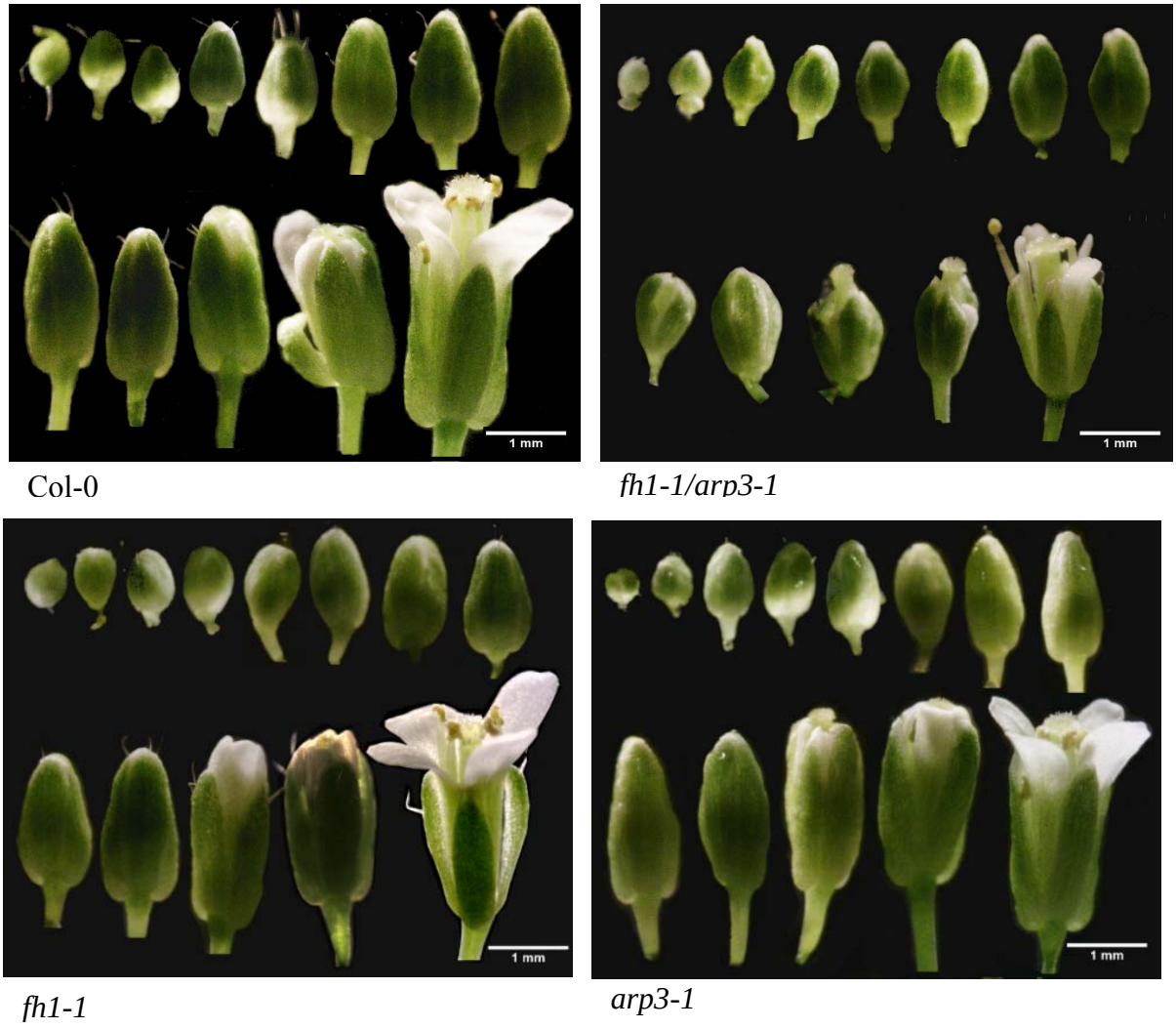

Col-0 *fh1-1/arp3-1*

fh1-1 *arp3-1*

Figure 3.27: Different stages of flower development of the wild type, the double mutant and both the single mutants. The flowers for all the stages were taken from a single florescence for each plant and imaged them with Zeiss dissection microscope (Zeiss Stemi 2000-C, West Germany).

3.5.2 Pollen structure and number of pollen produced

The size of pollen of the double mutant (*fh1-1/arp3-1*) was smaller compared to the wild type and the two single mutants (Figure 3.28). Almost all of the pollen in the wild type and the mutants were normal in size and shape (Figure 3.28), whereas some of the pollen were normal and some were tiny and distorted with irregular pollen coat topology in the double mutant (Figure 3.29). The tectum were uniformly distributed over the pollen coat in normal pollens of the double mutant, similar to that of the wild type and both the single mutants, but the expanded tectum over the pollen

coat made the exine nearly collapsed in distorted pollens of the double mutant (Figure 3.28). Visibly there were no differences in pollen size, shape and exine structure among the wild type, *fh1-1* and *arp3-1* single mutants (Figure 3.28).

Figure 3.28: Scanning electron microscopy (SEM) images of mature pollens of the wild type, the double mutant and both the single mutants. The pollens were taken from newly bloomed flowers for each sample.

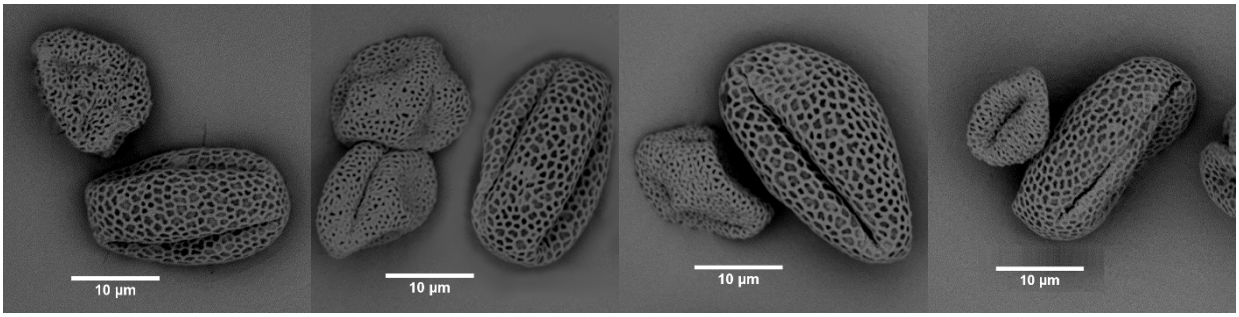

Figure 3.29: The SEM images show the normal and distorted pollens of the double mutant (*fh1-1/arp3-1*). The distorted pollens are very small compared to the normal pollens. The surface (exine) structure of the distorted pollens was also different than that of normal pollens.

3.5.3 *In vitro* pollen germination rate

At 6 hrs post spreading the pollen into the culture plate, few pollens of the double mutant were germinated that were almost half compared to the wild type and both the single mutants under *in vitro* pollen germination test (Figure 3.30). Within that time point, the pollen tubes of the double mutant were also shortest in length compared to the wild type and both the single mutant (Figure 3.30). The pollen tube lengths of both the single mutants were moderate, whereas the wild type produced the longest pollen tube within that time point (Figure 3.30). Average *in vitro* pollen germination rate of the double mutant was 37% which was significantly lower (at an average 31.37% lower) than the wild type and two single mutants (Figure 3.31). There was no significant difference of *in vitro* pollen germination rate among the wild type and two single mutants (Figure 3.31).

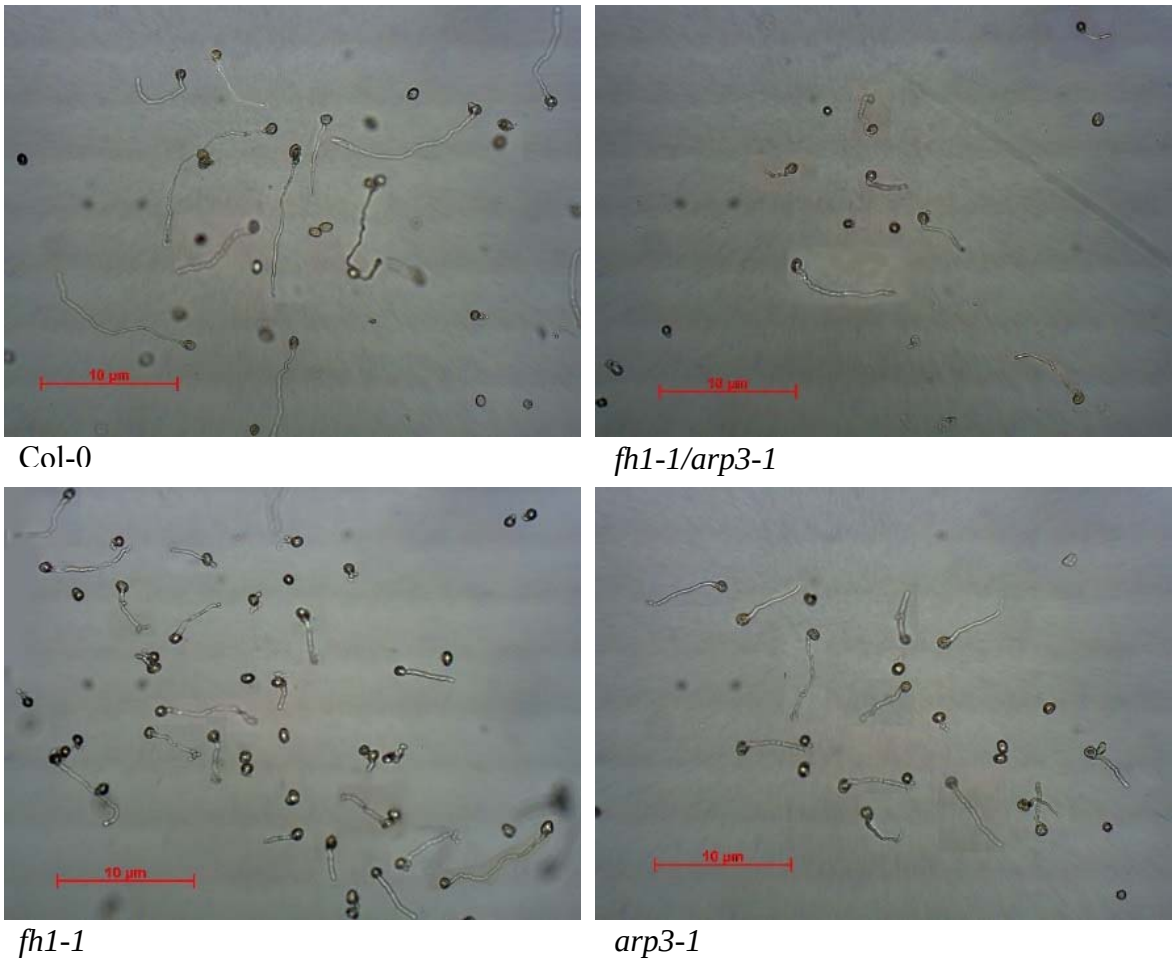

Col-0 *fh1-1/arp3-1*

fh1-1 *arp3-1*

Figure 3.30: Light microscopic images show *in vitro* pollen germination of the wild type, the double mutant and both the single mutants. At 6 hrs post spreading the pollen in to the culture plate containing pollen culture media the images were taken using Zeiss Axiplan microscope.

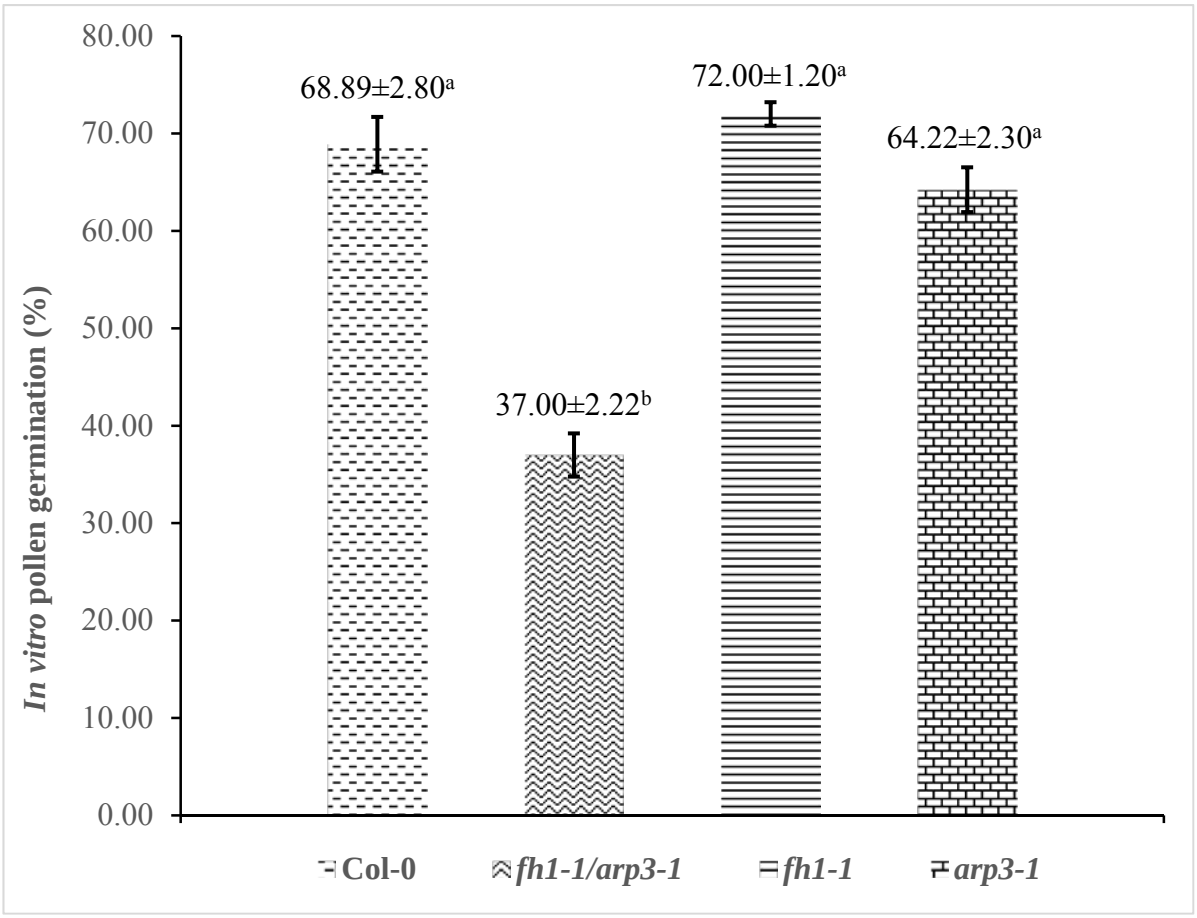

Figure 3.31: The histogram shows *in vitro* pollen germination rate of the wild type, the doublemutant and both the single mutants. Randomly 900 pollen grains from 3 different plates for each line were counted using dissection microscope to calculate the pollen germination rate. One way ANOVA with Holm-Sidak multiple comparison method was used for statistical analysis. The error bars represent the standard errors of the means.

3.5.4 Pollen tube germination on the stigma

The aniline blue staining of pollen tube inside self-pollinated pistil showed that fewer number of pollen tubes grew and passed through the transmitting tissue of the pistil in the double mutant, whereas the wild type and both the single mutant produced sufficient numbers of pollen tubes of which almost all were passing through the transmitting tissues of the pistils (Figure: 3.32). The pollen tubes of the double mutant and the *arp3-1* single mutant were passing through the transmitting tissue deviating the strait line, but the pollen tube formed homogenously and were

passing through the transmitting tissue straightly within the wild type and *fh1-1* single mutant pistil (Figure: 3.32).

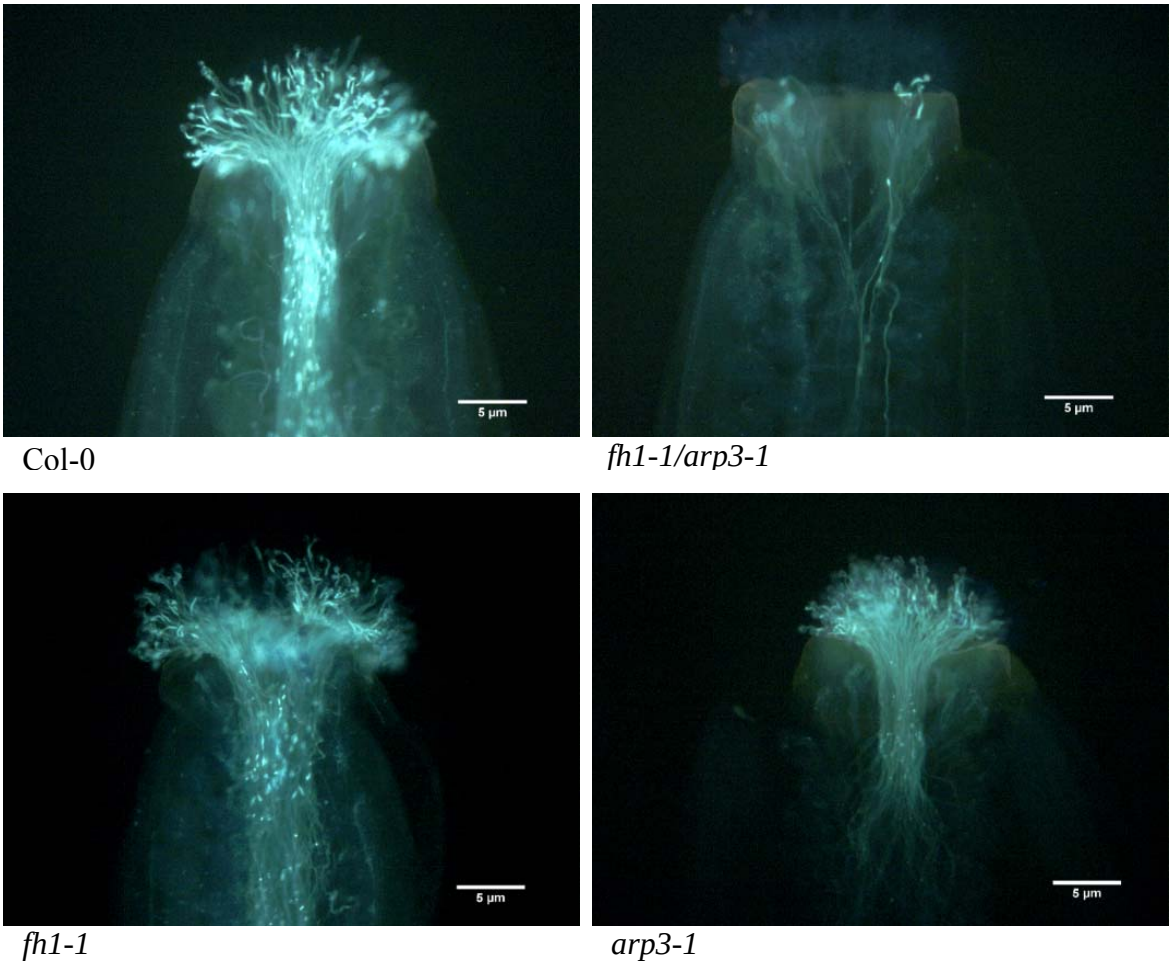

Figure 3.32: Growth of pollen tube along the transmitting tissues of pistils. The pistils were taken from the self-pollinated flowers of the wild type, the double mutant and both the single mutants. They were processed, stained with aniline blue and images were taken by Zeiss epifluorescence microscope using UV light.

3.5.5 Size of the silique

The silique size of the double mutant was very short compared to the wild type and both the single mutants (Figure 3.33). The average length of siliques of the double mutant was 3.97±0.80 mm which was significantly shorter than the wild type (12.90±0.73 mm) and single mutants *fh1-1* (13.32±1.106 mm) and *arp3-1* (11.83±0.71 mm) (Figure 3.34). Although the siliques of the double

mutant were short but their width were enough to contain the viable seeds. The transparent siliques (Figure 3.35) showed the seed content of the siliques of all the mutants and wild type. The seed content of the double mutant siliques ranged from 1 to 6 and some siliques were empty, whereas the wild type and both the single mutant siliques were full of seeds with no empty siliques (Figure 3.35). The average seed content per silique in the double mutant was negligible (2.45 seeds/silique) compared to the wild type (42.25 seeds/silique), and the single mutants *fh1-1* (46.27 seeds/silique) and *arp3-1* (38.99 seeds/silique) (Figure 3.36).

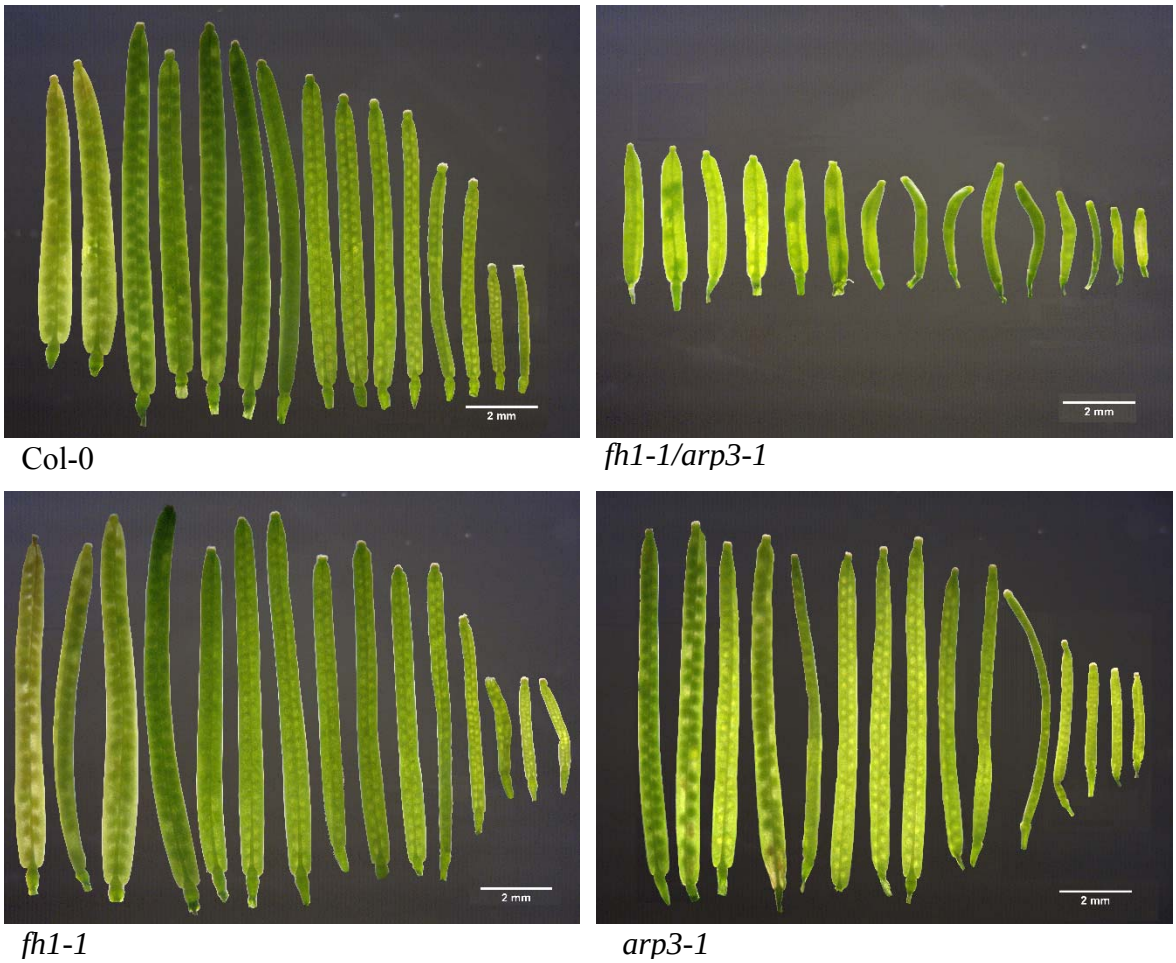

Col-0 *fh1-1/arp3-1*

fh1-1 *arp3-1*

Figure 3.33: Sizes of the siliques in different stages of their development. For each genotype, all the siliques were collected from a single branch of the mature plant. The images of different sizes of the siliques were taken by Zeiss dissection microscope (Zeiss Stemi 2000-C, West Germany).

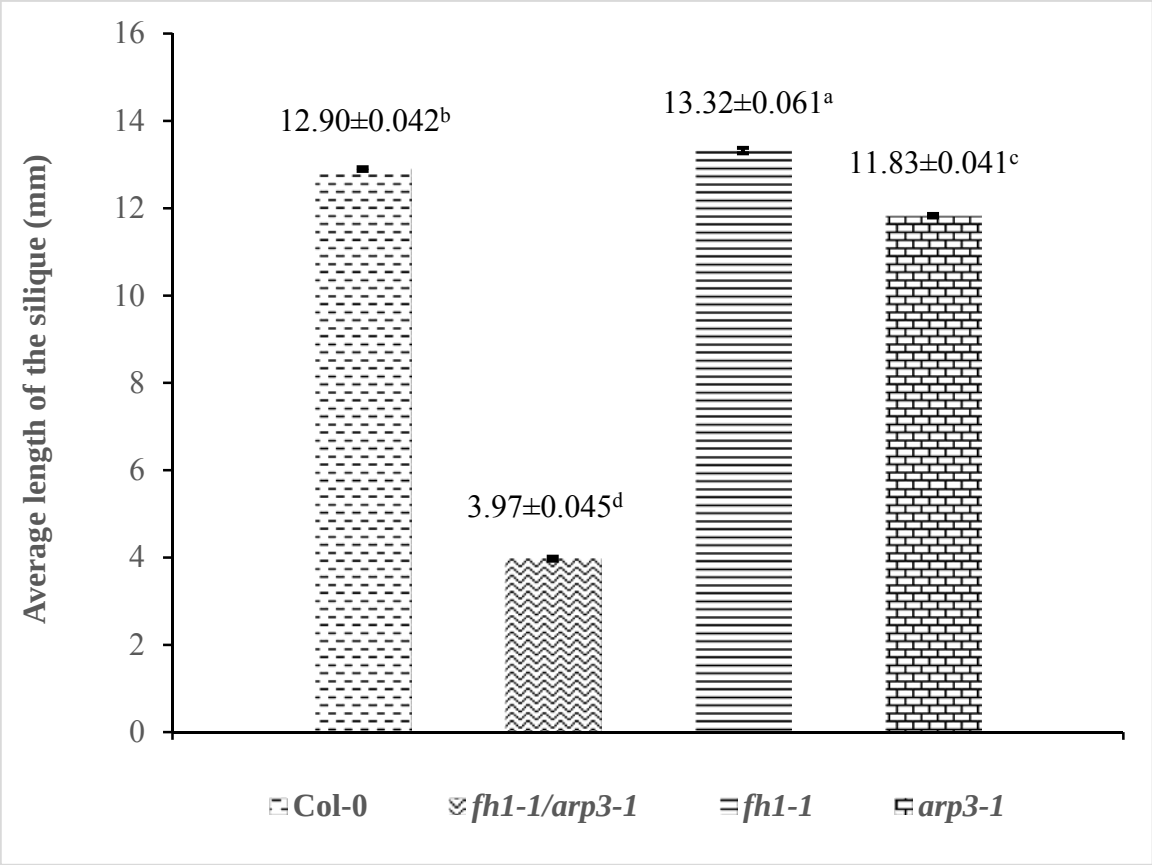

Figure 3.34: The histogram shows the average length of siliques of the wild type, the double mutant and both the single mutants. About 300 mature siliques from 20 different plants per line were collected and were imaged with dissection microscope (Zeiss Stemi 2000-C, West Germany). The ImageJ software was used to measure the length of the siliques from the images. Statistical analysis was performed by One way ANOVA with Holm-Sidak multiple comparison method. The error bars represent the standard error of the means.

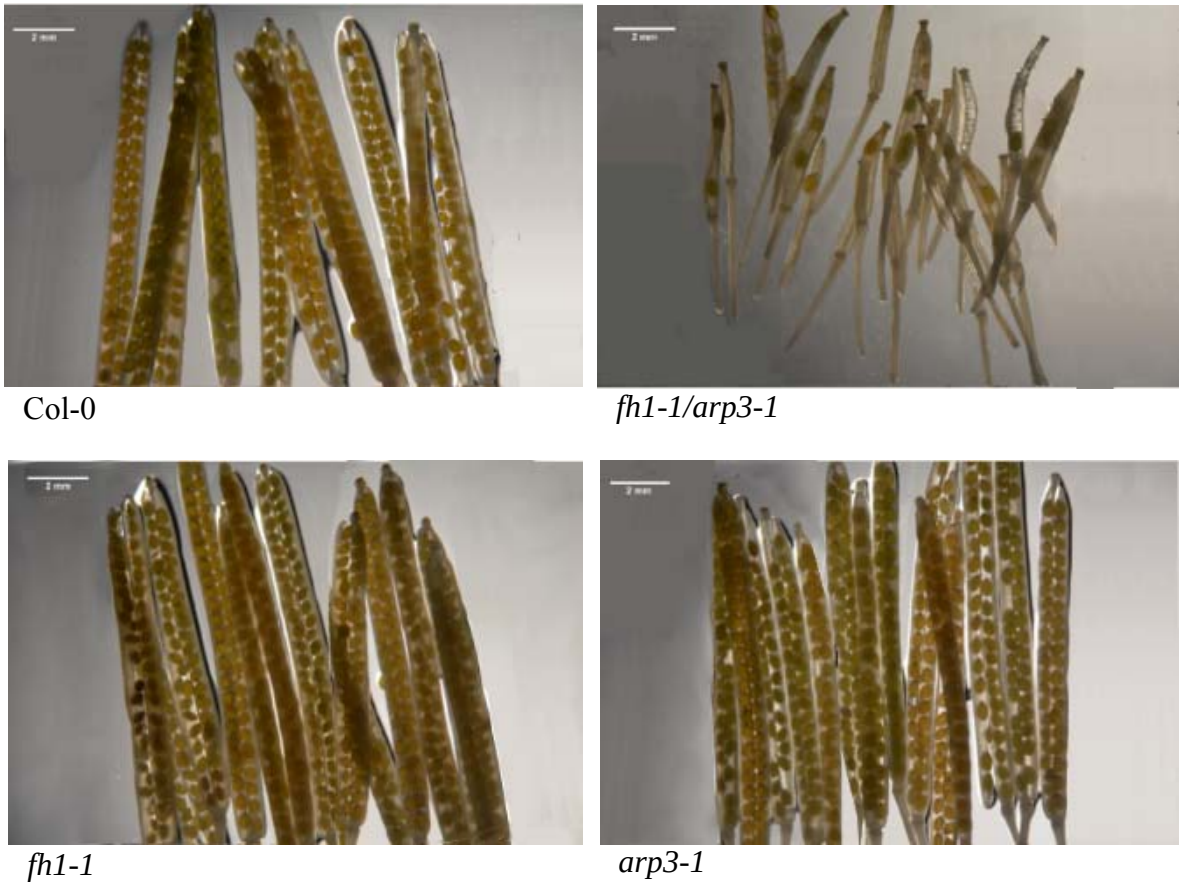

Figure 3.35: The seed content of the siliques of the double mutant, the wild type and both the single mutants. The siliques were decolorized which allowed to see not only seed but also the empty seed chamber. The images were taken by Zeiss dissection microscope (Zeiss Stemi 2000-C, West Germany).

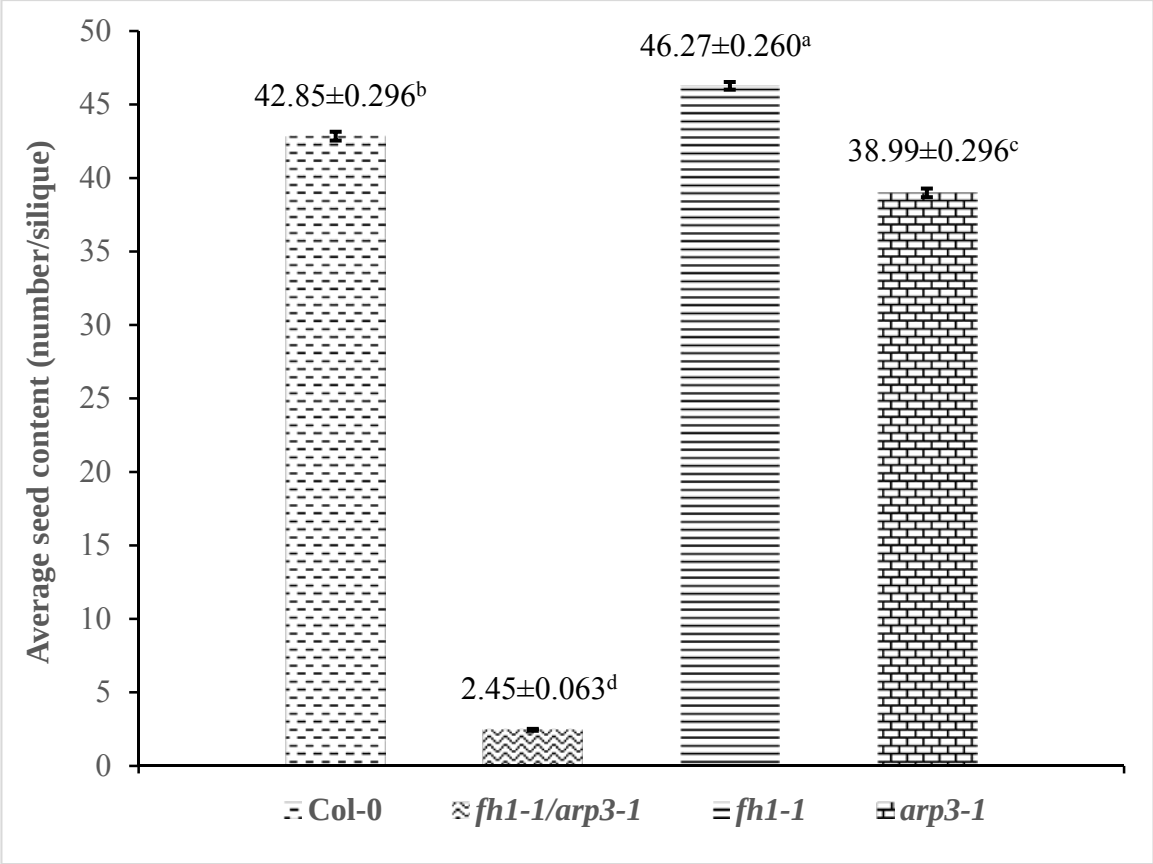

Figure 3.36: The histogram represents the average seed content of siliques of the double mutant, the wild type and both the single mutants. About 300 mature siliques from 20 different plants per line were collected and their seed contents were counted manually. Statistical analysis was performed by One way ANOVA with Holm-Sidak multiple comparison method. The error bars stand for the standard error of the means.

CHAPTER 4: DISCUSSION

4.1 *AtFH1* and *AtARP3* genes mutation affect normal plant morphology

The size, shape and growth of plant are regulated by a combination of genetic (mostly male and female gametophytes) and environmental (temperature, humidity, soil, water availability) factors (Bögre et al., 2008). Study with actin disrupted drug treatment in *Arabidopsis* revealed that after disruption of actin filament the plant was very small and sometimes contained unexpanded cells (Baluška et al., 2001). The dynamic actin organization and different actin-interacting proteins are found in abundance at the apex of tip-growing region of the cell (Miller et al., 1999).

The small plant and short leaves in the double mutant may be due to the arresting of the cell division or cell elongation processes. It was reported that *Arabidopsis* formin1 mutant produced short root phenotype but the molecular mechanism underlying the reduced root length is not clear (Rosero et al., 2013; Rosero et al., 2016). As the plant Formin protein family is one of the key regulator of microfilament and microtubules, they may play important roles in some of the fundamental processes including plant cell growth and plant development (Wang et al., 2012). The research conducted on physiological functions of plant formins summarized that they are involved in plant cell division and participate in plant cell tip growth and diffuse expansion (Wang et al., 2012). So *AtFH1* mutation in *fh1-1/arp3-1* plants may facilitate this phenotypic variation from wild type by affecting cell growth and expansion. On the other hand ARP2/3 complex controls the cell shape and cell morphology in higher plants (Uhrig et al., 2007). In an effort to predict the function of ARP2/3 complex in plant, *ARP2, ARP3, ARPC2* and *ARPC5* mutants were studied and the similar actin disrupted phenotypes were found (Mathur et al., 1999; Schwab et al., 2003; Szymanski et al., 1999). It was reported that *ARP2* mutation produced enlarged hypocotyl phenotype and outward bended epidermal cell layer in plant (El-Din El-Assal et al., 2004; Li, 2003; Saedler et al., 2004). *ARP3* may play the same roles in plant morphogenesis, but its unique roles in cell morphogenesis are less understood (Mathur, 2003).

Under this study, the *arp3-1* mutant showed more oval shape leaves with slightly pale green color compared to wild type, which are negligible in phenotypic differences, whereas *fh1-1* mutant

showed no differences in phenotypic appearance compared to the wild type. Based on the experimental evidence, it was suggested that there may be an equilibrium between formin and ARP2/3 complex activity in plant cells. As a result, disruption of ARP2/3 complex activity boosted up formin activity in some mutants (i.e., *napp-1*, *pirp-1*), although those mutants showed defective morphology of some specific cells, such as trichome cell (Mathur, 2005; Brembu et al., 2004). Consistence with this, *arp3-1* exhibited similar cell morphology, but did not show any significant differences in some of the developmental processes which may be due to increased activity of formins. These suggest the stronger phenotype of *fh1-1/arp3-1* mutant compared to the wild type is due to the effect of *AtFH1* and *AtARP3* double mutation. As both *AtFH1* and *AtARP3* are responsible for actin filaments assembly and elongation, disruption and disorganization of acting filaments may cause the unique phenotype of *fh1-1/arp3-1* plants. Because acting cytoskeletons play a fundamental role in several essential cellular processes in plant including morphogenesis, organogenesis and development (Barrero, 2002). The array of actin filament determines the division plane during cytokinesis, participates in cell elongation process and mediates cell wall depositions which are the critical steps in cell differentiation and plant developments (Kost et al., 1999). In addition, the microfilament configuration and distribution patterns in different plant cell type have already been established that ensures the specific phenotype of plants (Kost et al., 1999; Mathur et al., 1999). So the disruption in actin filament organization and abundance or distribution which are caused by *AtFH1* and *AtARP3* double mutations produced the distinguished phenotype in *fh1-1/arp3-1* plants. These suggest that *AtFH1* and *AtARP3* may be involved in plant morphogenesis through participating in cell division, cell elongation and organ development.

4.2 *AtFH1* and *AtARP3* are involved in normal root development of *Arabidopsis*

Root growth is the combination of cell division, anisotropic cell expansion and cell differentiation in the apical meristem, elongation, and differentiation zones, respectively (Rosero et al., 2013; Vaughn et al., 2011). During germination, the longest primary root apical meristem (RAM) is built up by division and reactivation of cell growth that determines the fate of root cells. Actin cytoskeleton is responsible for increasing the number of dividing cells (Kushwah et al., 2011), thus regulate root growth as well as root hair development (Thitamadee et al., 2002; Gilliland et al.,

2003; Abe and Hashimoto, 2005). Among the cytoskeletons, microtubules determine the polar axis and actin cytoskeletons regulate the delivery of growth materials to growing root cells during root growth (Blancaflor et al., 2006; Yang et al., 2014). Thus, actin cytoskeletons polymerizing protein mutations disorganize the actin cytoskeletons resulting cellular distortion or growth reduction (Mathur and Hülskamp, 2002).

The double mutant *fh1-1/arp3-1* expressed the shortest root phenotype compared to the wild type and the other two single mutants. This response appears to be associated with a slower primary root growth rate. This *fh1-1/arp3-1* double mutant is based on the mutation of *AtFH1* and *AtARP3* genes, both of which are responsible for nucleation, polymerization and assembly of actin cytoskeletons (Wang et al., 2014). The plant formin protein family is also involved in microtubule reorganization by mediating microfilament-microtubule crosstalk in *Arabidopsis* and thus is considered to be one of the key regulators of microfilament and microtubules (Rosero et al., 2016; Rosero et al., 2013; Blancaflor, 2000). Several articles reported that formin proteins regulate tip growth, cell division, and cell expansion (Cheung and Wu, 2004; Favery et al., 2004; Deeks et al., 2005; Fitz Gerald et al., 009; Li et al., 2010; Yang et al., 2011; Zhang et al., 2011). They also play important roles in some of the fundamental processes including plant cell growth and plant development (Wang et al., 2012). It is also now established that important actin cytoskeleton regulator ARP2/3 complex is required for the development of higher plants (Uhrig et al., 2007; El-Din El-Assal et al., 2004; Le et al., 2003; Li et al., 2003; Mathur et al., 2003; Saedler et al., 2004). The mutation in ARP2/3 complex components including *AtARP3* exhibited several developmental defects in *Arabidopsis thaliana*, such as uncoordinated trichome cell expansion resulting in distorted trichome (Hülskamp et al., 1994), elongated hypocotyl cell tear out the epidermal cell layer, abnormal epidermal pavement cell lobbing and outward bending (Uhrig et al., 2007; El-Din El-Assal et al., 2004; Le et al., 2003; Li et al., 2003; Mathur et al., 2003; Saedler et al., 2004), reduced and wavy growth of root hairs in *ARP2* mutant (Li et al., 2003; Mathur et al., 2003). As mentioned, root growth is the result of cell division in the meristematic zone, anisotropic cell expansion in the elongation zone and cell differentiation in the differentiation zone, *AtFH1* may modulate root growth through participating in cell division, cell tip growth and diffuse expansion of plant cells (Wang et al., 2012). The *AtFH1* mutation in *fh1-1/arp3-1* plants may facilitate this phenotypic variation from the wild type by altering the dynamic organization of actin

cytoskeletons in root cells or affecting cell growth and expansion. That the single mutant *fh1-1* and wild type did not show any significant difference in root growth was a confirmation of (Rosero et al., 2013). In that experiment, the *AtFH1* gene mutant showed a distinct root growth phenotype when the seedlings were grown on actin and microtubule disrupting drug treated media. Conversely, the same mutant did not show any root growth phenotype compared to wild type under normal conditions, suggesting the plant formin proteins containing the same conserved functional domains may lead to the functional redundancy between plant formin protein members (Rosero et al., 2013).

At 4 days after germination, both the *fh1-1/arp3-1* double mutant and *arp3-1* single mutant seedlings produced thicker primary roots than the wild type and *fh1-1* single mutant. In addition, altered production of the lateral roots in the double mutant and *arp3-1* single mutant was largely absent in the *fh1-1* single mutants and wild type seedlings. These results suggest that *AtARP3* is responsible for thickening of the primary root and formation of lateral root at the early seedling stage of *Arabidopsis thaliana*.

By contrast the *arp3-1* mutant showed significantly higher root growth rate compared to the wild type. Root growth rate in *AtARP3* encoded *DIS1* mutant was reported to have no difference after gravistimulation compared to the wild type *Arabidopsis* (Zou et al., 2016) and the authors suggested *DIS1*/*ARP3* had no effect on root growth. But our present study suggested that *AtARP3* has a negative effect on root growth, although some studies reported that *AtARP3*, a component of ARP2/3 complex stimulated root growth in varied environmental conditions, i.e., *arp3* mutant showed short root phenotype under increasing fluence rate of monochromatic red, F-red and blue light conditions (Dyachok et al., 2011). In animal cells, finger like protrusion that contains mostly actin bundles is initiated by ARP2/3 complex, but it is not needed for elongation of the protrusion which needs formins to push the membrane forward to elongate the protrusion (Lee et al., 2010). Similarly in plant system formins are responsible for tip growth of the cells and participate in cell division (Wang et al., 2012). The previous study revealed that ARP2/3 mutants exhibited over production of actin cables indicating enhance function of formins in these mutants (Brembu et al., 2004) which may be the reason for increased root growth rate in *arp3-1* mutant under the present study.

Furthermore, a single class I formin *ATFH8* gene mutant *atfh8-1* seedlings exhibited similar root growth rate compared to the wild type (Xue et al., 2011). In the present study, the *fh1-1* and wild type plants also did not show any significant difference in root growth rate. Because *Arabidopsis* class I formins share characteristics clade specific and conserved domain structures, it is rare to get distinct phenotypic effects through a single formin mutation due to functional redundancy (Grunt et al., 2008; Deeks et al., 2002; Rosero et al., 2013). Consistent with this, most of the characteristics studied were largely similar between *fh1-1* mutant and wild type plants. In root growth and development, actin cytoskeletons play much more important roles than microtubules, because *fh1-1* mutant exhibited short root phenotype with lower root growth rate compared to the wild type upon actin disrupted drug treatment, whereas disruption of microtubules by inhibitor treatment showed a similar effect in *fh1-1* mutant and wild type plants (Rosero et al., 2013). These provide evidence that the short root phenotype and lower root growth rate in *fh1-1/arp3-1* double mutant seedlings are the effect of double mutations of *AtFH1* and *AtARP3* genes, both of which are responsible for actin cytoskeleton polymerization. LatB treated *fh1-1* showed distorted cell expansion such as short and expanded cells in small and wider roots, suggesting *AtFH1* mutation causes cell expansion defect rather than cell division (Rosero et al., 2013; Baluska et al., 2001). Thus, it is suggested both *AtFH1* and *AtARP3* are responsible for mediating the actin depended cell expansion in root elongation zone.

There are two different hypotheses related to actin cytoskeleton involvement in root gravisensing: the actin-tether model (Baluska and Hasenstein, 1997) and the tensegrity model (Yoder et al., 2001). According to the actin-tether model, a distinct connection of actin cytoskeleton or microfilaments (MFs) between the amyloplast and plasma membrane mediate the gravisensing, indicating disruption of AFs results in reduced gravitropic response. The actin cytoskeleton disrupted double mutant *fh1-1/arp3-1* exhibited increased gravitropic response that is in contrast to this model but supportive of the latter model in which disruption of actin cytoskeleton network in the central region of columella cell mediates the gravisensing (Yoder et al., 2001). The *fh1-1* single mutant and wild type seedlings showed similar bending in roots upon gravistimulation indicating the disruption of linear actin cytoskeleton may have no effect on gravitropism as formin proteins are responsible for polymerizing linear actin cytoskeleton. But in rice, a class II formin

(that nucleate the actin filaments) mutant *bui1* showed strong positive gravitropic response with enhanced bending angle in the root tip (Yang et al., 2011). This suggest that class I formin *AtFH1* functions on gravitropism may be rescued by other formin members in *Arabidopsis* (Grunt et al., 2008; Deeks et al., 2002; Rosero et al., 2013). Formin mediated PIN protein redistribution and auxin transport in root cells of higher plants were not reported yet. So formin1 induced root gravitropic response is not well reported. But *AtFH1* was reported to be involved in microtubule reorganization in *Arabidopsis* (Rosero et al., 2013; Rosero et al., 2016). Treatment with actin disrupting drugs induces microtubule reorganization in the roots indicating the importance of actin-microtubule crosstalk in root growth and gravitropism (Blancaflor, 2000). This suggests that along with actin cytoskeleton, *AtFH1* modulate gravitropism by reorganizing microtubule in root. But it was reported that *ARP3* has specific role in gravitropism (Reboulet et al., 2010; Zou et al., 2016). By contrst, *ARP3* gene mutant *dis1* showed the impaired root tip curvature that was reduced curvature compared to wild type in dark grown seedling but there were no significant differences in light grown seedlings (Reboulet et al., 2010). Consistent with this result, light grown *arp3-1* single mutant did not show any significant difference in root curvature compared to wild type after gravistimulation under the present study. LatB treated *Arabidopsis* root showed increased sedimentation of amyloplast in columella cells that promoted root curvature (Hou et al., 2004). Consistent with these findings, the higher gravitropic response of *fh1-1/arp3-1* plants may be due to the disruption of actin cytoskeleton through the mutation of both actin polymerizing *AtFH1* and *AtARP3* genes. This suggest that *AtFH1* and *AtARP3* genes are both involved in controlling the actin mediated gravitropism in higher plants.

The cytoskeleton reorganization and vesicle trafficking provide the driving force for the elongation of root hairs (for review, see Libault et al., 2010). Plant formins that are responsible for the nucleation and polymerization of linear actin cytoskeleton also regulate tip growth, cell division, and cell expansion (Cheung and Wu, 2004b; Favery et al., 2004; Deeks et al., 2005; Fitz Gerald et al., 009; Li et al., 2010; Yang et al., 2011; Zhang et al., 2011). Another important branched actin cytoskeleton polymerizer *ARP3* is well reported to be involved in cell shape formation in trichome and epidermal pavement cells (Pei et al., 2012; Mathur, 2003; Blancaflor et al., 2006), but it also participates in tip growth and cell morphogenesis (Pei et al., 2012; Finka et al., 2008). So the short root hair in the *fh1-1/arp3-1* double mutant and *arp3-1* single mutant compared to the wild type

may be due to lack of *AtFH1* and *AtARP3* mediated proper actin cytoskeleton organization. It was reported that rice formin1 (*OsFH1*) plays an important role in root hair development, as *OsFH1* mutant showed stunted or defective growth and elongation of root hair when seedlings were grown in submerged condition in solution, whereas air born roots showed normal root hair development (Huang et al., 2013). Consistent with this, *fh1-1* single mutant did not show any distortion or stunted growth in root hair compared to the wild type under the present study. The over expression of full length *Arabidopsis* formin8 gene exhibited distinguishable changes in root hair development and its actin cytoskeleton organization (Yi et al., 2005). As a possible impact of *AtFH1* mutation in combination with *AtARP3* mutation may contribute to the root hair phenotype of *fh1-1/arp3-1*, as *AtFH1* single gene mutation effect can be minimized by other formin members due to functional redundancy (Rosero et al., 2013). There were some conflicting results reported about the involvement of ARP2/3 complex in root hair development (Guimil and Dunand, 2007). Some experimental results showed that SCAR/WAVE-ARP2/3 mutants had no effect on root hair development (Le et al., 2003; Brembu et al., 2004; El-Din El-Assal et al., 2004; Djakovic et al., 2006), but some results showed mild root hair phenotype (Li et al., 2003; Mathur, 2003). The shorter root hairs of *arp3-1* single mutant is phenocopied early research findings where loss of *ARP3* functions produced shorter and sometimes sinuous root hairs (Pei et al., 2012; Mathur, 2003). In another experiment the root epidermal cells were studied in *arp3-1* mutant and were found to have a slightly wavy pattern of root hairs, but other root epidermal cells were normal (Li et al., 2003). In a special condition of growing root hair rapidly the *dis1*/*arp3* mutant showed sinuous, shorter root hair (350 ± 200 μm), whereas the wild type showed longer root hair (800 ± 150 μm) (Mathur, 2003). These results support the short root hair phenotype of *fh1-1/arp3-1* double mutant and *arp3-1* single mutant may be contributed by the mutation of *AtARP3*.

The root hair density was well studied in response to nutrient deficiency (i.e., phosphorus) and metallic toxicity in the soil (Bahmani et al., 2016; Stetter et al., 2017). The direct relation between actin cytoskeleton and root hair density was not reported. But it was reported that plant hormones auxin, ethylene and strigolactones control root hair density through their complex effects on general root growth (Stetter et al., 2017). In an experiment *ROOT HAIR DEFFECTIVE6* mutant *rhd6* exhibited reduced number of root hairs compared to wild type but that effect was rescued by addition of auxin (IAA) and ethylene precursor (ACC) (Masucci and Schiefelbein, 1994; Menand

et al., 2007). It is likely that actin cytoskeleton may be involved in regulating the cellular auxin homeostasis, and disruption of *AtFH1* and *AtARP3* genes may result in the reduced root hair density in double mutant *fh1-1/arp3-1* and single mutant *arp3-1* compared to wild type, since actin cytoskeletons are normally redistributed to establish the proper auxin gradient through the whole plant (Lanza et al., 2012) by facilitating the auxin transporting machinery within the plants (Muday and Murphy, 2002). As most of the characteristics of *fh1-1* mutant are similar to the wild type may be due to the functional redundancy of other formin members and this is why the *fh1-1* single mutant exhibited increased root hair density.

The *fh1-1/arp3-1* is an actin disrupted double mutant possessed two actin filament polymerizing *AtFH1* and *AtARP3* genes mutations. Based on the spatial and temporal expression pattern of *Arabidopsis* formin like protein6 (*AtFH6*), it was reported that this protein may be involved in the early differentiation of the vascular tubular cells in the root apex during lateral root development (Favery et al., 2004). In the intact plant, the *Arabidopsis* formin protein8 (*AtFH8*) is involved in both primary and lateral root growth and development, as LatB treated *atfh8-1* exhibited reduced growth of primary and lateral roots compared to the wild type which was rescued by PAtFH8:AtFH8–GFP complementation, but the *atfh8-1* mutant and wild type *Arabidopsis* did not show any significant difference in root length, root growth rate and lateral root development because other formins might compensate the loss of *AtFH8* functions due to the functional redundancy (Xue et al., 2011). These findings suggest that *AtFH1* may be involved in the growth and development of lateral root and its mutation might contribute to the lateral root phenotype of *fh1-1/arp3-1* double mutant. As there was no significant difference in lateral root growth and development between *fh1-1* single mutant and wild type plants, this may be due to the functional redundancy of other formin members of *Arabidopsis thaliana.*

Research has been conducted on the initiation site of the lateral root and concluded that the root apical meristem is the initiation site of lateral root in plants (Dubrovsky et al., 2000). In some Polygonaceae and Cucurbitaceae, the lateral root primordia are initiated during the late embryogenesis of lateral root founder cells when they were in the meristematic state, suggesting that the ability for the initiation of lateral root is restricted within the root apical meristem (Gladish and Rost, 1993). It was also reported that the lateral root initiation was seen within approximately

1.4 mm up from root tip (Beeckman et al., 2001). In case of *fh1-1/arp3-1* and *arp3-1* we did not know the initiation time of lateral root in the founder cells, but the visible initiation of lateral roots was at the elongation zone of the primary root whereas visible initiation sites of lateral roots were consistent with previous findings in case of the *fh1-1* mutant and the wild type.

There are several genes reported to be responsible for the density of lateral root in *Arabidopsis*, but the involvement of actin cytoskeleton in this perspective was not reported. The mutation studies showed that a cyclin triple mutant *cyca2;234* exhibited reduced number of lateral roots compared to wild type (Chen et al., 2015). Another experiment reported that a double mutant *aura1aura2* with two genes (*AURA1, AURA2*) mutation produced few lateral roots which might be due to the cytokinesis defects and mis-oriented cell plates observed in lateral root primordia (Van Damme et al., 2011). It is well reported that actin and microtubule cytoskeletons are responsible for the determination of division plane in prophase stage and formation of cell plate during cytokinesis (Müller et al., 2009; Liu et al., 2011; Rasmussen et al., 2013; Li et al., 2015). Hormonal regulations are also important for normal density of lateral roots, as inhibition of shoot to root auxin flow using auxin transport inhibitor naphthylphthalamic acid (NPA) resulted in reduced number of lateral roots and this phenomenon was rescued through application of IAA apical to the inhibitor application (Reed et al., 1998). The Polaris gene mutant (*pls*) that showed enhanced ethylene signaling produced reduced lateral roots (Chilley et al., 2006) indicating over production of ethylene reduced the density of lateral roots. So the disruption of actin cytoskeleton in *fh1-1/arp3-1* double mutant might contribute to the reduced number of lateral roots by altering the cytokinesis in root apical cells or through inhibition of auxin movement from shoot to root by disrupting the proper actin cytoskeleton organizations.

The effect of ARP2/3 complex on lateral root growth and development has not been reported yet, but ARP2/3 complex and formins both are important for actin cytoskeleton polymerization. It was reported that formin mediated actin bundle is increased in ARP2/3 complex mutant and ARP2/3 complex activator NAP and PIR protein mutant (Brembu et al., 2004). It was also reported that *AtFH8* is specifically expressed in root meristem, vasculature and outgrowth point of lateral root and is involved in cell division and lateral root initiation (Xue et al., 2011). So increasing formin activity in ARP2/3 complex component mutant *arp3-1* may be responsible for increased lateral

root density in this mutant. Actin cytoskeleton is important for the distribution of auxin efflux or influx carrier in the root cells and disruption of actin filament organization by acting filament depolymerizing drug altered the localization of auxin transporter resulted in defective response of auxin on lateral root initiation (Hou et al., 2003; Yamamoto and Kiss, 2002). The proper response of auxin is mostly depended on appropriate organization of actin cytoskeleton (Lanza et al., 2012). The above discussions suggest that *AtFH1* may be directly involved in initiation timing, localization and development of lateral root, *AtARP3* is involved in this process mostly by maintaining the proper actin cytoskeleton organization in the root cells through polymerizing and assembling the branched actin cytoskeleton in *Arabidopsis thaliana*.

4.3 *AtFH1* and *AtARP3* are required for normal cell morphogenesis

In order to study cell growth and morphogenesis, *Arabidopsis* provides an excellent model system for studying root hairs, pavement cells, and trichome cells (Mathur and Hülskamp, 2002). The development of jigsaw puzzle shaped interdigitating pavement cell layers in the epidermis of cotyledons and leaves are associated with the coordinated cell wall expansions among the neighboring cells (Ivakov and Persson, 2013; Jacques et al., 2014). The assembly of protruding microtubule bundles (Panteris and Galatis, 2005), some microtubule-binding proteins, microtubule cytoskeleton (Wang et al., 2007; Ambrose et al., 2007), ARP2/3 complex mediated nucleation and assembly of actin cytoskeleton (Mathur, 2005), myosins (Ojangu et al., 2012), and the active function of membrane trafficking apparatus (Falbel et al., 2003; Zhang et al., 2011a) at the indentation or the neck region are involved for the formation of harmonized lobes in the pavement cells .

The jigsaw puzzle shape pavement cells of the mature leaves of wild type *Arabidopsis* exhibited a wavy cell outline of elongated lobes (Li et al., 2003) which is consistent with the findings of the present study. It was reported that formin 1 mutant produced the increased lobbing resulting in less circular pavement cells (Rosero et al., 2016), so the most elongated lobes in *fh1-1/arp3-1* double mutant and *fh1-1* single mutant may be the result of the *AtFH1* mutation. This is a contradictory result, because after initiation of the lobe, the outward protrusion of the lobe depends on the enrichment of the actin cytoskeleton at the lobe tip areas (Armour et al., 2015). Due to the

functional redundancy of the members of *Arabidopsis* formin family (Rosero et al., 2016), *AtFH1* mutation may cause the over expression of some formin members which can increase actin polymerization at the lobe tip (thick bundles of actin cytoskeleton at the lobe tips were observed under the present study) resulting in elongated lobes in the pavement cells. The *AtFH1* mutation caused stabilization of actin cytoskeleton and increased the end dynamics of microtubules in the root epidermal cells (Rosero et al., 2016). The *AtFH1* mutation in both *fh1-1/arp3-1* double mutant and *fh1-1* single mutant may modulate the microtubule dynamics to initiate lobes and stabilize the actin cytoskeletons at the lobe tip to elongate, which may be another possibility of increased lobbing within these mutants. The development of pavement cell lobes are linked to the cortical filamentous actin (F-actin) and hence ARP2/3 complex plays an important role in this process (Li et al., 2003). Early research revealed that mutants of ARP2/3 complex components like *arp2-1, arp2-2, arp3-1* and *arpc5-1* produced short lobes resulting less wavy outlines of pavement cells. Quantitatively the lobe height was dramatically reduced without affecting the neck width of the pavement cells in all of these mutants (Li et al., 2003). Consistent with these findings the reduced lobe height of the pavement cell in *arp3-1* mutant under the present study suggests that the branch actin cytoskeleton polymerization in the pavement cell especially at the initiated lobe tip is essential for the elongation of pavement cell lobes. The WAVE protein that is responsible for the activation of ARP2/3 complex (Frank et al., 2004; Gautreau et al., 2004) works alongside the ARP2/3 complex. Mutations in ARP2/3 complex components and WAVE genes results in misdirected cell expansion, as a result pavement cells fail to produce lobe (Mathur, 2003). The aberrant pavement cell shapes were observed in all the SCAR/WAVE and ARP2/3 genes mutants (Guimil and Dunand, 2007). The lobes in the epidermal pavement cells were almost absent in all *ARP2*, *ARP3*, *ARPC5* genes mutants (Hülskamp et al., 1994; Li et al., 2003; Mathur, 2003). All of these results prove that *AtARP3* is obviously needed for the elongation of lobes in the interdigitating epidermal pavement cells in *Arabidopsis* leaves.

The actin cytoskeleton and microtubule distribution and arrangement are crucial for pavement cell morphogenesis (Fu et al., 2002; Lin et al., 2013a). The lobe outgrowth is mediated by the cortical actin cytoskeleton through promoting the local growth in the pavement cells (Frank and Smith, 2002). During the lobe formation, the actin cables are arranged along the growth axis and dynamic actin cytoskeletons localize to the tip of the growing lobes of the pavement cells (Han et al., 2015).

In wild type *Arabidopsis*, the actin filaments formed dense actin cable network in the pavement cells whereas constitutive expresser of pathogenesis-related gene1 mutants *cpr1-j594* and *cpr1-j2928* would not been able to form obvious actin cable network in the pavement cells resulted reduced lobbing (Han et al., 2015). The compact actin cables network in wild type and lack of obvious network in *arp3-1* mutant under this study are consistent with those previous results. Although the actin cable network is not so organized in *fh1-1* mutant's pavement cells, *AtFH1* may be involved in the elongation of lobe by microtubule reorganization as it was reported that *AtFH1* is involved in microtubule end dynamics (Rosero et al., 2016). In the *fh1-1/arp3-1* double mutant lack of actin filaments indicated that they may be unable to be bound to the ABD2 domain. Another striking result may be a compensation about the elongated lobe formation in the double mutant *fh1-1/arp3-1,* where the double mutant of monomeric actin *act2act7* showed severely reduced lobbing in pavement cells (Kandasamy et al., 2009). So not only the actin cytoskeleton but also the monomeric actin may be responsible for elongated lobe in the pavement cells in *fh1-1/arp3-1* double mutant. The above discussions indicate that during lobe elongation *AtARP3* is directly involved by polymerizing the actin cytoskeleton and *AtFH1* is involved by reorganizing microtubule in the epidermal pavement cells.

The trichomes are the established model for studing the directional cell expansion in *Arabidopsis* (Schwab et al., 2000; Szymanski et al., 2000; Wasteneys, 2000; Smith, 2003). As the tip growth, cell division, and cell expansion are controlled by plant formins (Cheung and Wu, 2004; Favery et al., 2004 Deeks et al., 2005; Fitz Gerald et al., 2009; Li et al., 2010; Yang et al., 2011; Zhang et al., 2011b), the normal trichome structure in *fh1-1* single mutant may be due to the functional overlap of other formin family members (Rosero et al., 2016). The less distortion of *fh1-1/arp3-1* trichomes may also be due to the overexpression of other formin member (s) in absence or partial expression of *AtFH1*. The microtubules play an important role at the early stage of trichome cell development and its branching that have been revealed by the cell biological approaches (Mathur et al., 1999). There are several microtubule cytoskeleton associated proteins including kinesin-like protein (Oppenheimer et al., 1997), katanin-like protein (Burk et al., 2001), and α-tubulin (Abe et al., 2004) were reported to be involved in trichome branching. It was also reported that the FH2 domain of some plant formins modulate the formation of microtubule bundles by binding to the microtubules (Li et al., 2010b; Zhang et al., 2011b; Yang et al., 2011). These indicate that plant

formins are involved in trichome cell shape and branching, but it is difficult to get the distinct phenotype by single mutation of plant formins due to functional redundancy between the native members (Grunt et al., 2008; Deeks et al., 2002; Rosero et al., 2013) that reflected in normal trichome morphology of *fh1-1* single mutant and the less distorted trichome morphology in *fh1-1/arp3-1* double mutant. On the other hand eight genes including *ARP3* of the distorted group control the directionality of the expansion of trichome cells (Hülskamp et al., 1994; Schwab et al., 2000). The mutation in any of the distorted genes causes irregular growth of the trichomes which results in twisted or distorted trichome phenotype. In this distorted gene mutant the growth aberration of trichome cells occurred after initiation of the branches (Schwab et al., 2000) resulted in short or visually no branches. Consistence with this result his result, *arp3-1* single mutant exhibited similar trichome morphology under the present study. So *AtARP3* is responsible for the expansion growth of trichome cells especially after initiation of the branch when rapid expansion of branches is needed.

The F-actin formed intricate three-dimensional network of actin cytoskeleton and actin bundle parallel to the long axis of stalk and branches of mature trichome (Szymanski et al., 1999). Studies on the trichome distorted protein mutant *grl* showed very loosely organized actin filament bundle through the stalk and those bundle were less apparent to the branch tip of mature trichome (Szymanski et al., 1999). Consistent with these findings, both the distorted trichome producing double mutant *fh1-1/arp3-1* and single mutant *arp3-1* exhibited very loose actin filament bundling through the stalk compared to the wild type and almost diffused to the branch tip in case of *arp3-1* single mutant, but F-actin bundles were similarly apparent to the stalk and branch in case of double mutant. In some expanded areas of the stalk of trichome in *fh1-1/arp3-1* double mutant and *arp3-1* single mutant, the direction of the actin filaments was normal, but those areas were more vacuolated compared to the wild type. The similar findings also reported in the case of *grl* mutant where a normal F-actin distribution was observed in some over expanded areas of branches (Szymanski et al., 1999). The actin filaments in the trichome of *fh1-1* single mutant were uniformly distributed in the form of a compact long F-actin bundle along the stalk and branches as revealed in the wild type. In the branch point of trichome, *fh1-1* produced a dense actin filament nest that was only difference in the actin filament distribution between the trichome cells of *fh1-1* single mutant and the wild type. It was reported that cortical microtubule affected the initiation of

trichome branches and disruption of microtubule binding protein resulted in unusual number of branches (Tian et al., 2015; Nakamura and Hashimoto, 2009; Kong et al., 2010; Buschmann et al., 2009; Burk et al., 2001; Oppenheimer et al., 1997). On the other hand actin filament is responsible for elongation of trichome cells and disruption of actin filament through drug treatment or mutation of actin related proteins like ARP2/3 complex components exhibited abnormal trichome elongation with normal branch numbers (Mathur, 2003; Basu, 2004; Deeks et al., 2004; El-Din El-Assal et al., 2004; Szymanski, 2005; Djakovic et al., 2006). These indicated that mutation in the protein(s) responsible for microfilament and microtubule crosstalk will produce the distorted trichomes with unusual number of branches (Tian et al., 2015). As the formin proteins are involve in microtubule and microfilament crosstalk (Wang et al., 2012; Rosero et al., 2016; Rosero et al., 2013), it may be reflected in the double mutant. In agreement with these findings, *arp3-1* single mutant produced distorted trichome with impaired actin cytoskeleton distribution and normal branch numbers. By contrast, most of the trichomes in the double mutant *fh1-1/arp3-1* were two branched and actin cytoskeleton distributions were mostly affected in this mutant. Due to the functional redundancy other members of the formin protein family may rescued the effect of mutation in *fh1-1* single mutant (Rosero et al., 2016; Rosero et al., 2013).

The mesophyll cells are the major site of chlorophyll biosynthesis in plants. So, absorption of carbon dioxide (CO_2), production of oxygen (O_2), chloroplast biogenesis and chlorophyll synthesis are directly correlated to the proper development and functions of mesophyll cells. There are several genes involved in chlorophyll synthesis pathway and the mutation of genes caused the depletion in the chlorophyll amount resulted in pale color leaves on plants (Guan et al., 2016). The chlorophyll mutant of *Arabidopsis thaliana (*chlorina mutant- *ch3)* contained the chlorophyll amount about 1/10 to the amount of the wild-type *Arabidopsis* (Velemínský and Röbbelen, 1966). Consistent with this result, the mutation of *AtFH1* and *AtARP3* genes in the double mutant resulted in the reduced chlorophyll content and unusual color of the leaves. The experimental results showed that the chlorophyll content is proportional to the photosynthesis rate of the plant leaf (Haberlandt, 1882). It was also reported that the photosynthesis rate is positively correlated with the number of chloroplasts in the leaf (Kariya and Tsunoda, 1972). So, the lower number of chloroplasts in mesophyll cells may be one reason for the diminished content of chlorophyll in this double mutant comparing to the wild type. No significant difference in chlorophyll content of

mesophyll cells between wild type and *fh1-1* single mutant indicated that single *AtFH1* gene has no effect on chlorophyll biosynthesis or chloroplast development. Otherwise *AtFH1* mutation was complimented by other formin members due to functional redundancy (Grunt et al., 2008; Deeks et al., 2002; Rosero et al., 2013). Although *arp3-1* mutant contained lower number of chloroplasts in mesophyll cells it synthesized more chlorophyll like wild type and *fh1-1* single mutant. This may be due to chloroplast distribution pattern inside the mesophyll cells or internal structural difference of chloroplasts. Because the amount of total chlorophyll is mainly dependent on the structure of chloroplast like the thylakoid membrane stacking and granum differentiation. The chlorophyll content of *Arabidopsis* is also depended on the developmental and environmental condition (Velemínský and Röbbelen, 1966). Using map based cloning, a chloroplast precursor gene *YGL* was isolated and predicted to encode for cpSRP43 protein and *YGL* is responsible for chloroplast development. In that experiment *ygl-1* mutant showed yellow-green leaves through all developmental stages (Guan et al., 2016) indicating lower chlorophyll content. The above findings revealed that not only the chloroplast number of the cell but also the structure and development of chloroplast are responsible for chlorophyll content of plant's leaves. So individually *AtFH1* or *AtARP3* gene may have no effect on chlorophyll content, but collectively they may be involved in chloroplast biogenesis and development and hence they alter the chlorophyll content of the leaves in the double mutant plant.

There are eight different proteins that are essential for cp-actin filament (chloroplast-actin filament) based chloroplast movement and positioning (Suetsugu and Wada, 2016). Among them CHLOROPLAST UNUSUAL POSITIONIGN1 (*CHUP1*), KINESIN-LIKE PROTEIN FOR ACTIN-BASED CHLOROPLAST MOVEMENT (*KAC*) and a glutaredoxin-like protein THRUMIN 1 (*THRUM1*) are the actin binding proteins that are responsible for generation of cp-actin filament *in vitro* (Suetsugu and Wada, 2016; Oikawa et al., 2003; Suetsugu et al., 2010; Whippo et al., 2011). It was reported that the single mutant *chup1* and double mutant *kac1kac2* exhibited unusual chloroplast movement and defective anchoring of chloroplast to the plasma membrane (Oikawa et al., 2003; Oikawa et al., 2008; Suetsugu et al., 2010). As both *AtFH1* and *AtARP3* are actin binding proteins and responsible for actin filaments polymerization, they have the role on chloroplast movement, positioning and anchoring to the plasma membrane. In the mesophyll cells of double mutant *fh1-1/arp3-1,* a few fine actin filaments were seen to form the

thin actin filament network associating to the chloroplast compared to the wild type and both single mutants that may cause the unusual positioning and movement of the chloroplasts resulting in lower chlorophyll contents, because cp-actin filaments reorganization is needed for mediating light accumulation response of chloroplasts (positive response to mild light for sufficient light accumulation) and light avoidance response of chloroplast (negative response to strong light for avoiding photo damage) (Iwabuchi and Takagi, 2010). So these responses ensure the higher photosynthesis rate resulted in increased chlorophyll content. In *arp3-1* mutant actin cytoskeleton organization was normal comparing to the wild type indicating chloroplasts can show the proper accumulation and avoidance responses resulting in normal chlorophyll synthesis. In *fh1-1* mutant chloroplasts were tightly associated with the fine actin filaments of thin actin filament network which was much compact than the wild type. This indicated single formin gene mutation may induce the expression of functionally redundant one or more other formin members for nucleation and elongation of more actin filaments (Rosero et al., 2016; Rosero et al., 2013; Wang et al., 2012). So, it may be concluded that the positioning is more important than the number of chloroplasts for chlorophyll biosynthesis and *AtFH1* and *AtARP3* may be involved in proper chloroplast movement and positioning by reorganizing the actin cytoskeleton in mesophyll cells.

4.4 The overall fertility of *Arabidopsis* is vastly affected by combined mutation of both *AtFH1* and *AtARP3* genes

Through mutation studies several genes were identified to be involved in floral organ development in *Arabidopsis*. ABC model's genes mutants produced positional and structural abnormalities in floral organs, such as *ap1* (*apetala1)* mutant exhibited leaf like sepals and no petals, in *ap2* mutant sepals were replaced by carpels and petals were replaced by stamens, stamens were transformed into carpels and petals were transformed into sepals in *ap3* and *pl* (*pistillata*) mutants, *ag* (*agamous)* mutant showed multiple secondary flower primordia in the center of the flower, and the *SEPALLATA* gene mutant did not produce any visible flower phenotype (Myakushina et al., 2009). Besides these well-known genes several other genes have been identified to contribute to the flower phenotype. In an experiment, the transcription factor TCPs targeting micro-RNA (*miR319a*) mutant *miR319a*^{129} produced short and narrow petals, and short and abnormal stamens (Nag et al., 2009). Similarly the double mutant *fh1-1/arp3-1* exhibited short and narrow petals and

stamens of variable sizes compared to the wild type and both *fh1-1* and *arp3-1* single mutants under the present study. One of the targets of *miR319a* is TCP3 (Nag et al., 2009), and interestingly the TCP3 negatively regulates the auxin response (Koyama et al., 2010). In *miR319a*^{129} mutant, TCP was upregulated (Nag et al., 2009) indicating that auxin response was suppressed in that mutant which may be a possible reason for flower abnormality. It was reported that disruption of the genes that are associated with signaling, biosynthesis, and transport of auxin resulted in flowers with multiple abnormalities (Okada et al., 1991; Smith and Zhao, 2016; Cecchetti et al., 2008; Wu et al., 2006). Both *pin1* mutant and polar auxin transport inhibitor treated plants exhibited similar but severely defective flower phenotypes (Okada et al., 1991). A double mutant of auxin response factor (ARF) genes *arf6 arf8* showed various defects in flowers, such as shortened petals and stamen filaments, failure to release pollen and production of abnormal ovules (Smith and Zhao, 2016; Nagpal, 2005; Wu et al., 2006). Although direct actin filament mediated floral development is not reported, but actin cytoskeleton is essential for proper auxin homeostasis and its response through the whole plant (Lanza et al., 2012). So tiny flower, short and narrow petals, aberrant stamen length may be the consequences of auxin suppressions by actin cytoskeleton disruption in *fh1-1/arp3-1* double mutant.

Chromosome rearrangement and deletion in the T-DNA insertion mutants can lead to the defect in pollen development (Nacry et al., 1998; Tax and Vernon, 2001; Oh et al., 2003). Random targeting of pollen expressed genes causes the pollen development defect in *Arabidopsis thaliana* (Procissi et al., 2001) which is the general effect of mutation on the pollen development. In the present study along with the normal pollen, the double mutant produced some tiny, shrunken and irregular shaped pollen grains. The double mutant not only produced very low amount of pollen but also *in vitro* pollen germination rate of the double mutant was around half of the wild type and both single mutants. This indicates the abnormal pollen grains in the double mutant were non-viable and/or aborted. The first *Arabidopsis* male gametophytic mutant SIDECAR POLLEN (*scp*) mutant plants (Chen and McCormick, 1996) produced aborted pollen and very low amount of pollen grains (Procissi et al., 2001), indicating the double mutant is a male gametophytic mutant. That indication was more apparent when crossing between wild type pistil and double mutant pollen resulted in short silique resembling double mutant's silique.

It was reported that before hydration of pollen, the actin cytoskeletons existed as a form of compact bundle which was dispersed to thin actin network uniformly throughout the whole pollen after hydration or activation during germination in *arsr45-1* mutant. This dispersion caused de-polymerization of some actin cytoskeletons that was higher than the wild type contributing to increased amount of monomeric actin resulting in higher rate of germination compared to the wild type (Cao et al., 2013). This is why, the actin cytoskeleton disrupted double mutant *fh1-1/arp3-1* might not been able to contribute enough monomeric actin to the pollen cytoplasm upon activation of the pollen resulted poor germination rate (*in vitro* and *in vivo*). As reported, overexpression of *LISR28* (an ortholog of *AtSR35*) inhibited pollen germination, because upon pollen hydration, all the actin filaments of the bundle dispersed to the whole pollen without de-polymerization of the actin filaments contributing no monomeric actin (Cao et al., 2013). Among the *Arabidopsis* formins, *AtFH3* which is responsible for actin bundle nucleation in pollen grains was highly expressed in pollen and suppressing of *AtFH3* with RNAi resulted in reduction of actin filaments in *AtFH3* RNAi pollen (Ye et al., 2009). This indicates upon pollen hydration, less amount of monomeric actin will be contributed to *AtFH3* RNAi pollen resulting in a lower rate of germination (Ye et al., 2009). As *AtFH1* is also responsible for nucleation, assembly and elongation of actin filaments (Michelot, 2005; Wear and Cooper, 2004), it may have an influence on pollen germination. But due to the functional redundancy among the formin family members (Rosero et al., 2016; Rosero et al., 2013), may contribute to the similar pollen germination rate in *fh1-1* single mutant compared to the wild type. Early research reported that *ARP3* encoded *DIS1* was not required for pollen germination, as *dis1* plants produced siliques with normal seed set (Le et al., 2003). Consistent with this result *arp3-1* mutant exhibited pollen germination rate similar to that of the wild type and produced lots of seeds. It is also possible that ARP2/3 complex components may be supplemented with redundant functionality (Harries et al., 2005) resulting in no significance difference within *in vitro* pollen germination rates of *arp3-1* compared to the wild type.

The cell wall materials, proteins and other membrane components are transported to the pollen tube growing tip during germination and rapid tube growth through vesicle trafficking system (Krichevsky et al., 2007; Chebli et al., 2013), facilitated by F-actin cytoskeleton. In the present study, the pollen tube growth was slow within *in vitro* culture in *fh1-1/arp3-1* double mutant. It

was reported that inhibition of the main *Arabidopsis* pollen formin *AtFH3* expression resulted in reduced pollen tube growth (Ye et al., 2009) and inhibition of *AtFH5*, another important pollen formin altered the pollen tube growth (Cheung et al., 2010; Mathur and Hülskamp, 2001). It is also reported that *AtFH1* may regulate actin filament nucleation at the apical region of pollen tube, but in contrast ARP2/3 complex did not have any obvious effect on pollen tube (Qu et al., 2015). These results suggest that the slow growth of pollen tube (*in vitro*) in the double mutant may be due to the partial mutation of *AtFH1* not by the null mutation of *AtARP3*. This is also supported by actin filament growth outward linearly from the apical membrane (Qu et al., 2015). But *in vitro* pollen tube growth in both *fh1-1* and *arp3-1* was reduced compared to the wild type indicated that both *AtFH1* and *AtARP3* have positive impact on pollen tube growth.

The silique size and seed content of siliques are also dependent on the proper actin cytoskeleton dynamics, as reported that ARP2/3 complex activating NAP and PIR proteins encoding genes mutant of *Arabidopsis Atnap-1* and *Atpir-1* exhibited short and reduced seed containing siliques (Li et al., 2004). In the present study the double mutant *fh1-1*/ *arp3-1* also showed very short siliques with empty seed chamber resulted in a few seeds in the silique. As this double mutant possessed two main stream actin cytoskeleton polymerizing proteins mutation which might cause the disruption in actin organization in siliques resulted in short silique phenotype. But the empty seed chamber indicated the seed abortion caused by partial female gametophyte lethality (Shockey et al., 2016). The double mutant also produced some empty siliques that also indicated female gametophytic lethality, because ovary developed but seed set did not occurr. As it was reported that post pollination development of the ovary needs auxin (Vivian-Smith et al., 2001; O'Neill and Nadeau, 2010; Gustafson, 1936) and this auxin is supplied first by pollen and pollen tube, later fertilized ovule (O'Neill and Nadeau, 2010; Gustafson, 1939). These results indicated that pollination occurred with viable pollen grains in the double mutant, but it would not been able to produce seed due to female gametophyte lethality. In the present study, there were no differences in seed set of *fh1-1* and *arp3-1* single mutants compared to the wild type. Due to the functional redundancy among the family members, *AtFH1* mutation may not affect any gametophytic development. In case of *arp3-1* mutant it was supported by the findings of (Le et al., 2003) where *ARP3* encoded *DIS1* mutant *dis1* showed normal seed set in the silique suggested *AtARP3* may not affect gametophytic development in *Arabidopsis*.

CHAPTER 5: SUMMARY AND CONCLUSIONS

In all eukaryotic cells actin exists in both monomeric G-actin and filamentous F-actin forms. F-actin belongs to the actin cytoskeleton that is polymerized from the G-actin by the action of several actin cytoskeleton polymerizing proteins, such as *AtFH1* and *AtARP3* in *Arabidopsis thaliana*. The following summarized discussions of the findings indicate that *AtFH1* and *AtARP3* affect several biological processes by reorganization of actin cytoskeleton in *Arabidopsis*.

On phenotypic observations, *fh1-1/arp3-1* mutant produced small plants with short, narrow and pale green leaves compared to the wild type and both the single mutants. The mature plants of the double mutant were less branched with short siliques, some of which lacked seeds, whereas the wild type and both the single mutants produced similar highly branched plants with plenty of normal siliques with a full seed set. At the rosette leaf stage the average size of the whole plants of *fh1-1/arp3-1* mutants was significantly smaller than the wild type and both the single mutants. There was no significant difference in plant size between *fh1-1* single mutant and the wild type, but *arp3-1* mutant produced significantly smaller plants compared to the wild type and the *fh1-1* single mutant at the rosette leaf stage.

Seedlings of the *fh1-1/arp3-1* mutant line exhibited a short root phenotype with a significantly lower growth rate compared to the wild type, as well as the other single mutants. The double mutant and *arp3-1* mutant produced significantly thicker primary root compared to the wild type and the *fh1-1* single mutant at 4 DAG. The double mutant showed the highest root gravitropic response compared to the wild type and both the single mutants, whereas no significant differences were observed in gravitropic responses among the wild type and the single mutants. The root hair length was significantly different among all the mutants and the wild type where the double mutant produced the shortest root hairs with lowest root hair density and *fh1-1* single mutant produced the longest root hairs with highest root hair density, though there was no significant difference in root hair density between the double mutant and *arp3-1* single mutant. The double mutant showed unusual localization of the lateral roots that were emerged in a bunch from the root shoot junction and were distributed within one-third region from the base of the primary roots. Both the single mutants and the wild type plants produced lateral root along the whole length of primary root

mostly in alternate arrangements. The wild type and all the mutants exhibited significantly different density of lateral roots where the double mutant and *fh1-1* mutant showed the lowest and highest lateral root density respectively.

There was no significant difference in leaf epidermal pavement cell circularity of the double mutant, as well as *arp3-1* mutant compared to the wild type, but *fh1-1* mutant showed the lowest circularity producing highest lobbing in the pavement cells. In the double mutant a few actin filaments crosslinked each other and distributed irregularly in the pavement cells. The *arp3-1* mutant exhibited no changes of actin cytoskeleton network having a few long actin filaments irregularly and un-uniformly distributed in the pavement cells. The *fh1-1* single mutant produced loose and thin actin cytoskeleton network comparing to the wild type.

The double mutant and the *arp3-1* mutant produced distorted leaf trichomes compared to the wild type and the *fh1-1* single mutant. Some trichomes of the double mutant were very long and expanded stalked with long branch that were not found in *arp3-1* mutant. The *fh1-1* single mutant showed the normal trichome phenotype similar to the wild type. Without stopping in the branch point the long actin filaments were eventually and longitudinally distributed from base to the end of the branch along the stalk in double mutant trichomes whereas, arising from the base of the trichome the actin filament elongated up to the branch point from where new actin filaments were distributed longitudinally to the end of the branch in wild type and both the single mutants. In the double mutant most of the areas along the circumferences of the stalk and branch were occupied by the vacuole and few actin filament were distributed in the trichome cells. The actin filaments were thin and loosely distributed in *arp3-1* single mutant compared to the wild type, but the direction of ATFs through the stalk and branches was similar to that of the wild type.

The chlorophyll content of the double mutant was only about 2/3 of wild type and all other single mutants. The wild type, the *fh1-1* and the *arp3-1* single mutants have no significant difference in chlorophyll content of the leaves, whereas *fh1-1/arp3-1* contained significantly lower amount of chlorophyll compared to that of the wild type and both the single mutants. All the mutants and wild type plants contained significantly different numbers of chloroplasts per mesophyll cells where the double mutant contained the lowest and the wild type contained the highest number of

chloroplast per mesophyll cell. In mesophyll cells of the double mutant, the longitudinal thick actin arrays were more apparent, but few fine actin filaments associating the chloroplasts were observed, whereas uniformly distributed thin actin filament network associating all the chloroplasts was seen in wild type mesophyll cells. In *fh1-1* single mutant apart from the longitudinal thick actin filament arrays, a compact thin actin filaments network covering the entire mesophyll cell was formed. The longitudinal thick actin filament arrays and randomly oriented thin actin filaments network both were clearly visible in the *arp3-1* single mutant.

The double mutant produced tiny flowers with distinct floral organ structures compared to the wild type and both the single mutants. The stamens and petals were vastly affected in the double mutant. The size of pollen grains of the double mutant was smaller compared to the wild type and both the single mutants. Almost all of the pollen grains in the wild type and both the single mutants were normal in size and shape, whereas some of the pollen grains were normal and some were tiny and distorted with irregular pollen coat topology in the double mutant. Average *in vitro* pollen germination rate of the double mutant was significantly lower than that of the wild type and both the single mutants. There was also no significant difference of *in vitro* pollen germination rate among the wild type and both the single mutants. The aniline blue staining of pollen tube inside self-pollinated pistil showed few number of pollen tubes were elongated and passing through the transmitting tissue of the pistil in a zigzag fashion in the double mutant, whereas the wild type and both the single mutant produced abundant pollen tubes, all of which passed straightly through the transmitting tissue of the pistil. The silique size of the double mutant was significantly shorter having $1/3^{rd}$ in length to the wild type and both the single mutants, although both the single mutants and wild type produced significantly different size siliques. The average seed content of the silique in the double mutant was around $1/20^{th}$ to the wild type and both the single mutants.

In addition *AtFH1* and *AtARP3* mutants exhibited altered biotic responses upon non-adapted powdery mildew Bgh inoculation. All the mutants showed significantly higher penetration rate, unusual collose deposition and aberrant actin cytoskeleton organization at the penetration site compared to the wild type. The mutants also showed anomalous abiotic responses upon exposure to the drought stress. All the mutants possessed lower leaf surface temperature compared to the wild type in different time points after imposing drought stress. The aberrant actin cytoskeleton

organization was observed in the guard cells of all the mutants. The detailed results of the biotic and abiotic stress responses of the mutants were added to the appendices.

This study conclude that *AtFH1* and *AtARP3* mediated actin cytoskeleton organization is important for normal plant phenotype, root development, some special cell morphogenesis and fertility in *Arabidopsis thaliana*. The experimental findings are evident enough to draw the final conclusion that *AtFH1* and *AtARP3* are involved in several developmental processes and they regulate these processes by triggering the actin cytoskeleton dynamics in *Arabidopsis thaliana*.

The future studies should be focused on in-depth molecular mechanism and signaling of *AtFH1* and *AtARP3* mediated root development and gravitropism. There were few studies reported weakly about the involvement of *AtARP3* in fertility, whereas no studies reported yet about *AtFH1* affected fertility in *Arabidopsis thaliana*. The findings of the present study indicate that both *AtFH1* and *AtARP3* have tremendous effect on root development and fertility of the *Arabidopsis thaliana*. So, both *AtFH1* and *AtARP3* mediated fertility including male and female gametophyte development of plant should be an emerging field of research.

REFERENCES

Aaziz, R., Dinant, S., and Epel, B.L. (2001). Plasmodesmata and plant cytoskeleton. Trends Plant Sci. *6*, 326–330.

Abe, T., and Hashimoto, T. (2005). Altered microtubule dynamics by expression of modified alpha-tubulin protein causes right-handed helical growth in transgenic Arabidopsis plants. Plant J. Cell Mol. Biol. *43*, 191–204.

Abe, T., Thitamadee, S., and Hashimoto, T. (2004). Microtubule defects and cell morphogenesis in the lefty1lefty2 tubulin mutant of Arabidopsis thaliana. Plant Cell Physiol. *45*, 211–220.

Abera Gebrie, S. (2016). Biotrophic Fungi Infection and Plant Defense Mechanism. J. Plant Pathol. Microbiol. *7*.

Adamowski, M., and Friml, J. (2015). PIN-Dependent Auxin Transport: Action, Regulation, and Evolution. Plant Cell Online *27*, 20–32.

Aist, J.R. (1976). Papillae and Related Wound Plugs of Plant Cells. Annu. Rev. Phytopathol. *14*, 145–163.

Ambrose, J.C., Shoji, T., Kotzer, A.M., Pighin, J.A., and Wasteneys, G.O. (2007). The Arabidopsis CLASP Gene Encodes a Microtubule-Associated Protein Involved in Cell Expansion and Division. PLANT CELL ONLINE *19*, 2763–2775.

An, Y.Q., Huang, S., McDowell, J.M., McKinney, E.C., and Meagher, R.B. (1996). Conserved expression of the Arabidopsis ACT1 and ACT 3 actin subclass in organ primordia and mature pollen. Plant Cell *8*, 15–30.

Andrés, F., and Coupland, G. (2012). The genetic basis of flowering responses to seasonal cues. Nat. Rev. Genet. *13*, 627–639.

Annis, S.L., and Goodwin, P.H. (1997). Recent advances in the molecular genetics of plant cell wall-degrading enzymes produced by plant pathogenic fungi. Eur. J. Plant Pathol. *103*, 1–14.

Armour, W.J., Barton, D.A., Law, A.M.K., and Overall, R.L. (2015). Differential Growth in Periclinal and Anticlinal Walls during Lobe Formation in Arabidopsis Cotyledon Pavement Cells. Plant Cell *27*, 2484–2500.

Assmann, S.M., and Wang, X.Q. (2001). From milliseconds to millions of years: guard cells and environmental responses. Curr. Opin. Plant Biol. *4*, 421–428.

Azarov, A.S., Tokarev, B.I., and Netchepurenko, A.E. (1990). Effect of sodium chloride on pollen germination and pollen tube growth in vitro in Arabidopsis thaliana (L.) Heynh (Arabidopsis Inf. Serv.).

Bahmani, R., Kim, D.G., Kim, J.A., and Hwang, S. (2016). The Density and Length of Root Hairs Are Enhanced in Response to Cadmium and Arsenic by Modulating Gene Expressions Involved in Fate Determination and Morphogenesis of Root Hairs in Arabidopsis. Front. Plant Sci. *7*.

Balkunde, R., Pesch, M., and Hülskamp, M. (2010). Trichome Patterning in Arabidopsis thaliana. In Current Topics in Developmental Biology, (Elsevier), pp. 299–321.

Baluska, F., and Hasenstein, K.H. (1997). Root cytoskeleton: its role in perception of and response to gravity. Planta *203*, S69-78.

Baluska, F., Salaj, J., Mathur, J., Braun, M., Jasper, F., Samaj, J., Chua, N.H., Barlow, P.W., and Volkmann, D. (2000). Root hair formation: F-actin-dependent tip growth is initiated by local assembly of profilin-supported F-actin meshworks accumulated within expansin-enriched bulges. Dev. Biol. *227*, 618–632.

Baluška, F., Jasik, J., Edelmann, H.G., Salajová, T., and Volkmann, D. (2001). Latrunculin B-Induced Plant Dwarfism: Plant Cell Elongation Is F-Actin-Dependent. Dev. Biol. *231*, 113–124.

Baluska, F., Jasik, J., Edelmann, H.G., Salajová, T., and Volkmann, D. (2001). Latrunculin B-induced plant dwarfism: Plant cell elongation is F-actin-dependent. Dev. Biol. *231*, 113–124.

Banno, H., and Chua, N.H. (2000). Characterization of the arabidopsis formin-like protein AFH1 and its interacting protein. Plant Cell Physiol. *41*, 617–626.

Barlow, P.W., and Baluska, F. (2000). CYTOSKELETAL PERSPECTIVES ON ROOT GROWTH AND MORPHOGENESIS. Annu. Rev. Plant Physiol. Plant Mol. Biol. *51*, 289–322.

Barrero, R.A. (2002). Arabidopsis CAP Regulates the Actin Cytoskeleton Necessary for Plant Cell Elongation and Division. PLANT CELL ONLINE *14*, 149–163.

Basu, D. (2004). Interchangeable functions of Arabidopsis PIROGI and the human WAVE complex subunit SRA1 during leaf epidermal development. Development *131*, 4345–4355.

Basu, D. (2005). DISTORTED3/SCAR2 Is a Putative Arabidopsis WAVE Complex Subunit That Activates the Arp2/3 Complex and Is Required for Epidermal Morphogenesis. PLANT CELL ONLINE *17*, 502–524.

Baum, S.F., Dubrovsky, J.G., and Rost, T.L. (2002). Apical organization and maturation of the cortex and vascular cylinder inArabidopsis thaliana (Brassicaceae) roots. Am. J. Bot. *89*, 908–920.

Bedinger, P.A., Hardeman, K.J., and Loukides, C.A. (1994). Travelling in style: the cell biology of pollen. Trends Cell Biol. *4*, 132–138.

Beeckman, T., Burssens, S., and Inzé, D. (2001). The peri-cell-cycle in Arabidopsis. J. Exp. Bot. *52*, 403–411.

Beemster, G.T., and Baskin, T.I. (1998). Analysis of cell division and elongation underlying the developmental acceleration of root growth in Arabidopsis thaliana. Plant Physiol. *116*, 1515–1526.

Beemster, G.T., and Baskin, T.I. (2000). Stunted plant 1 mediates effects of cytokinin, but not of auxin, on cell division and expansion in the root of Arabidopsis. Plant Physiol. *124*, 1718–1727.

Beltzner, C.C., and Pollard, T.D. (2004). Identification of functionally important residues of Arp2/3 complex by analysis of homology models from diverse species. J. Mol. Biol. *336*, 551–565.

Bielach, A., Podlesáková, K., Marhavy, P., Duclercq, J., Cuesta, C., Müller, B., Grunewald, W., Tarkowski, P., and Benková, E. (2012). Spatiotemporal regulation of lateral root organogenesis in Arabidopsis by cytokinin. Plant Cell *24*, 3967–3981.

Blancaflor, E.B. (2000). Cortical Actin Filaments Potentially Interact with Cortical Microtubules in Regulating Polarity of Cell Expansion in Primary Roots of Maize (Zea mays L.). J. Plant Growth Regul. *19*, 406–414.

Blancaflor, E.B. (2002). The cytoskeleton and gravitropism in higher plants. J. Plant Growth Regul. *21*, 120–136.

Blancaflor, E.B. (2013). Regulation of plant gravity sensing and signaling by the actin cytoskeleton. Am. J. Bot. *100*, 143–152.

Blancaflor, E.B., and Masson, P.H. (2003). Plant gravitropism. Unraveling the ups and downs of a complex process. Plant Physiol. *133*, 1677–1690.

Blancaflor, E.B., Wang, Y.-S., and Motes, C.M. (2006). Organization and function of the actin cytoskeleton in developing root cells. Int. Rev. Cytol. *252*, 219–264.

Blanchoin, L., and Staiger, C.J. (2010). Plant formins: Diverse isoforms and unique molecular mechanism. Biochim. Biophys. Acta BBA - Mol. Cell Res. *1803*, 201–206.

Blanchoin, L., Amann, K.J., Higgs, H.N., Marchand, J.B., Kaiser, D.A., and Pollard, T.D. (2000). Direct observation of dendritic actin filament networks nucleated by Arp2/3 complex and WASP/SCAR proteins. Nature *404*, 1007–1011.

Boavida, L.C., and McCormick, S. (2007). TECHNICAL ADVANCE: Temperature as a determinant factor for increased and reproducible in vitro pollen germination in Arabidopsis thaliana: Temperature effect on Arabidopsis pollen germination. Plant J. *52*, 570–582.

Boevink, P., Oparka, K., Santa Cruz, S., Martin, B., Betteridge, A., and Hawes, C. (1998). Stacks on tracks: the plant Golgi apparatus traffics on an actin/ER network. Plant J. Cell Mol. Biol. *15*, 441–447.

Boffey, S.A., Ellis, J.R., Selldén, G., and Leech, R.M. (1979). Chloroplast Division and DNA Synthesis in Light-grown Wheat Leaves. Plant Physiol. *64*, 502–505.

Bögre, L., Magyar, Z., and López-Juez, E. (2008). New clues to organ size control in plants. Genome Biol. *9*, 226.

Bork, P., Sander, C., and Valencia, A. (1992). An ATPase domain common to prokaryotic cell cycle proteins, sugar kinases, actin, and hsp70 heat shock proteins. Proc. Natl. Acad. Sci. U. S. A. *89*, 7290–7294.

Braun, M., Hauslage, J., Czogalla, A., and Limbach, C. (2004). Tip-localized actin polymerization and remodeling, reflected by the localization of ADF, profilin and villin, are fundamental for gravity-sensing and polar growth in characean rhizoids. Planta *219*, 379–388.

Breitsprecher, D., Jaiswal, R., Bombardier, J.P., Gould, C.J., Gelles, J., and Goode, B.L. (2012). Rocket launcher mechanism of collaborative actin assembly defined by single-molecule imaging. Science *336*, 1164–1168.

Brembu, T., Winge, P., Seem, M., and Bones, A.M. (2004). NAPP and PIRP encode subunits of a putative wave regulatory protein complex involved in plant cell morphogenesis. Plant Cell *16*, 2335–2349.

Burk, D.H., Liu, B., Zhong, R., Morrison, W.H., and Ye, Z.H. (2001). A katanin-like protein regulates normal cell wall biosynthesis and cell elongation. Plant Cell *13*, 807–827.

Buschmann, H., Hauptmann, M., Niessing, D., Lloyd, C.W., and Schaffner, A.R. (2009). Helical Growth of the Arabidopsis Mutant tortifolia2 Does Not Depend on Cell Division Patterns but Involves Handed Twisting of Isolated Cells. PLANT CELL ONLINE *21*, 2090–2106.

Cahill, D., Rookes, J., Michalczyk, A., McDonald, K., and Drake, A. (2002). Microtubule dynamics in compatible and incompatible interactions of soybean hypocotyl cells with Phytophthora sojae. Plant Pathol. *51*, 629–640.

Cao, L.-J., Zhao, M.-M., Liu, C., Dong, H.-J., Li, W.-C., and Ren, H.-Y. (2013). LlSR28 is involved in pollen germination by affecting filamentous actin dynamics. Mol. Plant *6*, 1163–1175.

Carol, P., Stevenson, D., Bisanz, C., Breitenbach, J., Sandmann, G., Mache, R., Coupland, G., and Kuntz, M. (1999). Mutations in the Arabidopsis gene IMMUTANS cause a variegated phenotype by inactivating a chloroplast terminal oxidase associated with phytoene desaturation. Plant Cell *11*, 57–68.

Cecchetti, V., Altamura, M.M., Falasca, G., Costantino, P., and Cardarelli, M. (2008). Auxin regulates Arabidopsis anther dehiscence, pollen maturation, and filament elongation. Plant Cell *20*, 1760–1774.

Chaerle, L., and Van Der Straeten, D. (2000). Imaging techniques and the early detection of plant stress. Trends Plant Sci. *5*, 495–501.

Chang, L., Ramireddy, E., and Schmülling, T. (2013). Lateral root formation and growth of Arabidopsis is redundantly regulated by cytokinin metabolism and signalling genes. J. Exp. Bot. *64*, 5021–5032.

Chebli, Y., Kroeger, J., and Geitmann, A. (2013). Transport logistics in pollen tubes. Mol. Plant *6*, 1037–1052.

Chen, Y.C., and McCormick, S. (1996). sidecar pollen, an Arabidopsis thaliana male gametophytic mutant with aberrant cell divisions during pollen development. Dev. Camb. Engl. *122*, 3243–3253.

Chen, C., Marcus, A., Li, W., Hu, Y., Calzada, J.-P.V., Grossniklaus, U., Cyr, R.J., and Ma, H. (2002). The Arabidopsis ATK1 gene is required for spindle morphogenesis in male meiosis. Dev. Camb. Engl. *129*, 2401–2409.

Chen, G., Bi, Y.R., and Li, N. (2005). EGY1 encodes a membrane-associated and ATP-independent metalloprotease that is required for chloroplast development. Plant J. Cell Mol. Biol. *41*, 364–375.

Chen, H., Cheng, Z., Ma, X., Wu, H., Liu, Y., Zhou, K., Chen, Y., Ma, W., Bi, J., Zhang, X., et al. (2013). A knockdown mutation of YELLOW-GREEN LEAF2 blocks chlorophyll biosynthesis in rice. Plant Cell Rep. *32*, 1855–1867.

Chen, N., Qu, X., Wu, Y., and Huang, S. (2009). Regulation of Actin Dynamics in Pollen Tubes: Control of Actin Polymer Level. J. Integr. Plant Biol. *51*, 740–750.

Chen, Q., Liu, Y., Maere, S., Lee, E., Van Isterdael, G., Xie, Z., Xuan, W., Lucas, J., Vassileva, V., Kitakura, S., et al. (2015). A coherent transcriptional feed-forward motif model for mediating auxin-sensitive PIN3 expression during lateral root development. Nat. Commun. *6*, 8821.

Cheung, A.Y., and Wu, H. (2004). Overexpression of an Arabidopsis formin stimulates supernumerary actin cable formation from pollen tube cell membrane. Plant Cell *16*, 257–269.

Cheung, A.Y., Niroomand, S., Zou, Y., and Wu, H.-M. (2010). A transmembrane formin nucleates subapical actin assembly and controls tip-focused growth in pollen tubes. Proc. Natl. Acad. Sci. U. S. A. *107*, 16390–16395.

Chilley, P.M., Casson, S.A., Tarkowski, P., Hawkins, N., Wang, K.L.-C., Hussey, P.J., Beale, M., Ecker, J.R., Sandberg, G.K., and Lindsey, K. (2006). The POLARIS peptide of Arabidopsis regulates auxin transport and root growth via effects on ethylene signaling. Plant Cell *18*, 3058–3072.

Cho, H.-T., and Cosgrove, D.J. (2002). Regulation of root hair initiation and expansin gene expression in Arabidopsis. Plant Cell *14*, 3237–3253.

Choi, W.-G., Toyota, M., Kim, S.-H., Hilleary, R., and Gilroy, S. (2014). Salt stress-induced Ca2+ waves are associated with rapid, long-distance root-to-shoot signaling in plants. Proc. Natl. Acad. Sci. U. S. A. *111*, 6497–6502.

Cole, R.A., Synek, L., Zarsky, V., and Fowler, J.E. (2005). SEC8, a subunit of the putative Arabidopsis exocyst complex, facilitates pollen germination and competitive pollen tube growth. Plant Physiol. *138*, 2005–2018.

Cooper, G.M. (2000). The cell: a molecular approach (Washington, DC: ASM Press [u.a.]).

Cvrcková, F. (2000). Are plant formins integral membrane proteins? Genome Biol. *1*, RESEARCH001.

Cvrcková, F., Novotný, M., Pícková, D., and Zárský, V. (2004). Formin homology 2 domains occur in multiple contexts in angiosperms. BMC Genomics *5*, 44.

Cvrčková, F., Oulehlová, D., and Žárský, V. (2014). Formins: Linking Cytoskeleton and Endomembranes in Plant Cells. Int. J. Mol. Sci. *16*, 1–18.

David Marks, M. (1994). Plant Development: The making of a plant hair. Curr. Biol. *4*, 621–623.

Dayel, M.J., and Mullins, R.D. (2004). Activation of Arp2/3 Complex: Addition of the First Subunit of the New Filament by a WASP Protein Triggers Rapid ATP Hydrolysis on Arp2. PLoS Biol. *2*, e91.

Deal, R.B., Kandasamy, M.K., McKinney, E.C., and Meagher, R.B. (2005). The nuclear actin-related protein ARP6 is a pleiotropic developmental regulator required for the maintenance of FLOWERING LOCUS C expression and repression of flowering in Arabidopsis. Plant Cell *17*, 2633–2646.

De Smet, I. (2012). Lateral root initiation: one step at a time: Minireview. New Phytol. *193*, 867–873.

De Smet, I., Tetsumura, T., De Rybel, B., Frei dit Frey, N., Laplaze, L., Casimiro, I., Swarup, R., Naudts, M., Vanneste, S., Audenaert, D., et al. (2007). Auxin-dependent regulation of lateral root positioning in the basal meristem of Arabidopsis. Dev. Camb. Engl. *134*, 681–690.

Deeks, M.J., Hussey, P.J., and Davies, B. (2002). Formins: intermediates in signal-transduction cascades that affect cytoskeletal reorganization. Trends Plant Sci. *7*, 492–498.

Deeks, M.J., Kaloriti, D., Davies, B., Malhó, R., and Hussey, P.J. (2004). Arabidopsis NAP1 is essential for Arp2/3-dependent trichome morphogenesis. Curr. Biol. CB *14*, 1410–1414.

Deeks, M.J., Cvrcková, F., Machesky, L.M., Mikitová, V., Ketelaar, T., Zársky, V., Davies, B., and Hussey, P.J. (2005). Arabidopsis group Ie formins localize to specific cell membrane domains, interact with actin-binding proteins and cause defects in cell expansion upon aberrant expression. New Phytol. *168*, 529–540.

Deng, X., Zhang, H., Wang, Y., He, F., Liu, J., Xiao, X., Shu, Z., Li, W., Wang, G., and Wang, G. (2014). Mapped clone and functional analysis of leaf-color gene Ygl7 in a rice hybrid (Oryza sativa L. ssp. indica). PloS One *9*, e99564.

DePina, A.S., and Langford, G.M. (1999). Vesicle transport: the role of actin filaments and myosin motors. Microsc. Res. Tech. *47*, 93–106.

Derksen, J., Rutten, T., Van Amstel, T., De Win, A., Doris, F., and Steer, M. (1995). Regulation of pollen tube growth. Acta Bot. Neerlandica *44*, 93–119.

Dhonukshe, P., Kleine-Vehn, J., and Friml, J. (2005). Cell polarity, auxin transport, and cytoskeleton-mediated division planes: who comes first? Protoplasma *226*, 67–73.

Dinh, T.T., Luscher, E., Li, S., Liu, X., Won, S.Y., and Chen, X. (2014). Genetic Screens for Floral Mutants in Arabidopsis thaliana: Enhancers and Suppressors. In Flower Development, J.L. Riechmann, and F. Wellmer, eds. (New York, NY: Springer New York), pp. 127–156.

Ditta, G., Pinyopich, A., Robles, P., Pelaz, S., and Yanofsky, M.F. (2004). The SEP4 Gene of Arabidopsis thaliana Functions in Floral Organ and Meristem Identity. Curr. Biol. *14*, 1935–1940.

Djakovic, S., Dyachok, J., Burke, M., Frank, M.J., and Smith, L.G. (2006). BRICK1/HSPC300 functions with SCAR and the ARP2/3 complex to regulate epidermal cell shape in Arabidopsis. Dev. Camb. Engl. *133*, 1091–1100.

Dolan, L., Janmaat, K., Willemsen, V., Linstead, P., Poethig, S., Roberts, K., and Scheres, B. (1993). Cellular organisation of the Arabidopsis thaliana root. Dev. Camb. Engl. *119*, 71–84.

Dominguez, R. (2010). Structural insights into de novo actin polymerization. Curr. Opin. Struct. Biol. *20*, 217–225.

Dominguez, R., and Holmes, K.C. (2011). Actin structure and function. Annu. Rev. Biophys. *40*, 169–186.

Dong, X., Nou, I.-S., Yi, H., and Hur, Y. (2015). Suppression of ASKβ (AtSK32), a Clade III Arabidopsis GSK3, Leads to the Pollen Defect during Late Pollen Development. Mol. Cells *38*, 506–517.

Dubrovsky, J.G., Doerner, P.W., Colón-Carmona, A., and Rost, T.L. (2000). Pericycle Cell Proliferation and Lateral Root Initiation in Arabidopsis. Plant Physiol. *124*, 1648–1657.

Dyachok, J., Zhu, L., Liao, F., He, J., Huq, E., and Blancaflor, E.B. (2011). SCAR Mediates Light-Induced Root Elongation in Arabidopsis through Photoreceptors and Proteasomes. Plant Cell *23*, 3610–3626.

Edlund, A.F., Swanson, R., and Preuss, D. (2004). Pollen and stigma structure and function: the role of diversity in pollination. Plant Cell *16 Suppl*, S84-97.

Egelman, E.H. (1985). The structure of F-actin. J. Muscle Res. Cell Motil. *6*, 129–151.

Egelman, E.H. (2003). A tale of two polymers: new insights into helical filaments. Nat. Rev. Mol. Cell Biol. *4*, 621–630.

Egelman, E.H., Francis, N., and DeRosier, D.J. (1982). F-actin is a helix with a random variable twist. Nature *298*, 131–135.

El-Din El-Assal, S., Le, J., Basu, D., Mallery, E.L., and Szymanski, D.B. (2004). *DISTORTED2* encodes an ARPC2 subunit of the putative *Arabidopsis* ARP2/3 complex. Plant J. *38*, 526–538.

Ellinger, D., Naumann, M., Falter, C., Zwikowics, C., Jamrow, T., Manisseri, C., Somerville, S.C., and Voigt, C.A. (2013). Elevated early callose deposition results in complete penetration resistance to powdery mildew in Arabidopsis. Plant Physiol. *161*, 1433–1444.

van den Ent, F., Amos, L.A., and Löwe, J. (2001). Prokaryotic origin of the actin cytoskeleton. Nature *413*, 39–44.

van den Ent, F., Møller-Jensen, J., Amos, L.A., Gerdes, K., and Löwe, J. (2002). F-actin-like filaments formed by plasmid segregation protein ParM. EMBO J. *21*, 6935–6943.

Faix, J., and Grosse, R. (2006). Staying in shape with formins. Dev. Cell *10*, 693–706.

Falbel, T.G., Koch, L.M., Nadeau, J.A., Segui-Simarro, J.M., Sack, F.D., and Bednarek, S.Y. (2003). SCD1 is required for cytokinesis and polarized cell expansion in Arabidopsis thaliana [corrected]. Dev. Camb. Engl. *130*, 4011–4024.

Fan, L.M., Wang, Y.F., Wang, H., and Wu, W.H. (2001). In vitro Arabidopsis pollen germination and characterization of the inward potassium currents in Arabidopsis pollen grain protoplasts. J. Exp. Bot. *52*, 1603–1614.

Favery, B., Chelysheva, L.A., Lebris, M., Jammes, F., Marmagne, A., De Almeida-Engler, J., Lecomte, P., Vaury, C., Arkowitz, R.A., and Abad, P. (2004). Arabidopsis formin AtFH6 is a plasma membrane-associated protein upregulated in giant cells induced by parasitic nematodes. Plant Cell *16*, 2529–2540.

Finka, A., Saidi, Y., Goloubinoff, P., Neuhaus, J.-M., Zrÿd, J.-P., and Schaefer, D.G. (2008). The knock-out of ARP3a gene affects F-actin cytoskeleton organization altering cellular tip growth, morphology and development in moss *Physcomitrella patens*. Cell Motil. Cytoskeleton *65*, 769–784.

Fitz Gerald, J.N., Hui, P.S., and Berger, F. (2009). Polycomb group-dependent imprinting of the actin regulator AtFH5 regulates morphogenesis in Arabidopsis thaliana. Dev. Camb. Engl. *136*, 3399–3404.

Folkers, U., Berger, J., and Hülskamp, M. (1997). Cell morphogenesis of trichomes in Arabidopsis: differential control of primary and secondary branching by branch initiation regulators and cell growth. Dev. Camb. Engl. *124*, 3779–3786.

Frank, M.J., and Smith, L.G. (2002). A small, novel protein highly conserved in plants and animals promotes the polarized growth and division of maize leaf epidermal cells. Curr. Biol. CB *12*, 849–853.

Frank, M., Egile, C., Dyachok, J., Djakovic, S., Nolasco, M., Li, R., and Smith, L.G. (2004). Activation of Arp2/3 complex-dependent actin polymerization by plant proteins distantly related to SCAR/WAVE. Proc. Natl. Acad. Sci. U. S. A. *101*, 16379–16384.

Franklin-Tong, null (1999). Signaling and the modulation of pollen tube growth. Plant Cell *11*, 727–738.

Friml, J., Wiśniewska, J., Benková, E., Mendgen, K., and Palme, K. (2002a). Lateral relocation of auxin efflux regulator PIN3 mediates tropism in Arabidopsis. Nature *415*, 806–809.

Friml, J., Benková, E., Blilou, I., Wisniewska, J., Hamann, T., Ljung, K., Woody, S., Sandberg, G., Scheres, B., Jürgens, G., et al. (2002b). AtPIN4 mediates sink-driven auxin gradients and root patterning in Arabidopsis. Cell *108*, 661–673.

Fu, Y. (2010). The actin cytoskeleton and signaling network during pollen tube tip growth. J. Integr. Plant Biol. *52*, 131–137.

Fu, Y., Li, H., and Yang, Z. (2002). The ROP2 GTPase controls the formation of cortical fine F-actin and the early phase of directional cell expansion during Arabidopsis organogenesis. Plant Cell *14*, 777–794.

Fu, Y., Gu, Y., Zheng, Z., Wasteneys, G., and Yang, Z. (2005). Arabidopsis Interdigitating Cell Growth Requires Two Antagonistic Pathways with Opposing Action on Cell Morphogenesis. Cell *120*, 687–700.

Fu, Y., Xu, T., Zhu, L., Wen, M., and Yang, Z. (2009). A ROP GTPase Signaling Pathway Controls Cortical Microtubule Ordering and Cell Expansion in Arabidopsis. Curr. Biol. *19*, 1827–1832.

Gabrielsen, E.K. (1948). Effects of Different Chlorophyll Concentrations on Photosynthesis in Foliage Leaves. Physiol. Plant. *1*, 5–37.

Galway, M.E., Masucci, J.D., Lloyd, A.M., Walbot, V., Davis, R.W., and Schiefelbein, J.W. (1994). The TTG gene is required to specify epidermal cell fate and cell patterning in the Arabidopsis root. Dev. Biol. *166*, 740–754.

Gao, X.-Q., Chen, J., Wei, P.-C., Ren, F., Chen, J., and Wang, X.-C. (2008). Array and distribution of actin filaments in guard cells contribute to the determination of stomatal aperture. Plant Cell Rep. *27*, 1655–1665.

Gao, X.-Q., Liu, C.Z., Li, D.D., Zhao, T.T., Li, F., Jia, X.N., Zhao, X.-Y., and Zhang, X.S. (2016). The Arabidopsis KINβγ Subunit of the SnRK1 Complex Regulates Pollen Hydration on the Stigma by Mediating the Level of Reactive Oxygen Species in Pollen. PLOS Genet. *12*, e1006228.

Gautreau, A., Ho, H.H., Li, J., Steen, H., Gygi, S.P., and Kirschner, M.W. (2004). Purification and architecture of the ubiquitous Wave complex. Proc. Natl. Acad. Sci. U. S. A. *101*, 4379–4383.

Geldner, N., Friml, J., Stierhof, Y.D., Jürgens, G., and Palme, K. (2001). Auxin transport inhibitors block PIN1 cycling and vesicle trafficking. Nature *413*, 425–428.

Gibbon, B.C., Kovar, D.R., and Staiger, C.J. (1999). Latrunculin B Has Different Effects on Pollen Germination and Tube Growth. Plant Cell *11*, 2349.

Gilliland, L.U., Pawloski, L.C., Kandasamy, M.K., and Meagher, R.B. (2003). Arabidopsis actin gene ACT7 plays an essential role in germination and root growth. Plant J. Cell Mol. Biol. *33*, 319–328.

Gladish, D.K., and Rost, T.L. (1993). The effects of temperature on primary root growth dynamics and lateral root distribution in garden pea (Pisum sativum L., cv. “Alaska”). Environ. Exp. Bot. *33*, 243–258.

Goldberg, R.B., de Paiva, G., and Yadegari, R. (1994). Plant embryogenesis: zygote to seed. Science *266*, 605–614.

Goode, B.L., and Eck, M.J. (2007). Mechanism and function of formins in the control of actin assembly. Annu. Rev. Biochem. *76*, 593–627.

Graceffa, P., and Dominguez, R. (2003). Crystal structure of monomeric actin in the ATP state. Structural basis of nucleotide-dependent actin dynamics. J. Biol. Chem. *278*, 34172–34180.

Gray, J. (2005). Guard cells: transcription factors regulate stomatal movements. Curr. Biol. CB *15*, R593-595.

Grebe, M. (2012). The patterning of epidermal hairs in Arabidopsis—updated. Curr. Opin. Plant Biol. *15*, 31–37.

Grierson, C., Nielsen, E., Ketelaarc, T., and Schiefelbein, J. (2014). Root Hairs. Arab. Book *12*, e0172.

Grunt, M., Žárský, V., and Cvrčková, F. (2008). Roots of angiosperm formins: The evolutionary history of plant FH2 domain-containing proteins. BMC Evol. Biol. *8*, 115.

Guan, H., Xu, X., He, C., Liu, C., Liu, Q., Dong, R., Liu, T., and Wang, L. (2016). Fine Mapping and Candidate Gene Analysis of the Leaf-Color Gene ygl-1 in Maize. PLOS ONE *11*, e0153962.

Guimil, S., and Dunand, C. (2007). Cell growth and differentiation in Arabidopsis epidermal cells. J. Exp. Bot. *58*, 3829–3840.

Gustafson, F. (1939). Auxin Distribution in Fruits and Its Significance in Fruit Development. Am. J. Bot. *26*, 189–194.

Gustafson, F.G. (1936). Inducement of Fruit Development by Growth-Promoting Chemicals. Proc. Natl. Acad. Sci. U. S. A. *22*, 628–636.

Haberlandt, G. (1882). Vt-rgleichciide Anatomie des assimilatorischen Gewebesystems der Pflanzcn. Jahrb Wiss Hot *13*.

Han, B., Chen, L., Wang, J., Wu, Z., Yan, L., and Hou, S. (2015). Constitutive Expresser of Pathogenesis Related Genes 1 Is Required for Pavement Cell Morphogenesis in Arabidopsis. PLOS ONE *10*, e0133249.

Hanson, J., and Lowy, J. (1963). The structure of F-actin and of actin filaments isolated from muscle. J. Mol. Biol. *6*, 46–IN5.

Harries, P.A., Pan, A., and Quatrano, R.S. (2005). Actin-related protein2/3 complex component ARPC1 is required for proper cell morphogenesis and polarized cell growth in Physcomitrella patens. Plant Cell *17*, 2327–2339.

Hashida, S., Takahashi, H., Kawai-Yamada, M., and Uchimiya, H. (2007). Arabidopsis thaliana nicotinate/nicotinamide mononucleotide adenyltransferase (AtNMNAT) is required for pollen tube growth. Plant J. Cell Mol. Biol. *49*, 694–703.

Hashimoto, Y., Ino, T., Kramer, P.J., Naylor, A.W., and Strain, B.R. (1984). Dynamic analysis of water stress of sunflower leaves by means of a thermal image processing system. Plant Physiol. *76*, 266–269.

Hepler, P.K., Vidali, L., and Cheung, A.Y. (2001). Polarized cell growth in higher plants. Annu. Rev. Cell Dev. Biol. *17*, 159–187.

Hetherington, A.M. (2001). Guard cell signaling. Cell *107*, 711–714.

Hetherington, A.M., and Woodward, F.I. (2003). The role of stomata in sensing and driving environmental change. Nature *424*, 901–908.

Higgs, H.N. (2005). Formin proteins: a domain-based approach. Trends Biochem. Sci. *30*, 342–353.

Hinchee, M.A.W., and Rost, T.L. (1992). The Control of Lateral Root Development in Cultured Pea Seedlings. III. Spacing Intervals. Bot. Acta *105*, 127–131.

Hiscock, S.J., and Allen, A.M. (2008). Diverse cell signalling pathways regulate pollen-stigma interactions: the search for consensus. New Phytol. *179*, 286–317.

Holweg, C., and Nick, P. (2004). Arabidopsis myosin XI mutant is defective in organelle movement and polar auxin transport. Proc. Natl. Acad. Sci. U. S. A. *101*, 10488–10493.

Honys, D., and Twell, D. (2004). Transcriptome analysis of haploid male gametophyte development in Arabidopsis. Genome Biol. *5*, R85.

Horner, H.T., and Palmer, R.G. (1995). Mechanisms of Genic Male Sterility. Crop Sci. *35*, 1527.

Hou, G., Mohamalawari, D.R., and Blancaflor, E.B. (2003). Enhanced gravitropism of roots with a disrupted cap actin cytoskeleton. Plant Physiol. *131*, 1360–1373.

Hou, G., Kramer, V.L., Wang, Y.-S., Chen, R., Perbal, G., Gilroy, S., and Blancaflor, E.B. (2004). The promotion of gravitropism in Arabidopsis roots upon actin disruption is coupled with the extended alkalinization of the columella cytoplasm and a persistent lateral auxin gradient. Plant J. Cell Mol. Biol. *39*, 113–125.

Huang, J., Kim, C.M., Xuan, Y., Liu, J., Kim, T.H., Kim, B.-K., and Han, C. (2013). Formin homology 1 (OsFH1) regulates root-hair elongation in rice (Oryza sativa). Planta *237*, 1227–1239.

Huang, L., Shi, X., Wang, W., Ryu, K.H., and Schiefelbein, J. (2017). Diversification of Root Hair Development Genes in Vascular Plants. Plant Physiol. *174*, 1697–1712.

Huang, S., An, Y.Q., McDowell, J.M., McKinney, E.C., and Meagher, R.B. (1997). The Arabidopsis ACT11 actin gene is strongly expressed in tissues of the emerging inflorescence, pollen, and developing ovules. Plant Mol. Biol. *33*, 125–139.

Hückelhoven, R. (2007). Cell wall-associated mechanisms of disease resistance and susceptibility. Annu. Rev. Phytopathol. *45*, 101–127.

Hülskamp, M., Misŕa, S., and Jürgens, G. (1994). Genetic dissection of trichome cell development in Arabidopsis. Cell *76*, 555–566.

Hussey, P.J., Ketelaar, T., and Deeks, M.J. (2006). Control of the actin cytoskeleton in plant cell growth. Annu. Rev. Plant Biol. *57*, 109–125.

Hwang, J.U., and Lee, Y. (2001). Abscisic acid-induced actin reorganization in guard cells of dayflower is mediated by cytosolic calcium levels and by protein kinase and protein phosphatase activities. Plant Physiol. *125*, 2120–2128.

Hwang, J.U., Suh, S., Yi, H., Kim, J., and Lee, Y. (1997). Actin Filaments Modulate Both Stomatal Opening and Inward K+-Channel Activities in Guard Cells of Vicia faba L. Plant Physiol. *115*, 335–342.

Ivakov, A., and Persson, S. (2013). Plant cell shape: modulators and measurements. Front. Plant Sci. *4*, 439.

Iwabuchi, K., and Takagi, S. (2010). Actin-based mechanisms for light-dependent intracellular positioning of nuclei and chloroplasts in Arabidopsis. Plant Signal. Behav. *5*, 1010–1013.

Jacobs, A.K., Lipka, V., Burton, R.A., Panstruga, R., Strizhov, N., Schulze-Lefert, P., and Fincher, G.B. (2003). An Arabidopsis Callose Synthase, GSL5, Is Required for Wound and Papillary Callose Formation. Plant Cell *15*, 2503–2513.

Jacques, E., Verbelen, J.-P., and Vissenberg, K. (2014). Review on shape formation in epidermal pavement cells of the Arabidopsis leaf. Funct. Plant Biol. *41*, 914.

Johnson, M.A., and Kost, B. (2010). Pollen Tube Development. In Plant Developmental Biology, L. Hennig, and C. Köhler, eds. (Totowa, NJ: Humana Press), pp. 155–176.

Johnson-Brousseau, S.A., and McCormick, S. (2004). A compendium of methods useful for characterizing Arabidopsis pollen mutants and gametophytically-expressed genes. Plant J. Cell Mol. Biol. *39*, 761–775.

Jones, H.G. (1999). Use of thermography for quantitative studies of spatial and temporal variation of stomatal conductance over leaf surfaces. Plant Cell Environ. *22*, 1043–1055.

Kabsch, W., Mannherz, H.G., Suck, D., Pai, E.F., and Holmes, K.C. (1990). Atomic structure of the actin: DNase I complex. Nature *347*, 37–44.

Kandasamy, M.K., and Meagher, R.B. (1999). Actin-organelle interaction: Association with chloroplast inArabidopsis leaf mesophyll cells. Cell Motil. Cytoskeleton *44*, 110–118.

Kandasamy, M.K., Deal, R.B., McKinney, E.C., and Meagher, R.B. (2004). Plant actin-related proteins. Trends Plant Sci. *9*, 196–202.

Kandasamy, M.K., Deal, R.B., McKinney, E.C., and Meagher, R.B. (2005). Silencing the nuclear actin-related protein AtARP4 in Arabidopsis has multiple effects on plant development, including early flowering and delayed floral senescence: Role of AtARP4 in plant development. Plant J. *41*, 845–858.

Kandasamy, M.K., McKinney, E.C., and Meagher, R.B. (2009). A single vegetative actin isovariant overexpressed under the control of multiple regulatory sequences is sufficient for normal Arabidopsis development. Plant Cell *21*, 701–718.

Kariya, K., and Tsunoda, S. (1972). Relationship of Chlorophyll Content, Chloroplast Area Index and Leaf Photosynthesis Rate in Brassica. Tohoku J. Agric. Res. *23*, 1–14.

Kim, M., Hepler, P.K., Eun, S.O., Ha, K.S., and Lee, Y. (1995). Actin Filaments in Mature Guard Cells Are Radially Distributed and Involved in Stomatal Movement. Plant Physiol. *109*, 1077–1084.

Kim, T.-H., Böhmer, M., Hu, H., Nishimura, N., and Schroeder, J.I. (2010). Guard cell signal transduction network: advances in understanding abscisic acid, CO2, and Ca2+ signaling. Annu. Rev. Plant Biol. *61*, 561–591.

Kimura, S., and Kodama, Y. (2016). Actin-dependence of the chloroplast cold positioning response in the liverwortMarchantia polymorphaL. PeerJ *4*, e2513.

Klahre, U., Becker, C., Schmitt, A.C., and Kost, B. (2006). Nt-RhoGDI2 regulates Rac/Rop signaling and polar cell growth in tobacco pollen tubes. Plant J. Cell Mol. Biol. *46*, 1018–1031.

Klimyuk, V.I., Persello-Cartieaux, F., Havaux, M., Contard-David, P., Schuenemann, D., Meiherhoff, K., Gouet, P., Jones, J.D., Hoffman, N.E., and Nussaume, L. (1999). A chromodomain protein encoded by the arabidopsis CAO gene is a plant-specific component of the chloroplast signal recognition particle pathway that is involved in LHCP targeting. Plant Cell *11*, 87–99.

Kobayashi, I., Kobayashi, Y., Yamaoka, N., and Kunoh, H. (1992). Recognition of a pathogen and a nonpathogen by barley coleoptile cells. III. Responses of microtubules and actin filaments in barley coleoptile cells to penetration attempts. Can. J. Bot. *70*, 1815–1823.

Kobayashi, Y., Kobayashi, I., Funaki, Y., Fujimoto, S., Takemoto, T., and Kunoh, H. (1997). Dynamic reorganization of microfilaments and microtubules is necessary for the expression of non-host resistance in barley coleoptile cells. Plant J. *11*, 525–537.

Kong, Z., Hotta, T., Lee, Y.-R.J., Horio, T., and Liu, B. (2010). The -Tubulin Complex Protein GCP4 Is Required for Organizing Functional Microtubule Arrays in Arabidopsis thaliana. Plant Cell *22*, 191–204.

Kost, B., Mathur, J., and Chua, N.H. (1999). Cytoskeleton in plant development. Curr. Opin. Plant Biol. *2*, 462–470.

Kovar, D.R., Harris, E.S., Mahaffy, R., Higgs, H.N., and Pollard, T.D. (2006). Control of the assembly of ATP- and ADP-actin by formins and profilin. Cell *124*, 423–435.

Koyama, T., Mitsuda, N., Seki, M., Shinozaki, K., and Ohme-Takagi, M. (2010). TCP Transcription Factors Regulate the Activities of ASYMMETRIC LEAVES1 and miR164, as Well as the Auxin Response, during Differentiation of Leaves in Arabidopsis. PLANT CELL ONLINE *22*, 3574–3588.

Krichevsky, A., Kozlovsky, S.V., Tian, G.-W., Chen, M.-H., Zaltsman, A., and Citovsky, V. (2007). How pollen tubes grow. Dev. Biol. *303*, 405–420.

Kubínová, Z., Janáček, J., Lhotáková, Z., Kubínová, L., and Albrechtová, J. (2014). Unbiased estimation of chloroplast number in mesophyll cells: advantage of a genuine three-dimensional approach. J. Exp. Bot. *65*, 609–620.

Kushwah, S., Jones, A.M., and Laxmi, A. (2011). Cytokinin-induced root growth involves actin filament reorganization. Plant Signal. Behav. *6*, 1848–1850.

Lanza, M., Garcia-Ponce, B., Castrillo, G., Catarecha, P., Sauer, M., Rodriguez-Serrano, M., Páez-García, A., Sánchez-Bermejo, E., Tc, M., Leo del Puerto, Y., et al. (2012). Role of Actin Cytoskeleton in Brassinosteroid Signaling and in Its Integration with the Auxin Response in Plants. Dev. Cell *22*, 1275–1285.

Lavenus, J., Goh, T., Roberts, I., Guyomarc'h, S., Lucas, M., De Smet, I., Fukaki, H., Beeckman, T., Bennett, M., and Laplaze, L. (2013). Lateral root development in Arabidopsis: fifty shades of auxin. Trends Plant Sci. *18*, 450–458.

Le, J., El-Assal, S.E.-D., Basu, D., Saad, M.E., and Szymanski, D.B. (2003). Requirements for Arabidopsis ATARP2 and ATARP3 during epidermal development. Curr. Biol. CB *13*, 1341–1347.

Lease, K.A., Wen, J., Li, J., Doke, J.T., Liscum, E., and Walker, J.C. (2001). A mutant Arabidopsis heterotrimeric G-protein beta subunit affects leaf, flower, and fruit development. Plant Cell *13*, 2631–2641.

Lee, K., Gallop, J.L., Rambani, K., and Kirschner, M.W. (2010). Self-assembly of filopodia-like structures on supported lipid bilayers. Science *329*, 1341–1345.

Lee, Y., Kim, E.-S., Choi, Y., Hwang, I., Staiger, C.J., Chung, Y.-Y., and Lee, Y. (2008). The Arabidopsis Phosphatidylinositol 3-Kinase Is Important for Pollen Development. PLANT Physiol. *147*, 1886–1897.

Li, S. (2003). The Putative Arabidopsis Arp2/3 Complex Controls Leaf Cell Morphogenesis. PLANT Physiol. *132*, 2034–2044.

Li, F., and Higgs, H.N. (2003). The mouse Formin mDia1 is a potent actin nucleation factor regulated by autoinhibition. Curr. Biol. CB *13*, 1335–1340.

Li, H., Lin, Y., Heath, R.M., Zhu, M.X., and Yang, Z. (1999). Control of pollen tube tip growth by a Rop GTPase-dependent pathway that leads to tip-localized calcium influx. Plant Cell *11*, 1731–1742.

Li, S., Blanchoin, L., Yang, Z., and Lord, E.M. (2003). The putative Arabidopsis arp2/3 complex controls leaf cell morphogenesis. Plant Physiol. *132*, 2034–2044.

Li, S., Sun, T., and Ren, H. (2015). The functions of the cytoskeleton and associated proteins during mitosis and cytokinesis in plant cells. Front. Plant Sci. *6*.

Li, X., Li, J.-H., Wang, W., Chen, N.-Z., Ma, T.-S., Xi, Y.-N., Zhang, X.-L., Lin, H.-F., Bai, Y., Huang, S.-J., et al. (2014). ARP2/3 complex-mediated actin dynamics is required for hydrogen peroxide-induced stomatal closure in Arabidopsis: H 2 O 2 and actin dynamics in ABA signalling. Plant Cell Environ. *37*, 1548–1560.

Li, Y., Sorefan, K., Hemmann, G., and Bevan, M.W. (2004). Arabidopsis NAP and PIR regulate actin-based cell morphogenesis and multiple developmental processes. Plant Physiol. *136*, 3616–3627.

Li, Y., Shen, Y., Cai, C., Zhong, C., Zhu, L., Yuan, M., and Ren, H. (2010). The Type II Arabidopsis Formin14 Interacts with Microtubules and Microfilaments to Regulate Cell Division. Plant Cell *22*, 2710–2726.

Li, Z.-Y., Li, B., and Dong, A.-W. (2012). The Arabidopsis Transcription Factor AtTCP15 Regulates Endoreduplication by Modulating Expression of Key Cell-cycle Genes. Mol. Plant *5*, 270–280.

Libault, M., Brechenmacher, L., Cheng, J., Xu, D., and Stacey, G. (2010). Root hair systems biology. Trends Plant Sci. *15*, 641–650.

Lichtenthaler, H.K., and Wellburn, A.R. (1983). Determinations of total carotenoids and chlorophylls *a* and *b* of leaf extracts in different solvents. Biochem. Soc. Trans. *11*, 591–592.

Lin, D., Cao, L., Zhou, Z., Zhu, L., Ehrhardt, D., Yang, Z., and Fu, Y. (2013). Rho GTPase signaling activates microtubule severing to promote microtubule ordering in Arabidopsis. Curr. Biol. CB *23*, 290–297.

Liu, null, and Luan, null (1998). Voltage-dependent K+ channels as targets of osmosensing in guard cells. Plant Cell *10*, 1957–1970.

Liu, P., Qi, M., Xue, X., and Ren, H. (2011). Dynamics and functions of the actin cytoskeleton during the plant cell cycle. Chin. Sci. Bull. *56*, 3504–3510.

Liu, Z., Persson, S., and Zhang, Y. (2015). The connection of cytoskeletal network with plasma membrane and the cell wall: Plant cell wall, plasma membrane and cytoskeleton nexus. J. Integr. Plant Biol. *57*, 330–340.

Livak, K.J., and Schmittgen, T.D. (2001). Analysis of Relative Gene Expression Data Using Real-Time Quantitative PCR and the 2−ΔΔCT Method. Methods *25*, 402–408.

Lodish, H.F., Berk, A., Zipursky, S.L., Matsudaira, P., Baltimore, D., and Darnell, J. (2000). Molecular cell biology (New York: W.H. Freeman).

Loraine, A.E., McCormick, S., Estrada, A., Patel, K., and Qin, P. (2013). RNA-Seq of Arabidopsis Pollen Uncovers Novel Transcription and Alternative Splicing. PLANT Physiol. *162*, 1092–1109.

Lord, E.M., and Russell, S.D. (2002). The mechanisms of pollination and fertilization in plants. Annu. Rev. Cell Dev. Biol. *18*, 81–105.

Lucas, M., Kenobi, K., von Wangenheim, D., Voβ, U., Swarup, K., De Smet, I., Van Damme, D., Lawrence, T., Péret, B., Moscardi, E., et al. (2013). Lateral root morphogenesis is dependent on the mechanical properties of the overlaying tissues. Proc. Natl. Acad. Sci. U. S. A. *110*, 5229–5234.

Luesse, D.R., DeBlasio, S.L., and Hangarter, R.P. (2006). Plastid Movement Impaired 2, a New Gene Involved in Normal Blue-Light-Induced Chloroplast Movements in Arabidopsis. PLANT Physiol. *141*, 1328–1337.

Machesky, L.M., Atkinson, S.J., Ampe, C., Vandekerckhove, J., and Pollard, T.D. (1994). Purification of a cortical complex containing two unconventional actins from Acanthamoeba by affinity chromatography on profilin-agarose. J. Cell Biol. *127*, 107–115.

Machesky, L.M., Mullins, R.D., Higgs, H.N., Kaiser, D.A., Blanchoin, L., May, R.C., Hall, M.E., and Pollard, T.D. (1999). SCAR, a WASp-related protein, activates nucleation of actin filaments by the Arp2/3 complex. Proc. Natl. Acad. Sci. U. S. A. *96*, 3739–3744.

Maisch, J., Fišerová, J., Fischer, L., and Nick, P. (2009). Tobacco Arp3 is localized to actin-nucleating sites in vivo. J. Exp. Bot. *60*, 603–614.

Malamy, J.E., and Ryan, K.S. (2001). Environmental regulation of lateral root initiation in Arabidopsis. Plant Physiol. *127*, 899–909.

Mancuso, S., Barlow, P.W., Volkmann, D., and Baluska, F. (2006). Actin turnover-mediated gravity response in maize root apices: gravitropism of decapped roots implicates gravisensing outside of the root cap. Plant Signal. Behav. *1*, 52–58.

Marhavý, P., Duclercq, J., Weller, B., Feraru, E., Bielach, A., Offringa, R., Friml, J., Schwechheimer, C., Murphy, A., and Benková, E. (2014). Cytokinin controls polarity of PIN1-dependent auxin transport during lateral root organogenesis. Curr. Biol. CB *24*, 1031–1037.

Martinière, A., Gayral, P., Hawes, C., and Runions, J. (2011). Building bridges: formin1 of Arabidopsis forms a connection between the cell wall and the actin cytoskeleton. Plant J. Cell Mol. Biol. *66*, 354–365.

Mass, R.L., Zeller, R., Woychik, R.P., Vogt, T.F., and Leder, P. (1990). Disruption of formin-encoding transcripts in two mutant limb deformity alleles. Nature *346*, 853–855.

Masucci, J.D., and Schiefelbein, J.W. (1994). The rhd6 Mutation of Arabidopsis thaliana Alters Root-Hair Initiation through an Auxin- and Ethylene-Associated Process. Plant Physiol. *106*, 1335–1346.

Mathur, J. (2003). Mutations in Actin-Related Proteins 2 and 3 Affect Cell Shape Development in Arabidopsis. PLANT CELL ONLINE *15*, 1632–1645.

Mathur, J. (2004). Cell shape development in plants. Trends Plant Sci. *9*, 583–590.

Mathur, J. (2005). The ARP2/3 complex: giving plant cells a leading edge. BioEssays News Rev. Mol. Cell. Dev. Biol. *27*, 377–387.

Mathur, J. (2006). Local interactions shape plant cells. Curr. Opin. Cell Biol. *18*, 40–46.

Mathur, J., and Chua, N.H. (2000). Microtubule stabilization leads to growth reorientation in Arabidopsis trichomes. Plant Cell *12*, 465–477.

Mathur, J., and Hülskamp, M. (2001). Cell growth: How to grow and where to grow. Curr. Biol. *11*, R402–R404.

Mathur, J., and Hülskamp, M. (2002). Microtubules and Microfilaments in Cell Morphogenesis in Higher Plants. Curr. Biol. *12*, R669–R676.

Mathur, J., Spielhofer, P., Kost, B., and Chua, N. (1999). The actin cytoskeleton is required to elaborate and maintain spatial patterning during trichome cell morphogenesis in Arabidopsis thaliana. Dev. Camb. Engl. *126*, 5559–5568.

Mathur, J., Mathur, N., and Hülskamp, M. (2002). Simultaneous visualization of peroxisomes and cytoskeletal elements reveals actin and not microtubule-based peroxisome motility in plants. Plant Physiol. *128*, 1031–1045.

Mathur, J., Mathur, N., Kernebeck, B., and Hülskamp, M. (2003). Mutations in actin-related proteins 2 and 3 affect cell shape development in Arabidopsis. Plant Cell *15*, 1632–1645.

McCormick, S. (1993). Male Gametophyte Development. PLANT CELL ONLINE *5*, 1265–1275.

McDowell, J.M., An, Y.Q., Huang, S., McKinney, E.C., and Meagher, R.B. (1996). The arabidopsis ACT7 actin gene is expressed in rapidly developing tissues and responds to several external stimuli. Plant Physiol. *111*, 699–711.

Meagher, R.B., McKinney, E.C., and Kandasamy, M.K. (2000). The Significance of Diversity in the Plant Actin Gene Family. In Actin: A Dynamic Framework for Multiple Plant Cell Functions, C.J. Staiger, F. Baluška, D. Volkmann, and P.W. Barlow, eds. (Dordrecht: Springer Netherlands), pp. 3–27.

Meagher, R.B., Deal, R.B., Kandasamy, M.K., and McKinney, E.C. (2005). Nuclear actin-related proteins as epigenetic regulators of development. Plant Physiol. *139*, 1576–1585.

Meagher, R.B., Kandasamy, M.K., Deal, R.B., and McKinney, E.C. (2007). Actin-related proteins in chromatin-level control of the cell cycle and developmental transitions. Trends Cell Biol. *17*, 325–332.

Meinke, D.W., and Sussex, I.M. (1979). Embryo-lethal mutants of Arabidopsis thaliana. A model system for genetic analysis of plant embryo development. Dev. Biol. *72*, 50–61.

Menand, B., Yi, K., Jouannic, S., Hoffmann, L., Ryan, E., Linstead, P., Schaefer, D.G., and Dolan, L. (2007). An Ancient Mechanism Controls the Development of Cells with a Rooting Function in Land Plants. Science *316*, 1477–1480.

Mercier, R. (2001). SWITCH1 (SWI1): a novel protein required for the establishment of sister chromatid cohesion and for bivalent formation at meiosis. Genes Dev. *15*, 1859–1871.

Merlot, S., Mustilli, A.-C., Genty, B., North, H., Lefebvre, V., Sotta, B., Vavasseur, A., and Giraudat, J. (2002). Use of infrared thermal imaging to isolate Arabidopsis mutants defective in stomatal regulation. Plant J. Cell Mol. Biol. *30*, 601–609.

Michelot, A. (2005). The Formin Homology 1 Domain Modulates the Actin Nucleation and Bundling Activity of Arabidopsis FORMIN1. PLANT CELL ONLINE *17*, 2296–2313.

Millard, T.H., Sharp, S.J., and Machesky, L.M. (2004). Signalling to actin assembly via the WASP (Wiskott-Aldrich syndrome protein)-family proteins and the Arp2/3 complex. Biochem. J. *380*, 1–17.

Miller, D.D., De Ruijter, N.C.A., Bisseling, T., and Emons, A. mie C. (1999). The role of actin in root hair morphogenesis: studies with lipochito-oligosaccharide as a growth stimulator and cytochalasin as an actin perturbing drug. Plant J. *17*, 141–154.

Morant, M., Jørgensen, K., Schaller, H., Pinot, F., Møller, B.L., Werck-Reichhart, D., and Bak, S. (2007). CYP703 is an ancient cytochrome P450 in land plants catalyzing in-chain hydroxylation of lauric acid to provide building blocks for sporopollenin synthesis in pollen. Plant Cell *19*, 1473–1487.

Morita, M.T. (2010). Directional gravity sensing in gravitropism. Annu. Rev. Plant Biol. *61*, 705–720.

Motamayor, J.C., Vezon, D., Bajon, C., Sauvanet, A., Grandjean, O., Marchand, M., Bechtold, N., Pelletier, G., and Horlow, C. (2000). Switch (swi1), an Arabidopsis thaliana mutant affected in the female meiotic switch. Sex. Plant Reprod. *12*, 209–218.

Motohashi, R., Ito, T., Kobayashi, M., Taji, T., Nagata, N., Asami, T., Yoshida, S., Yamaguchi-Shinozaki, K., and Shinozaki, K. (2003). Functional analysis of the 37 kDa inner envelope membrane polypeptide in chloroplast biogenesis using a Ds-tagged Arabidopsis pale-green mutant. Plant J. Cell Mol. Biol. *34*, 719–731.

Mouline, K., Véry, A.-A., Gaymard, F., Boucherez, J., Pilot, G., Devic, M., Bouchez, D., Thibaud, J.-B., and Sentenac, H. (2002). Pollen tube development and competitive ability are impaired by disruption of a Shaker K(+) channel in Arabidopsis. Genes Dev. *16*, 339–350.

Muday, G.K., and Murphy, A.S. (2002). An emerging model of auxin transport regulation. Plant Cell *14*, 293–299.

Müller, M., and Schmidt, W. (2004). Environmentally induced plasticity of root hair development in Arabidopsis. Plant Physiol. *134*, 409–419.

Müller, A., Guan, C., Gälweiler, L., Tänzler, P., Huijser, P., Marchant, A., Parry, G., Bennett, M., Wisman, E., and Palme, K. (1998). AtPIN2 defines a locus of Arabidopsis for root gravitropism control. EMBO J. *17*, 6903–6911.

Müller, S., Wright, A.J., and Smith, L.G. (2009). Division plane control in plants: new players in the band. Trends Cell Biol. *19*, 180–188.

Mullins, R.D., Heuser, J.A., and Pollard, T.D. (1998). The interaction of Arp2/3 complex with actin: nucleation, high affinity pointed end capping, and formation of branching networks of filaments. Proc. Natl. Acad. Sci. U. S. A. *95*, 6181–6186.

Myakushina, Y.A., Milyaeva, E.L., Romanov, G.A., and Nikiforova, V.Y. (2009). Mutation in LSU4 gene affects flower development in Arabidopsis thaliana. Dokl. Biochem. Biophys. *428*, 257–260.

Nacry, P., Camilleri, C., Courtial, B., Caboche, M., and Bouchez, D. (1998). Major chromosomal rearrangements induced by T-DNA transformation in Arabidopsis. Genetics *149*, 641–650.

Naested, H., Holm, A., Jenkins, T., Nielsen, H.B., Harris, C.A., Beale, M.H., Andersen, M., Mant, A., Scheller, H., Camara, B., et al. (2004). Arabidopsis VARIEGATED 3 encodes a chloroplast-targeted, zinc-finger protein required for chloroplast and palisade cell development. J. Cell Sci. *117*, 4807–4818.

Nag, A., King, S., and Jack, T. (2009). miR319a targeting of *TCP4* is critical for petal growth and development in *Arabidopsis*. Proc. Natl. Acad. Sci. *106*, 22534–22539.

Nagpal, P. (2005). Auxin response factors ARF6 and ARF8 promote jasmonic acid production and flower maturation. Development *132*, 4107–4118.

Nakamura, M., and Hashimoto, T. (2009). A mutation in the Arabidopsis -tubulin-containing complex causes helical growth and abnormal microtubule branching. J. Cell Sci. *122*, 2208–2217.

Nakamura, M., Toyota, M., Tasaka, M., and Morita, M.T. (2011). An Arabidopsis E3 ligase, SHOOT GRAVITROPISM9, modulates the interaction between statoliths and F-actin in gravity sensing. Plant Cell *23*, 1830–1848.

Oh, S.-A., Park, S.K., Jang, I., Howden, R., Moore, J.M., Grossniklaus, U., and Twell, D. (2003). halfman, an Arabidopsis male gametophytic mutant associated with a 150 kb chromosomal deletion adjacent to an introduced Ds transposable element. Sex. Plant Reprod. *16*, 99–102.

Oikawa, K., Kasahara, M., Kiyosue, T., Kagawa, T., Suetsugu, N., Takahashi, F., Kanegae, T., Niwa, Y., Kadota, A., and Wada, M. (2003). Chloroplast unusual positioning1 is essential for proper chloroplast positioning. Plant Cell *15*, 2805–2815.

Oikawa, K., Yamasato, A., Kong, S.-G., Kasahara, M., Nakai, M., Takahashi, F., Ogura, Y., Kagawa, T., and Wada, M. (2008). Chloroplast outer envelope protein CHUP1 is essential for chloroplast anchorage to the plasma membrane and chloroplast movement. Plant Physiol. *148*, 829–842.

Ojangu, E.-L., Tanner, K., Pata, P., Järve, K., Holweg, C.L., Truve, E., and Paves, H. (2012). Myosins XI-K, XI-1, and XI-2 are required for development of pavement cells, trichomes, and stigmatic papillae in Arabidopsis. BMC Plant Biol. *12*, 81.

Okada, K., Ueda, J., Komaki, M.K., Bell, C.J., and Shimura, Y. (1991). Requirement of the Auxin Polar Transport System in Early Stages of Arabidopsis Floral Bud Formation. Plant Cell *3*, 677.

Ó'Maoiléidigh, D.S., Graciet, E., and Wellmer, F. (2014). Gene networks controlling Arabidopsis thaliana flower development. New Phytol. *201*, 16–30.

O'Neill, S.D., and Nadeau, J.A. (2010). Postpollination Flower Development. In Horticultural Reviews, J. Janick, ed. (Oxford, UK: John Wiley & Sons, Inc.), pp. 1–58.

Opalski, K.S., Schultheiss, H., Kogel, K.-H., and Hückelhoven, R. (2005). The receptor-like MLO protein and the RAC/ROP family G-protein RACB modulate actin reorganization in barley attacked by the biotrophic powdery mildew fungus Blumeria graminis f.sp. hordei. Plant J. Cell Mol. Biol. *41*, 291–303.

Oppenheimer, D.G., Pollock, M.A., Vacik, J., Szymanski, D.B., Ericson, B., Feldmann, K., and Marks, M.D. (1997). Essential role of a kinesin-like protein in Arabidopsis trichome morphogenesis. Proc. Natl. Acad. Sci. U. S. A. *94*, 6261–6266.

Owen, H.A., and Makaroff, C.A. (1995). Ultrastructure of microsporogenesis and microgametogenesis inArabidopsis thaliana (L.) Heynh. ecotype Wassilewskija (Brassicaceae). Protoplasma *185*, 7–21.

Palmieri, M., and Kiss, J.Z. (2005). Disruption of the F-actin cytoskeleton limits statolith movement in Arabidopsis hypocotyls. J. Exp. Bot. *56*, 2539–2550.

Pantaloni, D., Boujemaa, R., Didry, D., Gounon, P., and Carlier, M.F. (2000). The Arp2/3 complex branches filament barbed ends: functional antagonism with capping proteins. Nat. Cell Biol. *2*, 385–391.

Panteris, E., and Galatis, B. (2005). The morphogenesis of lobed plant cells in the mesophyll and epidermis: organization and distinct roles of cortical microtubules and actin filaments. New Phytol. *167*, 721–732.

Paul, A.S., Paul, A., Pollard, T.D., and Pollard, T. (2008a). The role of the FH1 domain and profilin in formin-mediated actin-filament elongation and nucleation. Curr. Biol. CB *18*, 9–19.

Paul, M.J., Primavesi, L.F., Jhurreea, D., and Zhang, Y. (2008b). Trehalose metabolism and signaling. Annu. Rev. Plant Biol. *59*, 417–441.

Paxson-Sowders, D.M., Owen, H.A., and Makaroff, C.A. (1997). A comparative ultrastructural analysis of exine pattern development in wild-typeArabidopsis and a mutant defective in pattern formation. Protoplasma *198*, 53–65.

Pei, W., Du, F., Zhang, Y., He, T., and Ren, H. (2012). Control of the actin cytoskeleton in root hair development. Plant Sci. *187*, 10–18.

Péret, B., De Rybel, B., Casimiro, I., Benková, E., Swarup, R., Laplaze, L., Beeckman, T., and Bennett, M.J. (2009). Arabidopsis lateral root development: an emerging story. Trends Plant Sci. *14*, 399–408.

Picton, J.M., and Steer, M.W. (1982). A model for the mechanism of tip extension in pollen tubes. J. Theor. Biol. *98*, 15–20.

Pierson, E.S., and Cresti, M. (1992). Cytoskeleton and Cytoplasmic Organization of Pollen and Pollen Tubes. In International Review of Cytology, (Elsevier), pp. 73–125.

Pitts, R.J., Cernac, A., and Estelle, M. (1998). Auxin and ethylene promote root hair elongation in Arabidopsis. Plant J. Cell Mol. Biol. *16*, 553–560.

Pollard, T.D. (2007). Regulation of Actin Filament Assembly by Arp2/3 Complex and Formins. Annu. Rev. Biophys. Biomol. Struct. *36*, 451–477.

Pollard, T.D., and Cooper, J.A. (1986). Actin and actin-binding proteins. A critical evaluation of mechanisms and functions. Annu. Rev. Biochem. *55*, 987–1035.

Possingham, J.V., and Smith, J.W. (1972). Factors Affecting Chloroplast Replication in Spinach. J. Exp. Bot. *23*, 1050–1059.

Preuss, D. (1995). Being fruitful: genetics of reproduction in Arabidopsis. Trends Genet. TIG *11*, 147–153.

Preuss, D., Lemieux, B., Yen, G., and Davis, R.W. (1993). A conditional sterile mutation eliminates surface components from Arabidopsis pollen and disrupts cell signaling during fertilization. Genes Dev. *7*, 974–985.

Pring, M., Evangelista, M., Boone, C., Yang, C., and Zigmond, S.H. (2003). Mechanism of formin-induced nucleation of actin filaments. Biochemistry (Mosc.) *42*, 486–496.

Procissi, A., de Laissardière, S., Férault, M., Vezon, D., Pelletier, G., and Bonhomme, S. (2001). Five gametophytic mutations affecting pollen development and pollen tube growth in Arabidopsis thaliana. Genetics *158*, 1773–1783.

Procissi, A., Guyon, A., Pierson, E.S., Giritch, A., Knuiman, B., Grandjean, O., Tonelli, C., Derksen, J., Pelletier, G., and Bonhomme, S. (2003). KINKY POLLEN encodes a SABRE-like protein required for tip growth in Arabidopsis and conserved among eukaryotes. Plant J. Cell Mol. Biol. *36*, 894–904.

Qu, X., Jiang, Y., Chang, M., Liu, X., Zhang, R., and Huang, S. (2015). Organization and regulation of the actin cytoskeleton in the pollen tube. Front. Plant Sci. *5*.

Raskin, I., and Ladyman, J.A. (1988). Isolation and characterization of a barley mutant with abscisic-acid-insensitive stomata. Planta *173*, 73–78.

Rasmussen, C.G., Wright, A.J., and Müller, S. (2013). The role of the cytoskeleton and associated proteins in determination of the plant cell division plane. Plant J. Cell Mol. Biol. *75*, 258–269.

Reboulet, J.C., Kumar, P., and Kiss, J.Z. (2010). *DIS1* and DIS2 play a role in tropisms in Arabidopsis thaliana. Environ. Exp. Bot. *67*, 474–478.

Reed, R.C., Brady, S.R., and Muday, G.K. (1998). Inhibition of auxin movement from the shoot into the root inhibits lateral root development in Arabidopsis. Plant Physiol. *118*, 1369–1378.

Reeder, S.H., Lee, B.H., Fox, R., and Dobritsa, A.A. (2016). A Ploidy-Sensitive Mechanism Regulates Aperture Formation on the Arabidopsis Pollen Surface and Guides Localization of the Aperture Factor INP1. PLOS Genet. *12*, e1006060.

Robinson, R.C., Turbedsky, K., Kaiser, D.A., Marchand, J.B., Higgs, H.N., Choe, S., and Pollard, T.D. (2001). Crystal structure of Arp2/3 complex. Science *294*, 1679–1684.

Robles, P., and Pelaz, S. (2005). Flower and fruit development in Arabidopsis thaliana. Int. J. Dev. Biol. *49*, 633–643.

Rodríguez-Hernández, A.A., Muro-Medina, C.V., Ramírez-Alonso, J.I., and Jiménez-Bremont, J.F. (2017). Modification of AtGRDP1 gene expression affects silique and seed development in Arabidopsis thaliana. Biochem. Biophys. Res. Commun. *486*, 252–256.

Rohatgi, R., Ma, L., Miki, H., Lopez, M., Kirchhausen, T., Takenawa, T., and Kirschner, M.W. (1999). The interaction between N-WASP and the Arp2/3 complex links Cdc42-dependent signals to actin assembly. Cell *97*, 221–231.

Rosero, A., Žárský, V., and Cvrčková, F. (2013). AtFH1 formin mutation affects actin filament and microtubule dynamics in Arabidopsis thaliana. J. Exp. Bot. *64*, 585–597.

Rosero, A., Oulehlová, D., Stillerová, L., Schiebertová, P., Grunt, M., Žárský, V., and Cvrčková, F. (2016). Arabidopsis FH1 Formin Affects Cotyledon Pavement Cell Shape by Modulating Cytoskeleton Dynamics. Plant Cell Physiol. *57*, 488–504.

Rost, T., and Baum, S. (1988). On the Correlation of Primary Root Length, Meristem Size and Protoxylem Tracheary Element Position in Pea Seedlings. Am. J. Bot. *75*, 414–124.

Running, M.P., and Meyerowitz, E.M. (1996). Mutations in the PERIANTHIA gene of Arabidopsis specifically alter floral organ number and initiation pattern. Dev. Camb. Engl. *122*, 1261–1269.

Saedler, R., Mathur, N., Srinivas, B.P., Kernebeck, B., Hülskamp, M., and Mathur, J. (2004). Actin control over microtubules suggested by DISTORTED2 encoding the Arabidopsis ARPC2 subunit homolog. Plant Cell Physiol. *45*, 813–822.

Saito, C., Morita, M.T., Kato, T., and Tasaka, M. (2005). Amyloplasts and vacuolar membrane dynamics in the living graviperceptive cell of the Arabidopsis inflorescence stem. Plant Cell *17*, 548–558.

Sawers, R.J.H., Linley, P.J., Gutierrez-Marcos, J.F., Delli-Bovi, T., Farmer, P.R., Kohchi, T., Terry, M.J., and Brutnell, T.P. (2004). The Elm1 (ZmHy2) gene of maize encodes a phytochromobilin synthase. Plant Physiol. *136*, 2771–2781.

Schmid, M.F., Sherman, M.B., Matsudaira, P., and Chiu, W. (2004). Structure of the acrosomal bundle. Nature *431*, 104–107.

Scholz-Starke, J., Büttner, M., and Sauer, N. (2003). AtSTP6, a new pollen-specific H+-monosaccharide symporter from Arabidopsis. Plant Physiol. *131*, 70–77.

Schroeder, J.I., Allen, G.J., Hugouvieux, V., Kwak, J.M., and Waner, D. (2001). GUARD CELL SIGNAL TRANSDUCTION. Annu. Rev. Plant Physiol. Plant Mol. Biol. *52*, 627–658.

Schütz, I., Gus-Mayer, S., and Schmelzer, E. (2006). Profilin and Rop GTPases are localized at infection sites of plant cells. Protoplasma *227*, 229–235.

Schwab, B., Folkers, U., Ilgenfritz, H., and Hulskamp, M. (2000). Trichome morphogenesis in Arabidopsis. Philos. Trans. R. Soc. B Biol. Sci. *355*, 879–883.

Schwab, B., Mathur, J., Saedler, R., Schwarz, H., Frey, B., Scheidegger, C., and Hülskamp, M. (2003). Regulation of cell expansion by the DISTORTED genes in Arabidopsis thaliana: actin controls the spatial organization of microtubules. Mol. Genet. Genomics MGG *269*, 350–360.

Scott, R.J. (1994). Pollen exine – the sporopollenin enigma and the physics of pattern. In Molecular and Cellular Aspects of Plant Reproduction, R.J. Scott, and A.D. Stead, eds. (Cambridge: Cambridge University Press), pp. 49–82.

Scott, R.J., Spielman, M., and Dickinson, H.G. (2004). Stamen structure and function. Plant Cell *16 Suppl*, S46-60.

Shi, D., Zheng, X., Li, L., Lin, W., Xie, W., Yang, J., Chen, S., and Jin, W. (2013). Chlorophyll Deficiency in the Maize elongated mesocotyl2 Mutant Is Caused by a Defective Heme Oxygenase and Delaying Grana Stacking. PLoS ONE *8*, e80107.

Shishkova, S., Rost, T.L., and Dubrovsky, J.G. (2007). Determinate Root Growth and Meristem Maintenance in Angiosperms. Ann. Bot. *101*, 319–340.

Shivanna, K.R., Linskens, H.F., and Cresti, M. (1991). Pollen viability and pollen vigor. TAG Theor. Appl. Genet. Theor. Angew. Genet. *81*, 38–42.

Shockey, J., Regmi, A., Cotton, K., Adhikari, N., Browse, J., and Bates, P.D. (2016). Identification of Arabidopsis GPAT9 (At5g60620) as an Essential Gene Involved in Triacylglycerol Biosynthesis. Plant Physiol. *170*, 163–179.

Skalamera, D., and Heath, M.C. (1998). Changes in the cytoskeleton accompanying infection-induced nuclear movements and the hypersensitive response in plant cells invaded by rust fungi. Plant J. Cell Mol. Biol. *16*, 191–200.

Smith, L.G. (2003). Cytoskeletal control of plant cell shape: getting the fine points. Curr. Opin. Plant Biol. *6*, 63–73.

Smith, A.R., and Zhao, D. (2016). Sterility Caused by Floral Organ Degeneration and Abiotic Stresses in Arabidopsis and Cereal Grains. Front. Plant Sci. *7*.

Smith, L.G., and Oppenheimer, D.G. (2005). SPATIAL CONTROL OF CELL EXPANSION BY THE PLANT CYTOSKELETON. Annu. Rev. Cell Dev. Biol. *21*, 271–295.

Srikanth, A., and Schmid, M. (2011). Regulation of flowering time: all roads lead to Rome. Cell. Mol. Life Sci. CMLS *68*, 2013–2037.

Staiger, C.J., Baluška, F., Volkmann, D., and Barlow, P. (2010). Actin : A Dynamic Framework for Multiple Plant Cell Functions (Dordrecht: Springer Netherlands).

Steer, M.W., and Steer, J.M. (1989). Pollen tube tip growth. New Phytol. *111*, 323–358.

Steinebrunner, I., Wu, J., Sun, Y., Corbett, A., and Roux, S.J. (2003). Disruption of apyrases inhibits pollen germination in Arabidopsis. Plant Physiol. *131*, 1638–1647.

Stetter, M.G., Benz, M., and Ludewig, U. (2017). Increased root hair density by loss of WRKY6 in Arabidopsis thaliana. PeerJ *5*, e2891.

Stone, B.A., and Clarke, A.E. (1992). Chemistry and biology of 1,3-[beta]-Glucans (Australia: La Trobe University Press).

Su, S.-H., Gibbs, N.M., Jancewicz, A.L., and Masson, P.H. (2017). Molecular Mechanisms of Root Gravitropism. Curr. Biol. *27*, R964–R972.

Suetsugu, N., and Wada, M. (2016). Evolution of the Cp-Actin-based Motility System of Chloroplasts in Green Plants. Front. Plant Sci. *7*.

Suetsugu, S., and Takenawa, T. (2003). Regulation of Cortical Actin Networks in Cell Migration. In International Review of Cytology, (Elsevier), pp. 245–286.

Suetsugu, N., Yamada, N., Kagawa, T., Yonekura, H., Uyeda, T.Q.P., Kadota, A., and Wada, M. (2010). Two kinesin-like proteins mediate actin-based chloroplast movement in Arabidopsis thaliana. Proc. Natl. Acad. Sci. U. S. A. *107*, 8860–8865.

Suzuki, T., Masaoka, K., Nishi, M., Nakamura, K., and Ishiguro, S. (2008). Identification of kaonashi Mutants Showing Abnormal Pollen Exine Structure in Arabidopsis thaliana. Plant Cell Physiol. *49*, 1465–1477.

Svitkina, T.M. (2012). Actin bends over backward for directional branching. Proc. Natl. Acad. Sci. *109*, 2693–2694.

Szymanski, D.B. (2005). Breaking the WAVE complex: the point of Arabidopsis trichomes. Curr. Opin. Plant Biol. *8*, 103–112.

Szymanski, D.B., Marks, M.D., and Wick, S.M. (1999). Organized F-actin is essential for normal trichome morphogenesis in Arabidopsis. Plant Cell *11*, 2331–2347.

Szymanski, D.B., Lloyd, A.M., and Marks, M.D. (2000). Progress in the molecular genetic analysis of trichome initiation and morphogenesis in Arabidopsis. Trends Plant Sci. *5*, 214–219.

Takemoto, D., and Hardham, A.R. (2004). The cytoskeleton as a regulator and target of biotic interactions in plants. Plant Physiol. *136*, 3864–3876.

Takemoto, D., Jones, D.A., and Hardham, A.R. (2006). Re-organization of the cytoskeleton and endoplasmic reticulum in the Arabidopsis pen1-1 mutant inoculated with the non-adapted powdery mildew pathogen, Blumeria graminis f. sp. hordei. Mol. Plant Pathol. *7*, 553–563.

Talbot, M.J., and White, R.G. (2013). Methanol fixation of plant tissue for Scanning Electron Microscopy improves preservation of tissue morphology and dimensions. Plant Methods *9*, 36.

Tanaka, I. (1997). Differentiation of generative and vegetative cells in angiosperm pollen. Sex. Plant Reprod. *10*, 1–7.

Tax, F.E., and Vernon, D.M. (2001). T-DNA-associated duplication/translocations in Arabidopsis. Implications for mutant analysis and functional genomics. Plant Physiol. *126*, 1527–1538.

Taylor, L.P., and Hepler, P.K. (1997). POLLEN GERMINATION AND TUBE GROWTH. Annu. Rev. Plant Physiol. Plant Mol. Biol. *48*, 461–491.

Teng, N., Wang, J., Chen, T., Wu, X., Wang, Y., and Lin, J. (2006). Elevated CO2 induces physiological, biochemical and structural changes in leaves of Arabidopsis thaliana. New Phytol. *172*, 92–103.

Terao, T., Yamashita, A., and Katoh, S. (1985). Chlorophyll b-Deficient Mutants of RiceI. Absorption and Fluorescence Spectra and Chlorophyll a/b Ratios. Plant Cell Physiol.

Terashima, I., Hanba, Y.T., Tholen, D., and Niinemets, Ü. (2011). Leaf functional anatomy in relation to photosynthesis. Plant Physiol. *155*, 108–116.

Thitamadee, S., Tuchihara, K., and Hashimoto, T. (2002). Microtubule basis for left-handed helical growth in Arabidopsis. Nature *417*, 193–196.

Thorsness, M.K., Kandasamy, M.K., Nasrallah, M.E., and Nasrallah, J.B. (1993). Genetic Ablation of Floral Cells in Arabidopsis. Plant Cell *5*, 253–261.

Tian, J., Han, L., Feng, Z., Wang, G., Liu, W., Ma, Y., Yu, Y., and Kong, Z. (2015). Orchestration of microtubules and the actin cytoskeleton in trichome cell shape determination by a plant-unique kinesin. eLife *4*.

Tlałka, M., and Gabryś, H. (1993). Influence of calcium on blue-light-induced chloroplast movement in Lemna trisulca L. Planta *189*, 491–498.

Tominaga-Wada, R., Ishida, T., and Wada, T. (2011). New Insights into the Mechanism of Development of Arabidopsis Root Hairs and Trichomes. In International Review of Cell and Molecular Biology, (Elsevier), pp. 67–106.

Uhrig, J.F., Mutondo, M., Zimmermann, I., Deeks, M.J., Machesky, L.M., Thomas, P., Uhrig, S., Rambke, C., Hussey, P.J., and Hulskamp, M. (2007). The role of Arabidopsis SCAR genes in ARP2-ARP3-dependent cell morphogenesis. Development *134*, 967–977.

Underwood, W., and Somerville, S.C. (2008). Focal accumulation of defences at sites of fungal pathogen attack. J. Exp. Bot. *59*, 3501–3508.

Valster, A.H., Pierson, E.S., Valenta, R., Hepler, P.K., and Emons, A.M.C. (1997). Probing the Plant Actin Cytoskeleton during Cytokinesis and Interphase by Profilin Microinjection. Plant Cell *9*, 1815–1824.

Van Damme, D., De Rybel, B., Gudesblat, G., Demidov, D., Grunewald, W., De Smet, I., Houben, A., Beeckman, T., and Russinova, E. (2011). Arabidopsis α Aurora kinases function in formative cell division plane orientation. Plant Cell *23*, 4013–4024.

Van Gestel, K., Köhler, R.H., and Verbelen, J.-P. (2002). Plant mitochondria move on F-actin, but their positioning in the cortical cytoplasm depends on both F-actin and microtubules. J. Exp. Bot. *53*, 659–667.

Vaughn, L.M., Baldwin, K.L., Jia, G., Verdonk, J.C., Strohm, A.K., and Masson, P.H. (2011). The Cytoskeleton and Root Growth Behavior. In The Plant Cytoskeleton, B. Liu, ed. (New York, NY: Springer New York), pp. 307–326.

Velemínský, J., and Röbbelen, G. (1966). Beziehungen Zwischen Chlorophyllgehalt und Chloroplastenstruktur in Einer Chlorina-Mutante von Arabidopsis Thaliana (L.) Heynh. Planta *68*, 15–35.

Verbelen, J.-P., De Cnodder, T., Le, J., Vissenberg, K., and Baluska, F. (2006). The Root Apex of Arabidopsis thaliana Consists of Four Distinct Zones of Growth Activities: Meristematic Zone, Transition Zone, Fast Elongation Zone and Growth Terminating Zone. Plant Signal. Behav. *1*, 296–304.

Vermeer, J.E.M., and Geldner, N. (2015). Lateral root initiation in Arabidopsis thaliana: a force awakens. F1000Prime Rep. *7*.

Vermeer, J.E.M., von Wangenheim, D., Barberon, M., Lee, Y., Stelzer, E.H.K., Maizel, A., and Geldner, N. (2014). A spatial accommodation by neighboring cells is required for organ initiation in Arabidopsis. Science *343*, 178–183.

Vidali, L., and Hepler, P.K. (2001). Actin and pollen tube growth. Protoplasma *215*, 64–76.

Vidali, L., McKenna, S.T., and Hepler, P.K. (2001). Actin Polymerization Is Essential for Pollen Tube Growth. Mol. Biol. Cell *12*, 2534–2545.

Vilches-Barro, A., and Maizel, A. (2015). Talking through walls: mechanisms of lateral root emergence in Arabidopsis thaliana. Curr. Opin. Plant Biol. *23*, 31–38.

Vivian-Smith, A., Luo, M., Chaudhury, A., and Koltunow, A. (2001). Fruit development is actively restricted in the absence of fertilization in Arabidopsis. Dev. Camb. Engl. *128*, 2321–2331.

Volkmann, N., Amann, K.J., Stoilova-McPhie, S., Egile, C., Winter, D.C., Hazelwood, L., Heuser, J.E., Li, R., Pollard, T.D., and Hanein, D. (2001). Structure of Arp2/3 complex in its activated state and in actin filament branch junctions. Science *293*, 2456–2459.

Wahl, V., Ponnu, J., Schlereth, A., Arrivault, S., Langenecker, T., Franke, A., Feil, R., Lunn, J.E., Stitt, M., and Schmid, M. (2013). Regulation of flowering by trehalose-6-phosphate signaling in Arabidopsis thaliana. Science *339*, 704–707.

Wang, Z. (2015). Functional Analysis of the miR156 Regulatory Network in Arabidopsis Siliques. University of Western Ontario.

Wang, J., Zhang, R., Chang, M., Qu, X., Diao, M., Zhang, M., and Huang, S. (2014). Actin Cytoskeleton. In Plant Cell Biology, S. Assmann, and B. Liu, eds. (New York, NY: Springer New York), pp. 1–28.

Wang, X., Anderson, O.R., and Griffin, K.L. (2004). Chloroplast numbers, mitochondrion numbers and carbon assimilation physiology of Nicotiana sylvestris as affected by CO2 concentration. Environ. Exp. Bot. *51*, 21–31.

Wang, X., Zhu, L., Liu, B., Wang, C., Jin, L., Zhao, Q., and Yuan, M. (2007). Arabidopsis MICROTUBULE-ASSOCIATED PROTEIN18 functions in directional cell growth by destabilizing cortical microtubules. Plant Cell *19*, 877–889.

Wasteneys, G.O. (2000). The cytoskeleton and growth polarity. Curr. Opin. Plant Biol. *3*, 503–511.

Watanabe, N., Madaule, P., Reid, T., Ishizaki, T., Watanabe, G., Kakizuka, A., Saito, Y., Nakao, K., Jockusch, B.M., and Narumiya, S. (1997). p140mDia, a mammalian homolog of Drosophila diaphanous, is a target protein for Rho small GTPase and is a ligand for profilin. EMBO J. *16*, 3044–3056.

Wear, M.A., and Cooper, J.A. (2004). Capping protein: new insights into mechanism and regulation. Trends Biochem. Sci. *29*, 418–428.

Wegner, A. (1976). Head to tail polymerization of actin. J. Mol. Biol. *108*, 139–150.

Wegner, A., and Isenberg, G. (1983). 12-fold difference between the critical monomer concentrations of the two ends of actin filaments in physiological salt conditions. Proc. Natl. Acad. Sci. U. S. A. *80*, 4922–4925.

Wellburn, A.R. (1994). The Spectral Determination of Chlorophylls a and b, as well as Total Carotenoids, Using Various Solvents with Spectrophotometers of Different Resolution. J. Plant Physiol. *144*, 307–313.

Whippo, C.W., Khurana, P., Davis, P.A., DeBlasio, S.L., DeSloover, D., Staiger, C.J., and Hangarter, R.P. (2011). THRUMIN1 is a light-regulated actin-bundling protein involved in chloroplast motility. Curr. Biol. CB *21*, 59–64.

Woychik, R.P., Maas, R.L., Zeller, R., Vogt, T.F., and Leder, P. (1990). “Formins”: proteins deduced from the alternative transcripts of the limb deformity gene. Nature *346*, 850–853.

Wu, M.-F., Tian, Q., and Reed, J.W. (2006). Arabidopsis microRNA167 controls patterns of ARF6 and ARF8 expression, and regulates both female and male reproduction. Development *133*, 4211–4218.

Wu, Y., Yan, J., Zhang, R., Qu, X., Ren, S., Chen, N., and Huang, S. (2010). Arabidopsis FIMBRIN5, an actin bundling factor, is required for pollen germination and pollen tube growth. Plant Cell *22*, 3745–3763.

Wu, Z., Zhang, X., He, B., Diao, L., Sheng, S., Wang, J., Guo, X., Su, N., Wang, L., Jiang, L., et al. (2007). A chlorophyll-deficient rice mutant with impaired chlorophyllide esterification in chlorophyll biosynthesis. Plant Physiol. *145*, 29–40.

Xiao, Y., Tholen, D., and Zhu, X.-G. (2016). The influence of leaf anatomy on the internal light environment and photosynthetic electron transport rate: exploration with a new leaf ray tracing model. J. Exp. Bot. *67*, 6021–6035.

Xing, A., Williams, M.E., Bourett, T.M., Hu, W., Hou, Z., Meeley, R.B., Jaqueth, J., Dam, T., and Li, B. (2014). A pair of homoeolog ClpP5 genes underlies a *virescent yellow-like* mutant and its modifier in maize. Plant J. *79*, 192–205.

Xu, T., Wen, M., Nagawa, S., Fu, Y., Chen, J.-G., Wu, M.-J., Perrot-Rechenmann, C., Friml, J., Jones, A.M., and Yang, Z. (2010). Cell Surface- and Rho GTPase-Based Auxin Signaling Controls Cellular Interdigitation in Arabidopsis. Cell *143*, 99–110.

Xue, X.-H., Guo, C.-Q., Du, F., Lu, Q.-L., Zhang, C.-M., and Ren, H.-Y. (2011). AtFH8 Is Involved in Root Development under Effect of Low-Dose Latrunculin B in Dividing Cells. Mol. Plant *4*, 264–278.

Yamamoto, K., and Kiss, J.Z. (2002). Disruption of the Actin Cytoskeleton Results in the Promotion of Gravitropism in Inflorescence Stems and Hypocotyls of Arabidopsis. PLANT Physiol. *128*, 669–681.

Yang, L., Qin, L., Liu, G., Peremyslov, V.V., Dolja, V.V., and Wei, Y. (2014). Myosins XI modulate host cellular responses and penetration resistance to fungal pathogens. Proc. Natl. Acad. Sci. *111*, 13996–14001.

Yang, W., Ren, S., Zhang, X., Gao, M., Ye, S., Qi, Y., Zheng, Y., Wang, J., Zeng, L., Li, Q., et al. (2011). *BENT UPPERMOST INTERNODE1* Encodes the Class II Formin FH5 Crucial for Actin Organization and Rice Development. Plant Cell *23*, 661–680.

Yang, Y., Xiang, H., and Jack, T. (2003). pistillata-5, an Arabidopsis B class mutant with strong defects in petal but not in stamen development. Plant J. *33*, 177–188.

Ye, J., Zheng, Y., Yan, A., Chen, N., Wang, Z., Huang, S., and Yang, Z. (2009). Arabidopsis formin3 directs the formation of actin cables and polarized growth in pollen tubes. Plant Cell *21*, 3868–3884.

Yi, K., Guo, C., Chen, D., Zhao, B., Yang, B., and Ren, H. (2005). Cloning and functional characterization of a formin-like protein (AtFH8) from Arabidopsis. Plant Physiol. *138*, 1071–1082.

Yoder, T.L., Zheng, H.Q., Todd, P., and Staehelin, L.A. (2001). Amyloplast sedimentation dynamics in maize columella cells support a new model for the gravity-sensing apparatus of roots. Plant Physiol. *125*, 1045–1060.

Yoo, S.-C., Cho, S.-H., Sugimoto, H., Li, J., Kusumi, K., Koh, H.-J., Iba, K., and Paek, N.-C. (2009). Rice virescent3 and stripe1 encoding the large and small subunits of ribonucleotide reductase are required for chloroplast biogenesis during early leaf development. Plant Physiol. *150*, 388–401.

Yu, Q.-B., Jiang, Y., Chong, K., and Yang, Z.-N. (2009). AtECB2, a pentatricopeptide repeat protein, is required for chloroplast transcript *accD* RNA editing and early chloroplast biogenesis in *Arabidopsis thaliana*. Plant J. *59*, 1011–1023.

Yun, B.-W., Atkinson, H.A., Gaborit, C., Greenland, A., Read, N.D., Pallas, J.A., and Loake, G.J. (2003). Loss of actin cytoskeletal function and EDS1 activity, in combination, severely compromises non-host resistance in Arabidopsis against wheat powdery mildew. Plant J. Cell Mol. Biol. *34*, 768–777.

Zhang, X. (2005). IRREGULAR TRICHOME BRANCH1 in Arabidopsis Encodes a Plant Homolog of the Actin-Related Protein2/3 Complex Activator SCAR/WAVE That Regulates Actin and Microtubule Organization. PLANT CELL ONLINE *17*, 2314–2326.

Zhang, C., Mallery, E.L., and Szymanski, D.B. (2013a). ARP2/3 localization in Arabidopsis leaf pavement cells: a diversity of intracellular pools and cytoskeletal interactions. Front. Plant Sci. *4*.

Zhang, F., Luo, X., Hu, B., Wan, Y., and Xie, J. (2013b). YGL138(t), encoding a putative signal recognition particle 54 kDa protein, is involved in chloroplast development of rice. Rice *6*, 7.

Zhang, H., Li, J., Yoo, J.-H., Yoo, S.-C., Cho, S.-H., Koh, H.-J., Seo, H.S., and Paek, N.-C. (2006). Rice Chlorina-1 and Chlorina-9 encode ChlD and ChlI subunits of Mg-chelatase, a key enzyme for chlorophyll synthesis and chloroplast development. Plant Mol. Biol. *62*, 325–337.

Zhang, L., Zhang, H., Liu, P., Hao, H., Jin, J.B., and Lin, J. (2011a). Arabidopsis R-SNARE proteins VAMP721 and VAMP722 are required for cell plate formation. PloS One *6*, e26129.

Zhang, Z., Zhang, Y., Tan, H., Wang, Y., Li, G., Liang, W., Yuan, Z., Hu, J., Ren, H., and Zhang, D. (2011b). *RICE MORPHOLOGY DETERMINANT* Encodes the Type II Formin FH5 and Regulates Rice Morphogenesis. Plant Cell *23*, 681–700.

Zhao, Y., Zhao, S., Mao, T., Qu, X., Cao, W., Zhang, L., Zhang, W., He, L., Li, S., Ren, S., et al. (2011). The plant-specific actin binding protein SCAB1 stabilizes actin filaments and regulates stomatal movement in Arabidopsis. Plant Cell *23*, 2314–2330.

Zigmond, S.H. (2004). Beginning and ending an actin filament: control at the barbed end. Curr. Top. Dev. Biol. *63*, 145–188.

Zou, J.-J., Zheng, Z.-Y., Xue, S., Li, H.-H., Wang, Y.-R., and Le, J. (2016). The role of Arabidopsis Actin-Related Protein 3 in amyloplast sedimentation and polar auxin transport in root gravitropism. J. Exp. Bot. *67*, 5325–5337.

APPENDICES

Appendix-A Altered biotic stress responses of actin cytoskeleton disrupted mutants

Appx.A.1 Penetration rate of non-adapted powdery mildew

The first resistance response of the host plant against fungal pathogen attack is penetration resistance. The penetration resistance of plant against fungi refers to the process of prevention to restrict the invasion of fungal infection structure (Abera Gebrie, 2016). The penetration resistance is the cell wall associated plant defense and the first resistance response of the plant which is important in basal resistance (Hückelhoven, 2007). Upon its first touch on the plant surface the fungi secrete a variety of degrading enzymes including cellulases, polygalacturonases, xylanases, and proteinases (Annis and Goodwin, 1997) for degrading the host cell wall to grow through the apoplast. When the plants recognize these non-self activity and molecules, they respond by induction of apoplastic defense through strengthening the cell wall, forming the papillae and or poisoning of the pathogen (Annis and Goodwin, 1997).

Appx.A.1.1 Determination of powdery mildew penetration rate

The wild type, the double mutant and both the single mutants plants were inoculated with non-adapted powdery mildew fungi (*Blumeria graminis* f. sp. *Hordei,* Bgh) by tapping the heavily Bgh infected barley plant over the sample plants following the method described in supplementary (Yang et al., 2014). Inoculated leaves were cut from the plant and fixed in carnoy's solutions (ethanol: chloroform: glacial acetic acid = 6:3:1) (Chen et al., 2002) until the complete removal of chlorophyll in the leaves. The solutions were replaced with 100% ethanol and incubated overnight. Then the leaves were rehydrated to distilled water following 2 hrs incubation in each dilution solution in a dilution series of (90%, 80%, 70%, 60%, 50%, 40%, 30%, 20% and 10% of ethanol). After 2 hrs of rehydration in distilled water, the leaves were stained with aniline blue solution (0.05% aniline blue in acidic water) for 5 minutes that enabled the staining of conidia, appressoria and hyphae. The stained leaves were then taken in slides containing few drops of acidic water and

the fungal infections were studied under light microscope. The penetration percentage were calculated according to the equation, % penetration = number of haustoria/ number of mature appressoria x 100 (supplementary, Yang et al., 2014). At least 500 infection sites for each genotype were counted for the determination of penetration rate.

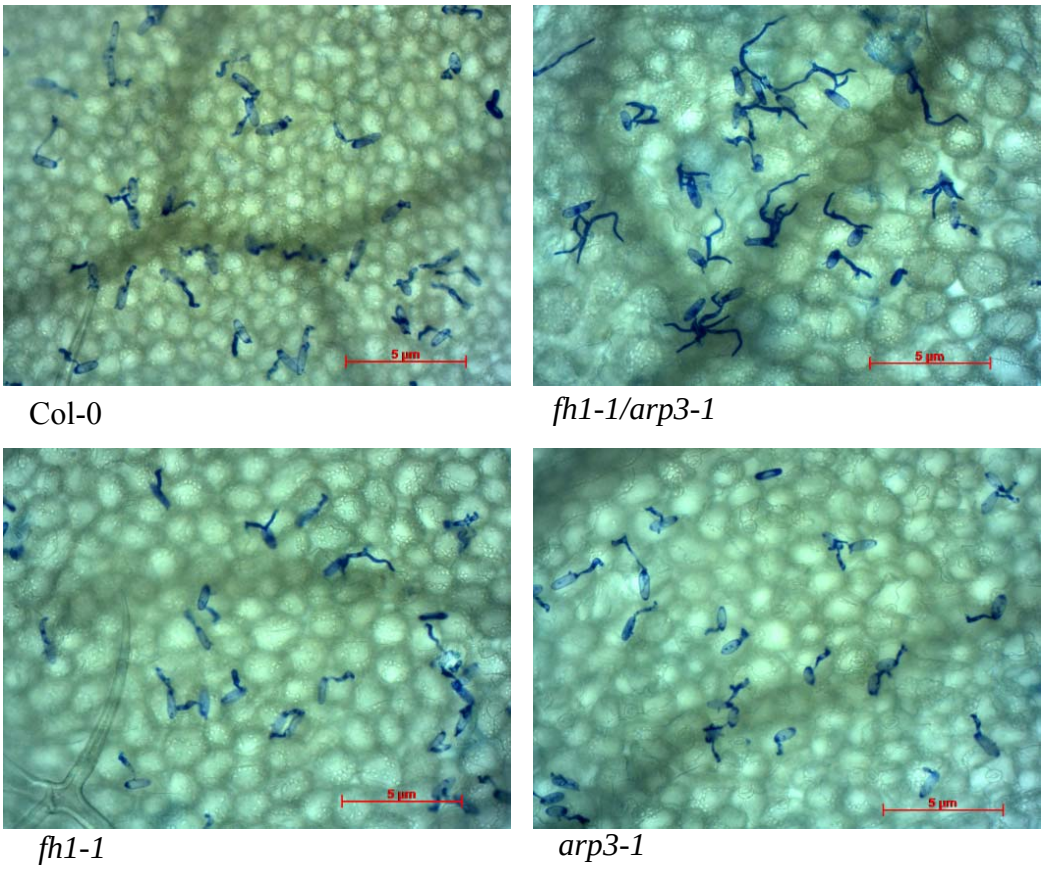

Figure appx.A.1.1: The infection of non-adapted powdery mildew, *Blumeria graminis* f. sp. *hordei* (Bgh) on the leaf of the wild type, the double mutant and both the single mutants. The inoculated leaves were fixed, rehydrated, stained with aniline blue and images were captured with Zeiss epifluorescence microscope.

Table appx.A.1.1: The rate of Bgh penetrations on the wild type, the double mutant and both the single mutants.

Leaf samples	Penetration rate (%) ± Std. Dev.				
	Haustorial primordia	**Haustorial growth**	**Cell death**	**Haustoria + Secondary hyphal growth**	**Total**
Col-0	2.45±0.26^{b}	1.50±0.60^{a}	2.26±0.54^{a}	1.52±0.35^{bc}	7.72±1.57^{d}
fh1-1/arp3-1	7.01±2.18^{b}	4.26±0.37^{a}	2.53±0.75^{a}	19.71±3.28^{a}	33.51±5.55^{a}
fh1-1	4.78±1.64^{b}	3.65±1.19^{a}	1.06±0.74^{a}	4.83±1.59^{b}	14.32±1.33^{c}
apr3-1	18.28±3.51^{a}	2.98±2.11^{a}	2.42±0.41^{a}	0.30±0.26^{c}	23.98±2.45^{b}

Appx.A.1.2 Results

The wild type (Col-0), the double mutant (*fh1-1/arp3-1*) and both the single mutants *fh1-1* and *arp3-1* were inoculated with *Bgh*. At 36 hpi the infected leaves from each plant were collected, fixed, dehydrated, re-hydrated, stained with aniline blue and examined under epifluorescence microscope for the determination of penetration frequency (Figure appx.A.1.1). The double mutant exhibited the highest total penetration percentage (33.51±5.55%) with the highest number of secondary hyphal growth compared to the wild type, conferring the penetration percentage 7.72±1.57% and both the single mutant having the penetration percentages of 14.32±1.33% in *fh1-1* and 23.98±2.45% in *arp3-1* respectively (Table appx.A.1.1). The total penetration rates of the wild type, the double mutant and both the single mutants were significantly difference to each other. The double mutant showed highest post invasion (haustoria + secondary hyphal growth) penetration rate and *fh1-1* single mutant followed the similar tendency, whereas, *arp3-1* exhibited highest pre-invasion (haustorial primordia) penetration rate (Figure appx.A.1.1; Table appx.A.1.1). There were no statistical significant differences in haustorial growth and cell death percentages among the wild type and all the mutants.

Appx.A.2 Cell wall apposition at the powdery mildew penetration site

The papilla that is formed by cell wall appositions (CWAs) beneath the cell wall at the fungal penetration site is the first penetration resistance of the plant (Aist, 1976). The main components of the CWAs are callose, lignin, cell wall proteins and reactive oxygen species which are deposited

at the inner surface of the cell wall and form the papillae (Underwood and Somerville, 2008). Callose or β (1,3) glucan, a linear polysaccharide, takes an important part of the basal plant resistance mechanism against fungal penetration by depositing itself at the papillae (Stone and Clarke, 1992). PMR4, one of the 12 callose synthase gene in *Arabidopsis thaliana* is responsible for the pathogen induced callose formation (Jacobs et al., 2003). A barley mlo mutant showed the higher penetration when callose synthesis was inhibited. Previous studies revealed that over expression of PMR4 in *Arabidopsis thaliana* enhanced early callose deposition upon powdery mildew infection conferring complete penetration resistance (Ellinger et al., 2013).

Appx.A.2.1 Callose detection upon powdery mildew inoculation

The powdery mildew fungi (*Blumeria graminis* f. sp. *Hordei,* Bgh) inoculated leaves from the wild type, the double mutant and both the single mutants were collected at 6, 12, 24 and 30 hpi and fixed them in carnoy's solutions until the removal of green color of the leaves. After removing the green color, the solutions were replaced with 100% ethanol and incubated overnight. Then the leaves were rehydrated to distilled water following 2 hrs incubation in each dilution solution in a dilution series of (90%, 80%, 70%, 60%, 50%, 40%, 30%, 20% and 10% of ethanol). After 2 hrs of rehydration in distilled water, the leaves were stained with 150 mM K_2HPO_4 (pH=9.5) containing 0.05% aniline blue overnight in dark. After staining the leaves were de-stained in Stained in 150 mM K_2HPO_4 (pH=9.5) overnight. The de-stained leaves were mounted with 30% glycerol in slides and images were taken under Zeiss Axioplan microscope.

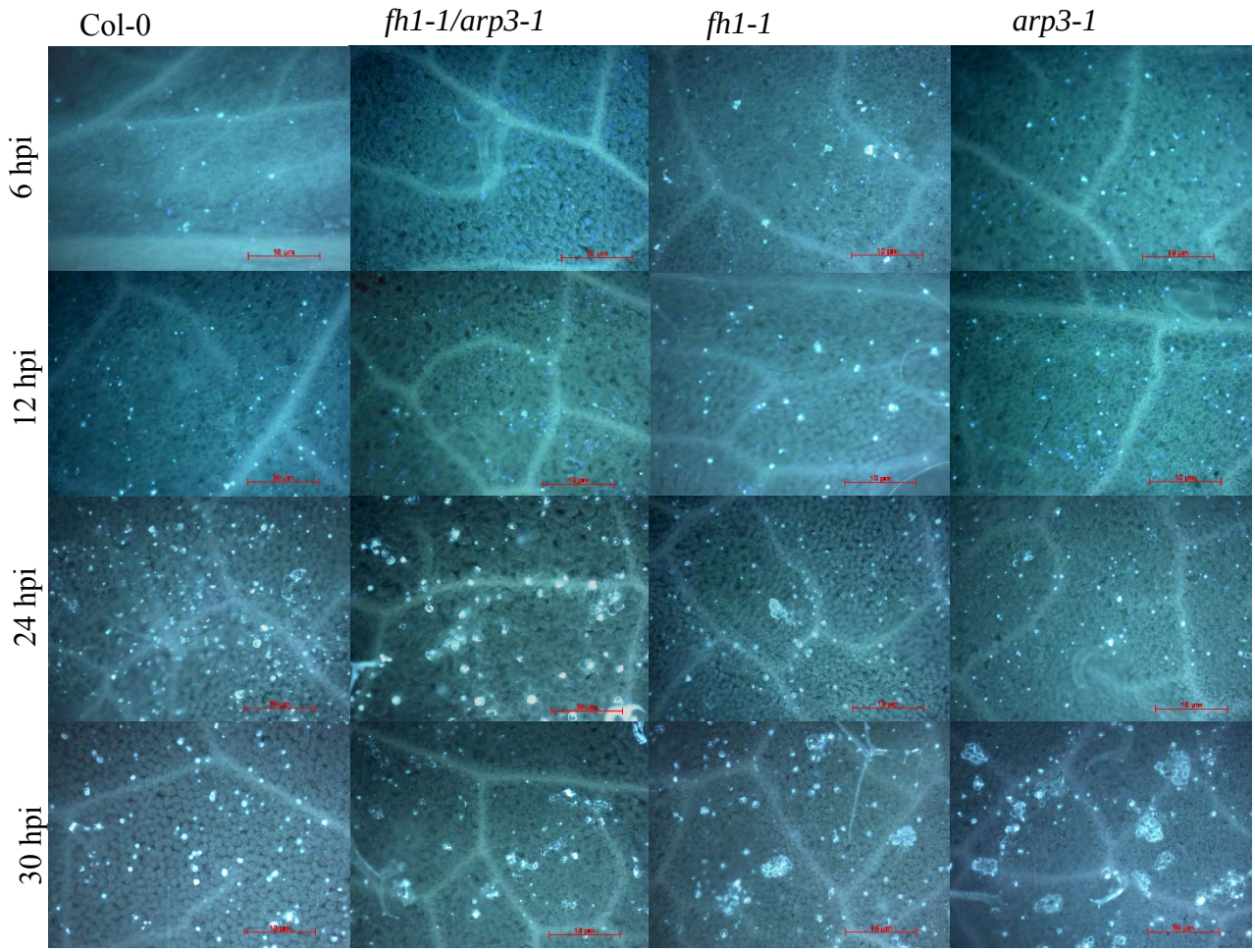

Figure appx.A.2.1: Callose deposition on the infected leaves of the wild type, the double mutant and both the single mutants in different hpi of inoculation with Bgh.

Appx.A.2.2 Results

The early callose deposition in 6 hpi in the double mutant plants was absent whereas the wild type and both the single mutants showed some deposition of callose within this time point. At 6 hpi single mutant *fh1-1* produced largest sizes of individual callose deposit than the wild type and *arp3-1* single mutant (Figure appx.A.2.1). The size of the callose deposits were almost similar up to 24 hpi in the wild type and both the single mutants (Figure appx.A.2.1). The amount of callose depositions in the wild type and both the single mutants were gradually increase up to 30 hpi within the time points of 6, 12, 24 and 30 hpi (Figure appx.A.2.1). In the double mutant few callose deposition was observed in 12 hpi that were drastically increased in both size and number of

deposits at 24 hpi (Figure appx.A.2.1). At 30 hpi the callose deposition in the double mutant was decreased but the trend of increasing callose depositions were continued in wild type and both the single mutants. At 30 hpi dense callose cores surrounded by large stained halos that were almost absent in the wild type were observed in the double mutant and both the single mutant. At this time point the highest number of callose surrounded halos were observed in *arp3-1* mutant, moderately in *fh1-1* mutant and lowest in the double mutant (Figure appx.A.2.1).

Appx.A.3 Reorganization of actin cytoskeleton at the powdery mildew penetration site

Actin cytoskeleton plays a multifaceted role in plant biology. It provides the major tracks that facilitate the intracellular transport of different cell organelles such as Golgi apparatus (Boevink et al., 1998), peroxisomes (Mathur et al., 2002) and mitochondria (Van Gestel et al., 2002) in the cellular level. The first defense response by the plant is the cytoplasmic aggregation beneath the pathogen attempted site of the cells. This aggregation is mediated with the internal cytoplasmic movement of the nucleus to the pathogen penetration site (Skalamera and Heath, 1998; Opalski et al., 2005). The actin filaments are redistributed to form a radial network at the targeted site of penetration in the cell of barley plant when it is inoculated by *Erysiphe pisi,* a nonhost powdery mildew of barley (Kobayashi et al., 1992). There are several researches on the compatible plant-microbe interaction on different plants such as flax-*Melanpsora lini* , soybean-*Phytophthora sojae* (Cahill et al., 2002) and barley-*Blumeria graminis* f.sp *hordei* (Bgh) (Schütz et al., 2006) revealed the similar reorganization and re-distribution of actin cytoskeleton inside the infected cells. So, disruption of actin cytoskeleton leaded to hamper the dynamic reorganization of actin cytoskeleton at the penetration site resulted higher penetration frequency of several fungi and oomycetes (Yang et al., 2014; Kobayashi et al., 1997; Takemoto et al., 2006; Yun et al., 2003).

Appx.A.3.1 Time lapse imaging of actin dynamics at Bgh infection site

Three week old plants of all the GFP expressing lines were inoculated with non-adapted powdery mildew fungi (*Blumeria graminis* f. sp. *Hordei,* Bgh) by tapping the heavily Bgh infected barley plant over the GFP expressing plants following the method described in supplementary (Yang et

al., 2014). The actin cytoskeleton dynamics within the infected cells of each sample were studied under the confocal laser scanning microscope (ZEISS LSM 510 Confor2, Carl Zeiss, West Germany) from 9 hours post inoculation (hpi) to 14 hpi and the time lapse images were taken with an interval of 10 minutes.

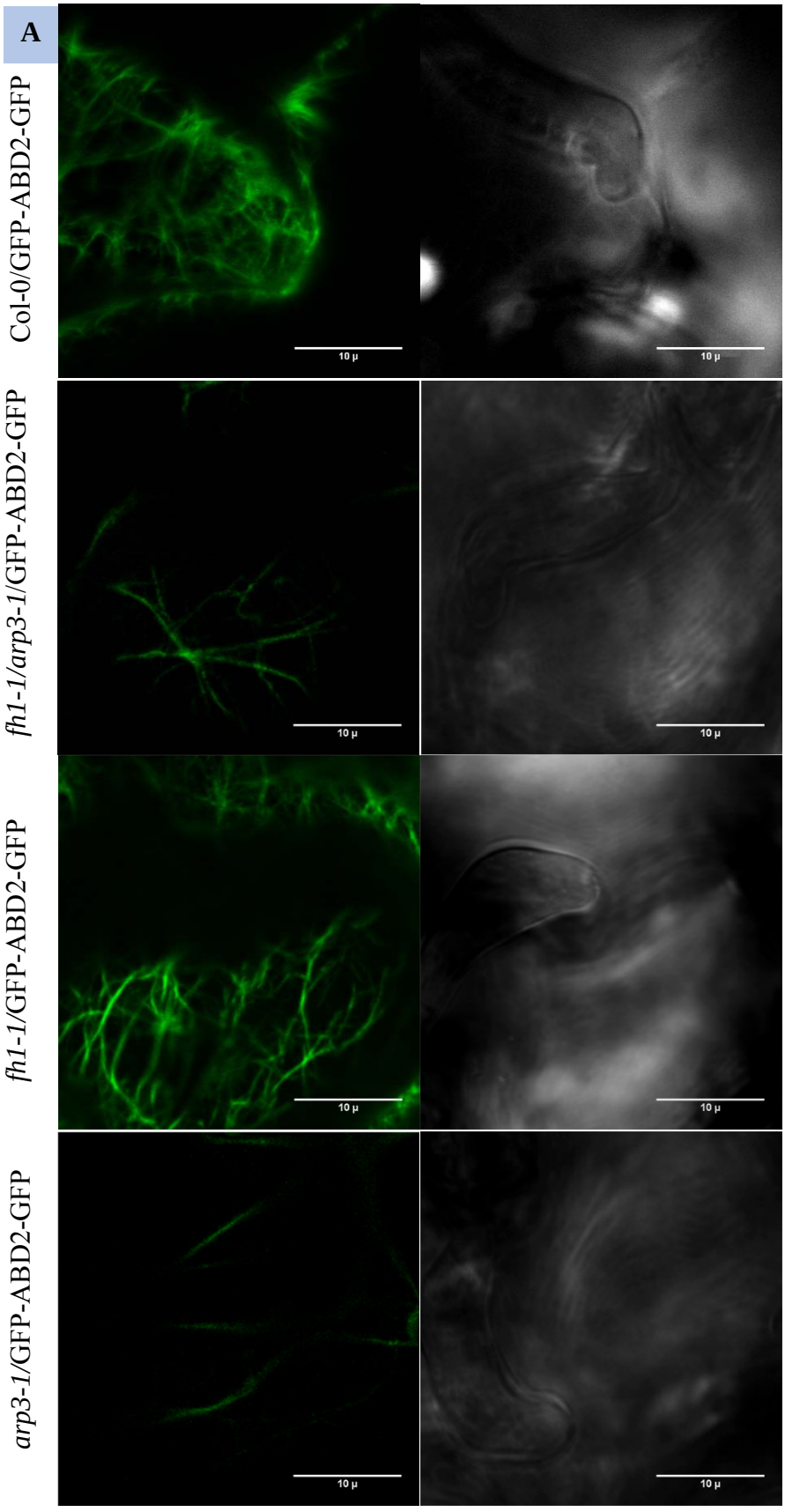
A
Col-0/GFP-ABD2-GFP
fh1-1/arp3-1/GFP-ABD2-GFP
fh1-1/GFP-ABD2-GFP
arp3-1/GFP-ABD2-GFP
10 µ

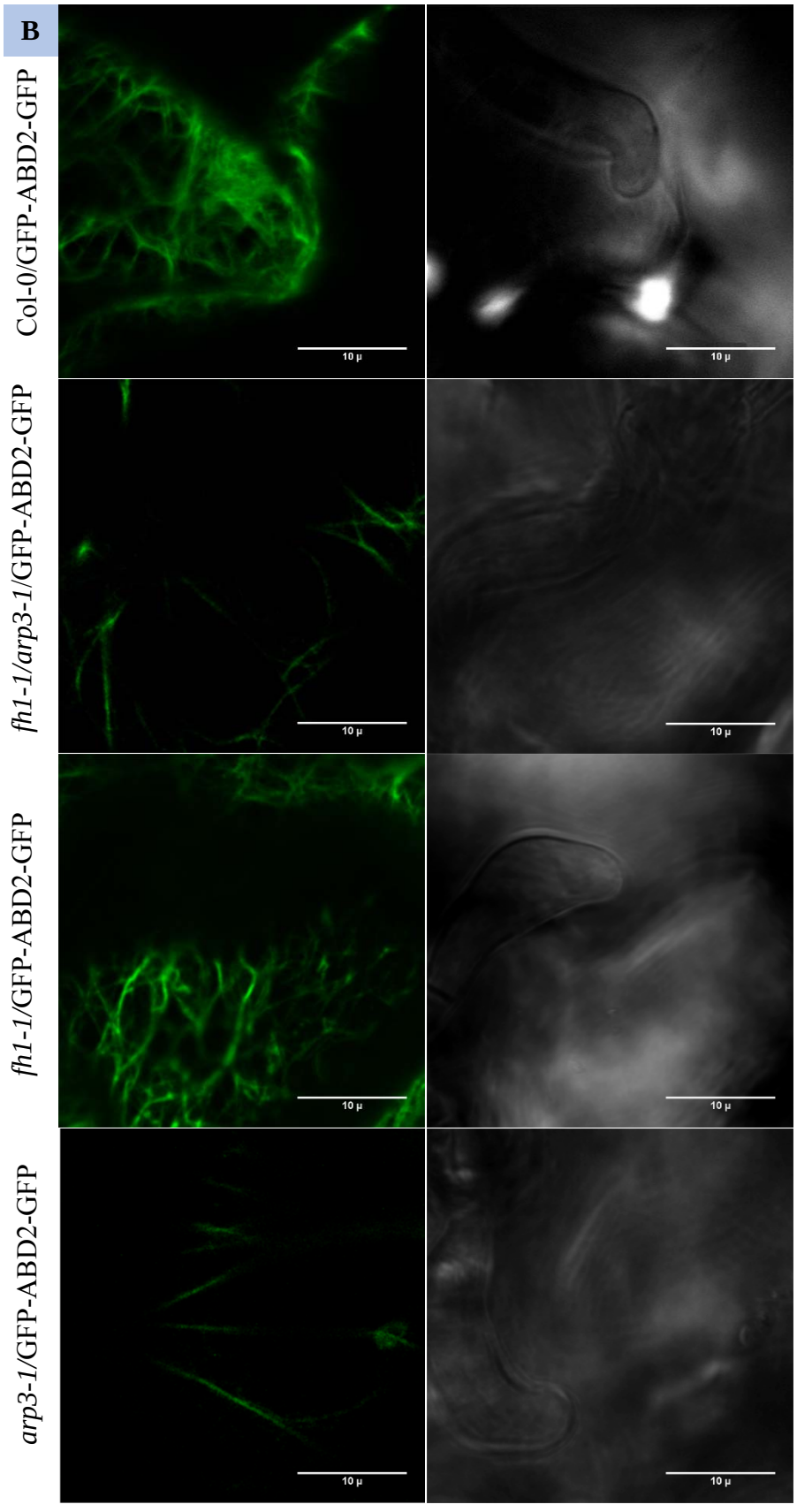
B
Col-0/GFP-ABD2-GFP
fh1-1/arp3-1/GFP-ABD2-GFP
fh1-1/GFP-ABD2-GFP
arp3-1/GFP-ABD2-GFP
10 µ

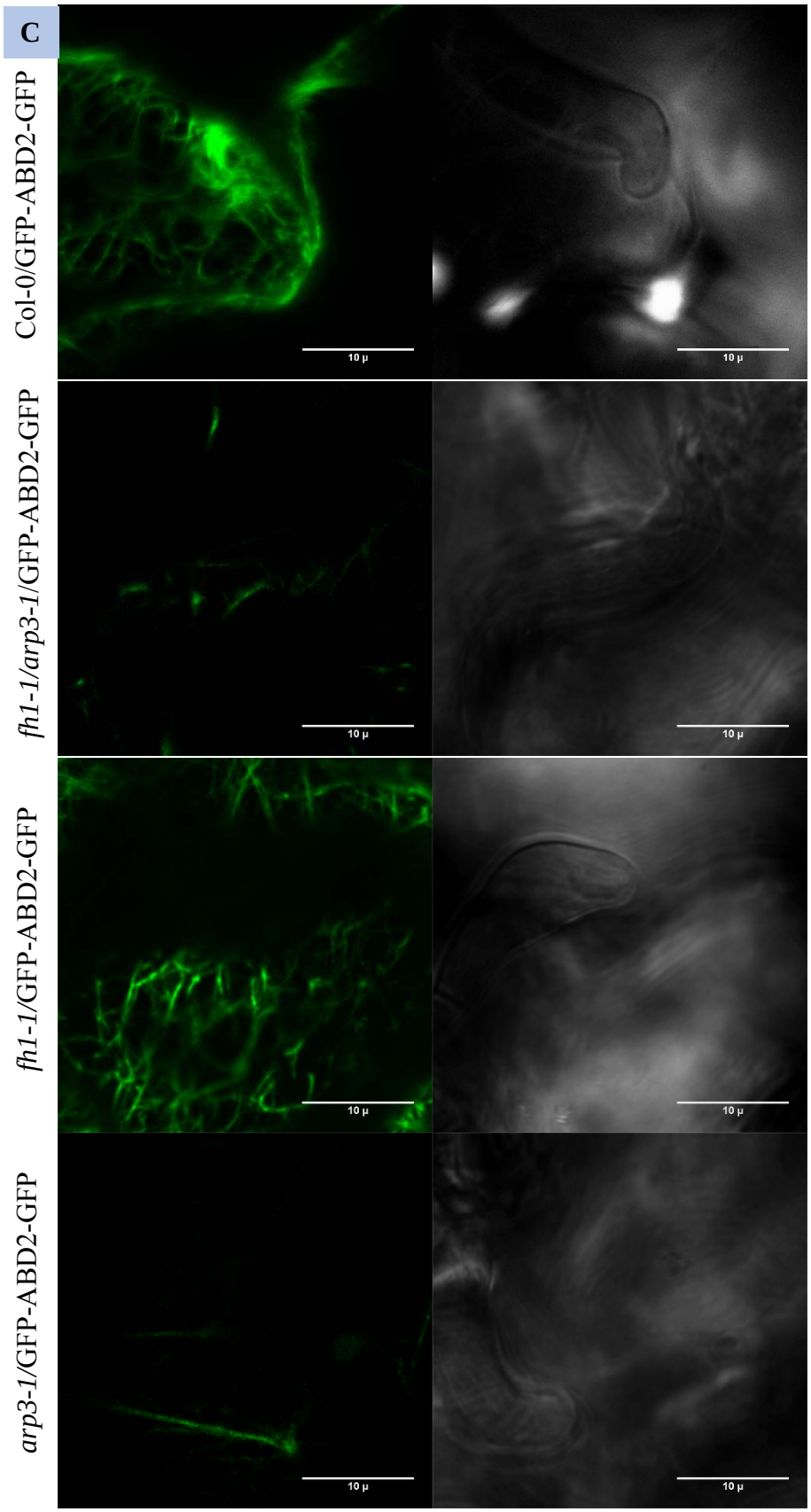
C
Col-0/GFP-ABD2-GFP
fh1-1/arp3-1/GFP-ABD2-GFP
fh1-1/GFP-ABD2-GFP
arp3-1/GFP-ABD2-GFP
10 µ

Figure appx.A.3.1: Actin cytoskeleton reorganization at the Bgh penetration site of the wild type, the *fh1-1/arp3-1* double mutant and both the single mutants *arp3-1* and *fh1-1* at 10.20 (A), 10.40 (B) and 11.00 (C) hpi.

Appx.A.3.2 Results

The GFP-ABD2-GFP expressing lines of the wild type, the double mutant and both the single mutants were inoculated with Bgh and actin cytoskeleton reorganization at the Bgh penetration sites were studied up to 6 hours from 8 hpi to 14 hpi for each sample under confocal microscope. In wild type (Col-0/ GFP-ABD2-GFP), at 10.20 hpi the actin cytoskeletons were started to accumulate at the Bgh penetration site, at 10.40 hpi they were started to form a radial network and at 11.00 hpi they formed a dense network of actin mesh at the Bgh penetration site (Figure appx.A.3.1- A, B and C). Although in the double mutant and *arp3-1* mutant the amount of actin cytoskeletons in the cell were very low, some tracks of actin filaments were continuously going to the penetration sites and few aggregations of actin filaments were observed (Figure appx.A.3.1- A, B and C). In case of *fh1-1* mutant the dynamic response of actin cytoskeletons at the Bgh penetration site were completely absent over time (Figure appx.A.3.1- A, B and C).

Appendix-B Anomalous abiotic stress responses of the actin cytoskeleton disrupted mutants

Appx.B.1 Leaf surface temperature upon exposure to drought stress

Stomata are the epidermal pore within the aerial part of the plants surrounded by two specialized guard cells that controls the gas exchanges and transpiration, the process through which plants loose excess water in the form of vapor. These guard cells control the opening and closing of the stomatal aperture in response to the endogenous and exogenous signals and fine tune the pore size to be fit to the environmental condition. The previous researches reported that a well-defined network of signaling events including turgor change, ion flux, metabolic change, protein modification, vesicle trafficking, actin rearrangement, and gene expression regulation within the guard cells control the stomatal movement (Hetherington and Woodward, 2003; Gray, 2005; Kim et al., 2010). The transduction pathway through which abscisic acid (ABA) regulates the stomatal movement have been established by several pharmacological and cell biological studies that have led to major advances in understanding the stomatal movements (Assmann and Wang, 2001; Hetherington, 2001; Schroeder et al., 2001).

The evaporation from any surface is associated with the latent heat loss, thereby transpiration causes the cooling of the leaf surface. A simple, scientific, efficient and non-destructive method to measure the leaf surface temperature is infrared thermography that provide the effective indicator of transpiration through measuring leaf temperature of captured plants (Chaerle and Van Der Straeten, 2000; Hashimoto et al., 1984; Jones, 1999). The infrared thermography was successfully introduced to isolate barley mutant that was unable to close the stomata and even after treatment with ABA (Raskin and Ladyman, 1988).

Appx.B.1.1 Determination of leaf temperature upon exposure to drought stress

The wild type, the double mutant and both the single mutants were grown in the growth chamber within above described conditions. The drought stress were imposed on 3 week old plants following (Merlot et al., 2002) with some modifications. Briefly the plants were grown as

previously described in a well-watered condition and at 3 week age of the plant watering was stopped for 72 to 120 hrs. A series of 60 images (at 30 second intervals) for each genotype of plants were taken within 72, 96 and 120 hours post watering (hpw) using infrared camera (FLIR T650sc, FLIR systems AB, Sweden). These images allowed capture of the leaf surface temperature and documented these information with the images.

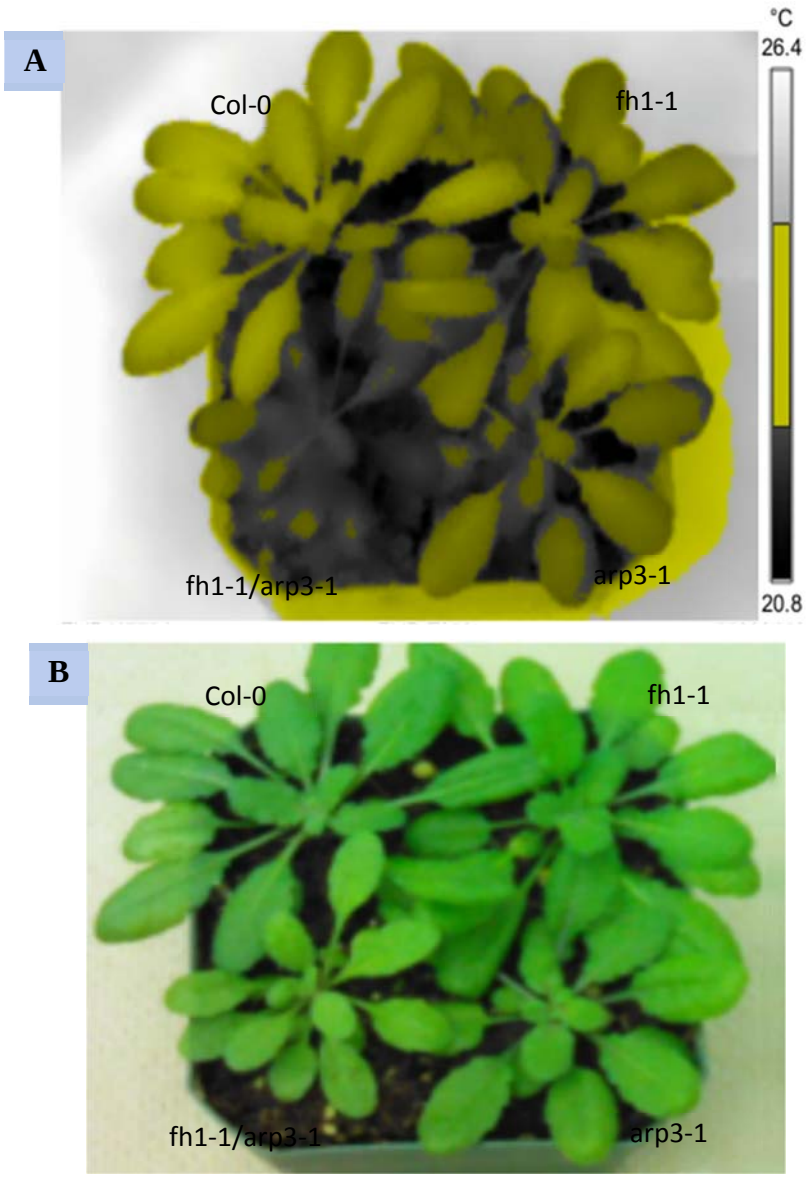

Figure appx.B.1.1: Infrared image (A) and normal camera image (B) of the same pot with the wild type, the double mutant and both the single mutants. The infrared image clearly shows the difference of leaf surface temperature of the double mutant differentiating the changes in color of leaf surfaces. The temperature scale is included with infrared image.

Table appx.B.1.1: Average leaf surface temperature of the wild type, the double mutant and both the single mutants in different hours post watering (hpw).

Genotype	**Leaf surface temperature ^{0}C ± Std. Dev.**		
	72 hpw	**96 hpw**	**120 hpw**
Col-0	25.00±1.430^a	24.08±0.091^a	23.48±0.145^a
fh1-1/arp3-1	23.62±1.301^b	23.34±0.086^b	22.53±0.180^b
fh1-1	24.28±1.407^c	23.82±0.086^c	23.22±0.141^c
arp3-1	24.17±1.375^{bc}	23.84±0.091^c	23.23±0.156^c

Appx.B.1.2 Results

The infrared image showed that the leaf surfaces of the double mutant *fh1-1/arp3-1* is colder having different leaf color compared to the wild type and both single mutants (Figure appx.B.1.1). This double mutant can easily be identified from other plants base on their leaf surface temperature that reflects on the color of the leaf in infrared image. The infrared thermography is very efficient to distinguish a fraction of temperature as the thermal camera is sensitive up to 0.1^0 C temperature (Merlot et al., 2002). The double mutant showed significantly lower leaf surface temperature compared to the wild type and both the single mutants in all the time points except 72 hpw when it exhibited similar leaf surface temperature to *arp3-1* mutant (Table appx.B.1.1). The wild type showed significantly higher leaf surface temperature than all the mutants in all the time points. There were no significant difference in leaf surface temperature between two single mutants in all the time points under the present study (Table appx.B.1.1).

Appx.B.2 Organization of the actin cytoskeleton in guard cells

During stomatal movement there are several changes occurred in the volume of guard cells and actin cytoskeleton participate in stomatal movement by regulating guard cell volume (Liu and Luan, 1998). The previous studies suggested that there is a positive correlation between actin filament orientation in guard cells and stomatal aperture (Li et al., 2014). In an open stomata the actin filaments are radially oriented and in a closed stomata they are longitudinally or randomly oriented in the guard cells of *Arabidopsis thaliana, Nicotiana tabacum Commelina communis* and *V. faba(* Gao et al., 2008; Zhao et al., 2011; Kim et al., 1995; Hwang and Lee, 2001). It was reported that actin filaments organization is regulated by cytoplasmic Ca^{++} concentration, protein

kinases, protein phosphatases, PI-3, PI-4 and ROS during stomatal movement (Hwang and Lee, 2001; Choi et al., 2014).

Appx.B.2.1 Visualization of actin dynamics in the guard cell

The leaves from three week old plants of all GFP expressing lines under drought stress were collected and The Z-stack images of the maximum number of clearly visible optical sections within the guard cells were taken with confocal laser scanning microscope (ZEISS LSM 510 Confor2, Carl Zeiss, West Germany) to visualize the actin cytoskeleton organization within the guard cells.

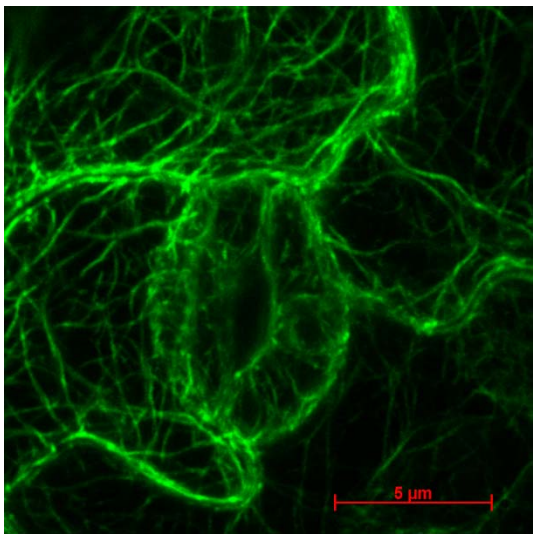

Col-0/GFP-ABD2-GFP

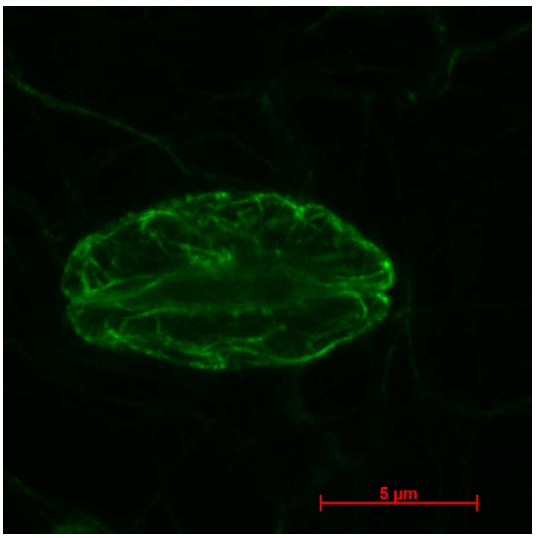

***fh1-1/arp3-1*/GFP-ABD2-GFP**

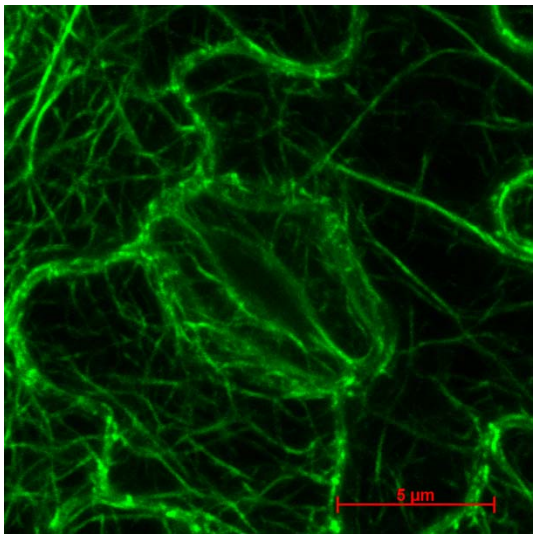

***fh1-1*/GFP-ABD2-GFP**

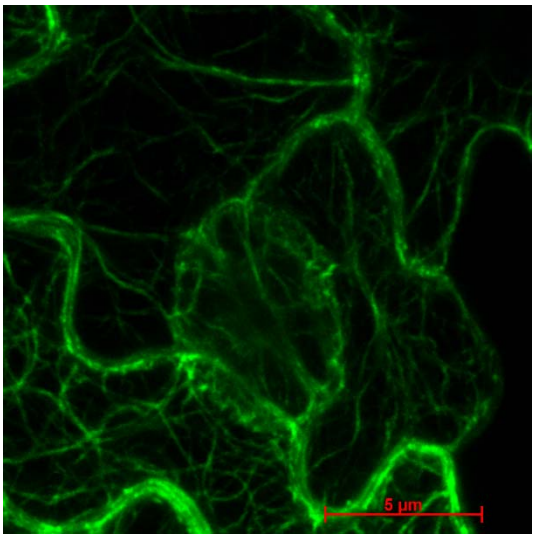

***arp3-1*/GFP-ABD2-GFP**

Figure appx.B.2.1: The actin cytoskeleton organization in the guard cells. The leaves were taken from 3 weeks GFP tagged ABD2 expressing lines under genetic background of the wild type, the double mutant and both the single mutants. The actin cytoskeleton organization in the guard cells of each plant leaves were visualized and captured the image with confocal microscope.

Appx.B.2.2 Results

The confocal images of moderately opened stomata showed that there were no thicker actin bundle strands at the periphery of the *fh1-1/arp3-1* guard cell whereas wild type and *fh1-1* had thicker and *arp3-1* had less thick strands (Figure appx.B.2.1). The transverse orientation of actin filaments in wild type and *fh1-1* mutant is readily organized. In *arp3-1* mutant had few transverse actin filaments but their organizations was smooth but in *fh1-1/arp3-1* mutant all the actin filaments are randomly organized (Figure appx.B.2.1).